DETECTION AND CHARACTERIZATION OF GLYCANS AND GLYCOCONJUGATES USING ION MOBILITY-MASS SPECTROMETRY

By

Larissa Spell Fenn

Dissertation

Submitted to the Faculty of the

Graduate School of Vanderbilt University

in partial fulfillment of the requirements

for the degree of

DOCTOR OF PHILOSOPHY

in

Chemistry

May, 2010

Nashville, Tennessee

Approved:

Professor John A. McLean

Professor Richard N. Armstrong

Professor Brian O. Bachmann

Professor Daniel C. Liebler

Dedicated

to

Joshua Fenn, who makes me aspire to breathe,

and

Daddy and Mom, Larry and Janice Spell, who made it possible for me to “dance”

ACKNOWLEDGEMENTS

I would like to begin by acknowledging and thanking my advisor, Dr. John A. McLean, for all of his guidance and taking a chance on me as his first graduate student. I feel very fortunate to have had such a great mentor. I would also like to thank Dr. Janel McLean for imparting her knowledge to me and for her friendship. Whitney Ridenour was my unofficial group member, and I appreciate all the ways she has assisted me, in the lab and out. I have enjoyed watching the McLean lab grow to its current members, Randi Gant-Branum, Josh Kerr, Michal Kliman, Jeff Enders, Cody Goodwin, Sevu Sundarapandian, Jody May, and Niki Arinze, and I wish everyone the best in their future endeavors.

I would also like to thank Dr. David Hercules for serving as my advisor during my rotation and while Dr. McLean was preparing for his transition from Texas. He started my passion for mass spectrometry and our weekly MS history lessons are something I will never forget.

My committee members, Dr. Richard Armstrong, Dr. Brian Bachmann, and Dr. Daniel Liebler, were great sources of ideas and were the encouragement I needed for all of the steps required in the quest for attaining my Ph.D. I appreciate all of the time they took to assist in my journey.

Of course, I would have never made it to this point without the teachers and professors who have fueled my passion for chemistry. Mr. John Williams first started my love while I was at Wayne County High School with his encouragement that I could do this. He is greatly missed. While at Mercer

University, the chemistry department, particularly Dr. Andrew Pounds and Dr. Caryn Seney, further cultivated my interest in chemistry and still serve as the type of people I aspire to be.

With the stressful work that was required during graduate school, I was happy to have friends that were able to distract me for a bit and help remind me to have fun. Rachel Snider was a great football buddy; weekends in Atlanta made me get away with Amy Griswold Martin, Blair Simpson, Hannah Carter, and Monica Harvell (not to mention a weekend in Las Vegas with Mary Frances Pilcher and the girls); and a few weekends in Philly with and visits to Nashville from Ashlee Snyder helped me take time to explore the cities around me. Updates from Dawn Stallard Jolly were also a highlight. Krystal Flowers moving to Nashville assisted me in getting out during my last year and also made for a great trip to Germany.

None of this would have been possible without the constant support from my family. Mom and Dad Fenn, Jeff and Debra, along with the Mallards, have taken me in as their own and I am proud to be a part of such an amazing family. I would also like to acknowledge Brandy Spell Geiger (with my new niece Autumn) and Mema, Ruby Morgan, for their support through my years of education. Larry and Janice Spell, Daddy and Mom, have supported me through all of my endeavors no matter how much the cost or how difficult it was for them to let me go out on my own.

Finally, I would like to acknowledge my creative and artistic husband, Joshua Fenn, who is my inspiration and makes me strive to be a better person.

He kept me sane during the long hours required for graduate work and was there whenever I needed him. I can only imagine what our future holds.

I would also like to acknowledge the financial support for this work which was provided by the Vanderbilt University College of Arts and Sciences, Vanderbilt Institute of Chemical Biology, Vanderbilt Institute for Integrative Biosystems Research and Education, Life Technologies/Molecular Probes, National Institutes of Health-NIDA (#HHSN271200677593C, #HHSN2712006775-63C), American Society for Mass Spectrometry Research Award, the US Defense Threat Reduction Agency HDTRA1-09-1-0013, the Spectroscopy Society of Pittsburgh, Ionwerks Inc., and Waters Corp. The synthetic carbohydrate compounds specified in forthcoming chapters were provided by the Carbohydrate Synthesis/Protein Expression Core of The Consortium for Functional Glycomics funded by the National Institute of General Medical Sciences grant GM62116.

TABLE OF CONTENTS

Page

Appendix

LIST OF TABLES

LIST OF FIGURES

LIST OF ABBREVIATIONS

ACN	acetonitrile
ATD	arrival time distribution
BA	boronic acid
CFG	The Consortium for Functional Glycomics
CID	collision-induced dissociation
Da	Dalton
DCM	dichloromethane
DDW	distilled, deionized water
Deoxyhex	deoxyhexose
DHB	2,5-dihydroxybenzoic acid
DMSO	dimethylsulphoxide
DTIM	drift tube ion mobility
ESI	electrospray ionization
FAIMS	high-field asymmetric waveform ion mobility spectrometry
FBA	ferrocene boronic acid
Gal	galactose
Glc	glucose
GlcNAc	*N*-acetylglucoseamine
Hex	hexose
HexNAc	*N*-acetylhexoseamine
HPLC	high-performance liquid chromatography

HPAE	high-pH anion-exchange chromatography
IM	ion mobility
IM-MS	ion mobility – mass spectrometry
IR	infrared
IRMPD	infrared multiphoton dissociation
LN	*N*-acetyl-D-lactoseamine
LNFP	lacto-*N*-fucopentaose
m/z	mass to charge ratio
MALDI	matrix-assisted laser desorption/ionization
MS	mass spectrometry
MS/MS	tandem mass spectrometry
MS^n	tandem mass spectrometry
NMR	nuclear magnetic resonance
PBA	4-[(2',6'-iisopropylphenoxy)phenylboronic acid]
PNGase F	peptide-N4-(acetyl-ß-glucosaminyl)-asparagine amidase F
PTM	post-translational modification
RNAse	ribonuclease
Sp	spacer on the end of synthetic glycans -$CH_2CH_2N_3$
THAP	2′,4′,6′-trihydroxyacetophenone
TOF	time-of-flight mass analyzer
TWIM	traveling wave ion mobility
v/v	volume to volume ratio
Wt	weight

CHAPTER I

INTRODUCTION

1.1 Challenges in Glycomics Research

Carbohydrates and glycans have significant roles in biological systems and are associated with many diseases that are currently of great interest. This section discusses these biological roles, associated diseases, and how glycans and glycoconjugates are currently detected and characterized to determine a disease state. A new methodology for rapid characterization utilizing ion mobility-mass spectrometry (IM-MS) is also proposed.

Glycomics has progressed into a critical area of study due to the implications of carbohydrate participation in many biological functions, and variations in glycosylation being associated with many disease states.[1-3] Protein glycosylation is one of the more intricate forms of post-translational modification (PTM) and is estimated to be present on 50% of eukaryotic proteins.[3] Glycoproteins have vital functions inside various organisms, and their associated glycans assist in the structure, function, and stability of proteins. Glycoproteins are involved in many important biological functions (*e.g.* embryonic development and the recognition of hormones, toxins, and other signals on the cell surface) and processes (*e.g.* coordination of immune function, cell division, and protein regulation and interactions).[4] With all of these important tasks of glycosylation,

detrimental effects may occur from variation or defects in glycosylation patterns. Several disease states such as Alzheimer's disease, HIV, cancer, and diabetes have characteristic defects in glycosylation patterns or unique glycoproteins associated with the disease.[3] The function of carbohydrates are derived from their composition and structure necessitating rapid and efficient structural determination from complex mixtures, including glycoconjugates such as glycoproteins and glycolipids.

Complete glycoprotein characterization involves the determination of: 1) glycosylation site or sites on the protein, 2) extent of occupancy at the site, 3) structure of the glycan attached at each site, and 4) all the various glycoforms present.[5] Current techniques proceed through each step sequentially and then combine the results in an attempt to fully characterize the glycoprotein of interest. Mass spectrometry (MS) has commonly been used to perform the first three steps of glycoprotein characterization. Characterization of all glycoforms is rarely performed due to the difficulty to detect less abundant glycoforms within a sample. For MS-based studies of glycoproteins, the main methods used are high-performance liquid chromatography (HPLC) techniques combined with MS and tandem MS (MS/MS or MS^n). Each assists in the steps to characterize the glycoprotein through the analysis of the digested glycopeptides, the detached glycans, or the complete glycoprotein.

To determine the site of attachment, a general technique is to use endoprotease digestion to cleave the protein into peptide fragments and isolate each glycosylation site onto a different peptide. HPLC or lectin-based affinity

chromatography then separates the glycopeptides from their non-glycosylated counterparts. Lectins are highly specific carbohydrate-binding proteins or glycoproteins that are extracted from natural sources. After HPLC separation, the glycopeptides are analyzed using MS^n or deglycosylated and sequenced using MS^n, scanning particularly for one of the two consensus sites for glycosylation: Asn-Xxx-(Ser, Thr), where Xxx can be any amino acid except proline, known to be the sequence of attachment for N-linked glycans; or a serine or threonine residues which are the sites of attachment for O-linked glycans.[5-7]

The next step is to characterize glycans attached to the glycoprotein. Glycans are typically removed from the protein and then analyzed separately because the complexity and size of the glycans typically places the glycoprotein in a range (*e.g.* >35kDa *m/z*) where MS resolution and sensitivity can begin to degrade.[6] The free or derivatized glycan can be removed chemically or enzymatically. Enzymatic approaches are most common for removal of N-linked glycans due to the specificity of enzymes such as peptide-N4-(acetyl-ß-glucosaminyl)-asparagine amidase F (PNGase F) which cleaves the glycan at the Asn/N-acetylglucosamine (GlcNAc) bond leaving an aspartate in place of the asparagine. There is no similar enzyme for O-linked glycan removal, and chemical deglycosylation such as hydrazinolysis or β-elimination is often used.[8-10] Another method is to use a nonspecific protease, such as Pronase, to digest the protein, but still leave the intact glycan with attached amino acids. The number of amino acids attached varies due to the possible steric hindrance by the glycan preventing amino acid cleavage.[11-13] The use of enzymatic or

chemical digestion simplifies analysis of the glycans, but most digests require extensive purification before MS analysis can be performed which requires more time for each experiment.

After removal from the protein and subsequent purification, usually with normal or reverse-phase HPLC, the glycans are characterized by MS. The choice of MS ionization source is critical when studying carbohydrates, and there are numerous advantages and challenges for each potential source. One of the advantages for electrospray ionization (ESI) is the ability to run online with HPLC separation. However, there are also challenges when using ESI such as the production of multiply-charged species which splits the already attenuated carbohydrate signal into several charge-state species. In addition, ESI does not tolerate impurities such as salts which are known to assist in the ionization and stabilization of the glycans.

As an alternative method of ionization, matrix-assisted laser desorption/ ionization (MALDI) can be used. In contrast with ESI, MALDI produces singly-charged ions and is more tolerant of salts leading to an abundance of metal cation-adducted species. However, MALDI cannot run online with HPLC and the laser desorption process can contribute to fragmentation of the carbohydrates in the source leading to a loss of signal. With these considerations, the optimal ionization source for each experiment can be determined.

When using MS to determine the structure of a glycan, sequencing is performed by MS/MS or MS^n to determine the monosaccharide units, or monomers, that compose the glycan. The glycans are generally constructed from

the same few monomers, many of which differ by linkages or stereocenters. For example, most glycans contain hexoses which can differ at the chiral centers (*i.e.* glucose vs. mannose) and anomeric carbons (*i.e.* α vs. β). To determine the linkages between the monomers, branching has to be taken into consideration. Even though many glycans have the same base structure they can vary greatly beyond the core.[14] The branches, or "antennae", can be dimeric, trimeric, tetrameric, and so on. Extensive characterization has been performed to determine the branching patterns of *N*-linked glycans leaving much to be discovered about the patterns that exist with other glycan types.

N-linked glycans contain a common trimannosyl-chitobiose core and are categorized into three different types: 1) "high mannose" which have all mannose on two antennae; 2) "hybrid" which has one antenna that has been further processed, and 3) "complex" which have further processing on two or more antennae (Figure 1.1).[5] The ability to separate these glycans into types is due to the well-characterized and more organized biosynthesis compared to O-linked glycans. The antennae of complex glycans can have three, four, or more antennae furthering the possible complexity of glycans for characterization.

1.1.2 Differentiating positional and structural carbohydrate isomers

The similarity of the monomers making up each glycan along with variations in branching provides the possibility for many positional and structural isomers. Structural or constitutional isomers have identical atomic composition but are arranged in different structures (*i.e.* identical monomer (individual

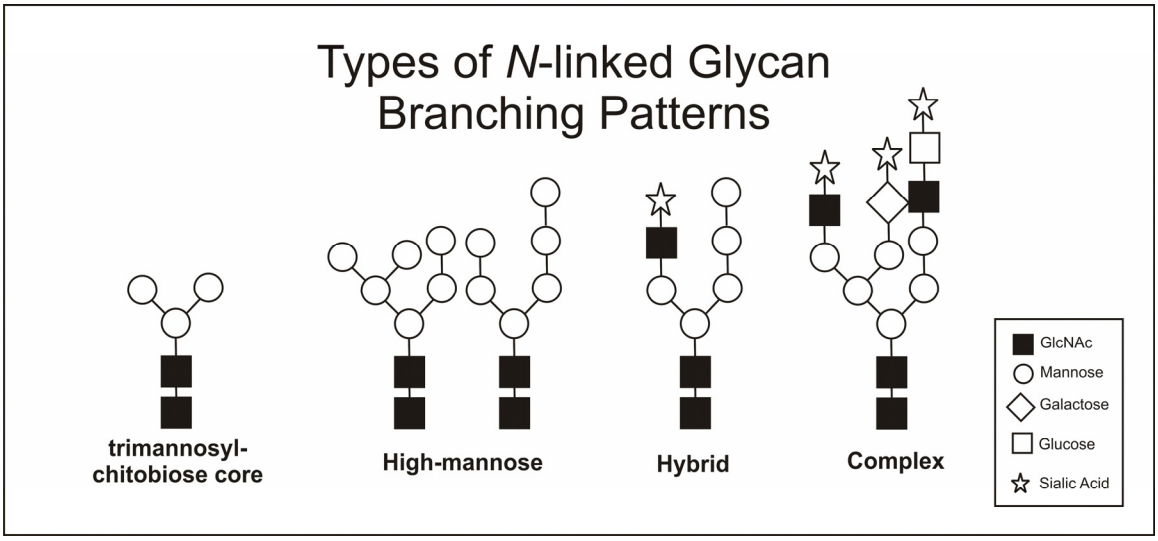

Figure 1.1 The *N*-linked glycan branching patterns which are separated into three types determined by the extent of processing after attachment to an asparagine on the glycoprotein of interest.

saccharide unit) linked on either of two antennae providing different topology) whereas positional isomers have the same number, type, sequence, and anomeric configurations but differ in the linkage position of a single monomer.[15,16] One method to differentiate isomeric carbohydrates is to analyze their structure using high-resolution techniques such as nuclear magnetic resonance (NMR) and X-ray crystallography.

Three-dimensional structural and conformational details can be used to differentiate isobaric glycans, and the topological structural information provides insight about the biological function of glycoproteins. Two ways of determining these high-resolution structures is through the use of NMR and X-ray crystallography. However, these methods are difficult for glycoproteins and in particular the associated glycans due to their complexity. Many carbohydrate and glycoprotein structures presently determined required extensive manipulation for stabilization of the glycan for X-ray crystallography, expression of the glycoproteins in non-glycosylating systems due to the large amount needed for NMR, or analysis of many sections of the structure all of which lead to doubt in the structural integrity of these findings.[17]

Methods for analyzing carbohydrates using MS-based methods have been developed due to the challenges using NMR and X-ray crystallography, but isomeric structures, which are also isobaric, makes the analysis of carbohydrates by MS challenging. Typically, HPLC and MS/MS fragmentation patterns are used to differentiate carbohydrate isomers by MS. In addition to the previously discussed HPLC methods used to separate and purify carbohydrates prior to MS

analysis (*e.g.* utilizing lectin, reverse-phase, or normal-phase columns[18]), other HPLC techniques such as high-pH anion-exchange (HPAE)[19,20] and porous graphitized carbon[21] have been explored to differentiate isobaric carbohydrates. HPAE, which is performed at a pH of approximately 13, can be used to separate positional isomers, but is difficult to combine with electrospray ionization because of the excessive amount of salts that are used requiring post separation sample clean-up prior to MS analysis.[19,20] Similarly, extensive and time-consuming sample cleanup is required after separation for many other types of HPLC such as lectin affinity chromatography. Although these HPLC methods can resolve some glycan isomers, due to a narrow range in polarity and similar carbohydrate size, typically tandem mass spectrometry is subsequently performed for complete structural elucidation.[18,22,23]

Fragmentation patterns produced using MS/MS or MS^n with collision-induced dissociation (CID)[24] and post-source decay[25,26] can sometimes distinguish isomeric carbohydrates. Carbohydrate fragmentation is described by nomenclature coined by Domon and Costello (Figure 1.2).[27] Generally two types of fragmentation occur in carbohydrates, glycosidic bond or cross-ring cleavages. Glycosidic bond cleavages are by far the most prevalent in positive-ion mode and provide information about sequence and branching of the monomers of the glycan. Cross-ring cleavages are two bond cleavages of a pyranose which provide information about the composition of the carbohydrate and are necessary to fully elucidate the structure of the glycan. However, these cleavages are not as abundant in positive-ion mode CID.[28] Therefore studies typically combine

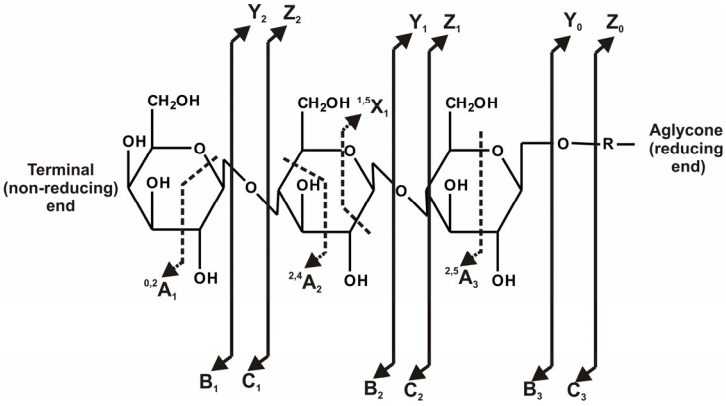

Figure 1.2 Carbohydrate fragmentation is specified in Domon-Costello nomenclature as depicted.[27]

multiple CID conditions such as negative-ion mode, changing the ionization or fragmentation energy,[29] varying the timescale for metastable decay prior to detection,[30] changing the ionizing cation, and utilizing other recently developed methods of ion activation (*i.e.* electron capture dissociation[31] and electron transfer dissociation[32]).

Collectively these challenges motivate the development of higher-throughput, more accurate, and less sample manipulation strategies for carbohydrate structure elucidation. Recently, 2D ion mobility-mass spectrometry (IM-MS) has been applied to the field of biological analysis.[33,34] Ion mobility, a well-developed separation technique, has been used extensively in the rapid detection of drugs and warfare agents due to its ease of use, low cost, speed, and sensitivity.[35] Ion mobility separates ions based on their apparent surface area or ion-neutral collision cross section.[36] When merged with MS, IM can separate gas-phase ions in one dimension based on their structure, and a second dimension related to their mass to charge (*m/z*). The advantages provided by IM-MS could be of great utility in the field of glycoproteomics.

This dissertation focuses on using IM-MS technologies for the study of carbohydrates and glycoproteins in the pursuit of simultaneous omics. Identification and conformational characterization of glycoproteins is pursued through studies of carbohydrate standards and separation of glycoprotein digests provided by the structural dimension of IM-MS. In this introductory chapter, IM-MS structural characterization will be summarized along with the theoretical background and instrumentation. The following sections describe an overview of

IM-MS instrumentation, the theory of IM separations, different types of IM separations, and data interpretation in IM-MS conformation space. Previous studies of carbohydrates and glycoproteins using IM-MS, and the specific questions addressed in this dissertation will also be discussed.

1.2 Ion Mobility-Mass Spectrometry Overview

Although gas-phase IM separations have existed for well over a century,[37] and coupling IM with MS has existed since the early 1960s,[38,39] the utility of IM-MS for biomolecular separations was not fully realized until combined with soft ionization techniques, such as electrospray ionization (ESI) and MALDI.[40,41] The first applications of IM-MS to determine peptide and protein structures were performed in the late 1990s.[42-44] Subsequent to these pioneering studies, research over the past decade has extended IM-MS techniques to the study of complex biological samples, such as whole cell lysates,[45] plasma,[46-49] homogenized tissue,[45,50,51] non-covalent complexes,[52-54] or directly from thin tissue sections.[55,56] However, until very recently, IM–MS was essentially available in only a limited number of laboratories where custom instruments were constructed. The recent introduction of commercially available IM–MS instrumentation, in several forms, has further fueled the integration of IM–MS techniques into life sciences research programs.

Ion mobility mass spectrometers are composed of an ion source, a mobility separation cell, a mass analyzer, and a detector as depicted in Figure

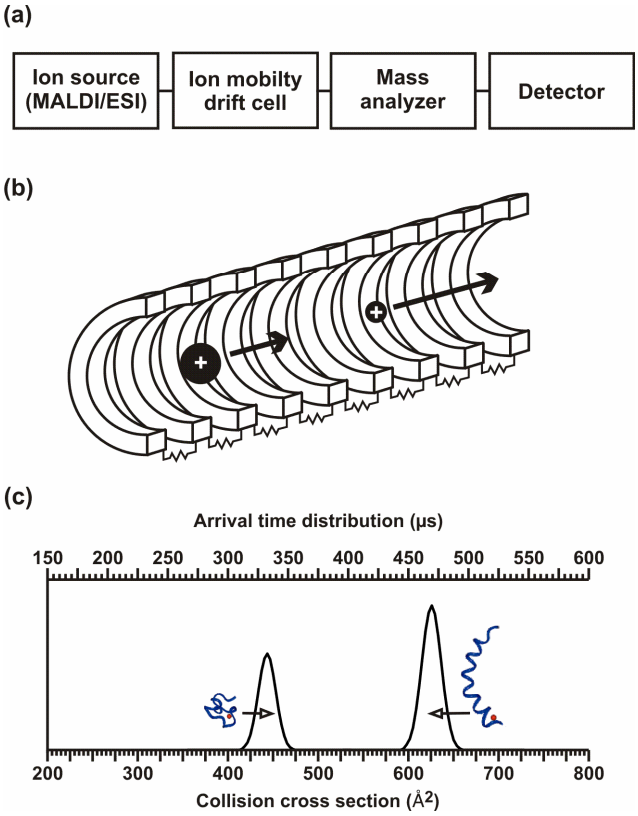

Figure 1.3 (a) A block diagram of the primary components of biological IM–MS instrumentation. (b) A conceptual depiction of an IM drift cell. A stack of ring electrodes are connected via resistors in series to form a voltage divider, which is typically designed to generate a relatively uniform electrostatic field along the axis of ion propagation. Ions of larger apparent surface area experience more collisions with the neutral drift gas and therefore elute more slowly than ions of smaller apparent surface area. (c) A hypothetical IM separation for peptide ions exhibiting two distinct structural subpopulations corresponding to globular (left) and to helical (right) conformations. The arrival time distribution data (top axis), or the observable, can be transformed into a collision cross-section profile (bottom axis) using Equation (4). With kind permission from Springer Science+Business Media: *Analytical and Bioanalytical Chemistry*, "Biomolecular Structural Separations by IM-MS: New Prospects for Systems Biology," 391, 2008, 905-909, L.S. Fenn and J.A. McLean, Figure 1.

1.3(a). There are many variations to the general design such as different ion sources (*i.e.* ESI, MALDI) and types of ion mobility separation cells used (*i.e.* whether the ions are dispersed in space or time). For most IM-MS applications time-of-flight (TOF) mass analyzers are used for timescale considerations. This research focuses on temporal ion dispersion through the use of drift tube or traveling wave ion mobility (DTIM and TWIM, respectively). In contrast with high energy ion-neutral gas-phase collisions used in collision induced dissociation (CID), both DTIM and TWIM separations utilize low energy gas-phase collisions to separate ions on the basis of predominantly molecular surface areas. Briefly, ions are injected into a drift tube filled with a neutral drift gas, usually helium or nitrogen, and migrate under the influence of a weak electrostatic field gradient [Figure 1.3(b)]. Larger ions have a lower mobility than smaller ions which result in longer drift times versus shorter drift times, respectively. This field is electrostatic for drift tube and electrodynamic for traveling wave separations, respectively. The migration of these ions is impeded by collisions with the neutral drift gas to a degree that is proportional to apparent surface area or collision cross section. Although the experimental parameter obtained from IM separations is the ion arrival time distribution (t_{ATD}), or the time between ion injection and ion detection, it can be converted to collision cross section or apparent surface area as illustrated in Figure 1.3(c). The following description details how this conversion is performed based on the kinetic theory of gases for drift tube separations. Derivation of ion-neutral collision cross section theory is presented in several excellent texts and reviews.[36,57,58] Procedures to estimate collision cross section

using TWIM are described elsewhere.[59,60] This research will utilize only DTIM for collision cross section calculations and the next section will present several of the key equations and practical considerations for determining ion-neutral collision cross sections in uniform electrostatic field IM instrumentation.

1.2.1 Theory of structural separations by ion mobility

Ion mobility rapidly separates ions on the basis of ion-neutral collision cross section, which in turn is related to the structure of the ion.[33,61-64] Briefly, ions are produced by MALDI or ESI and then introduced into the IM drift cell at room temperature. It should be noted that ionization is performed at the pressure of the drift cell, which results in ion collisional cooling and reduced fragmentation in comparison with contemporary high vacuum MALDI. The ions migrate across the drift cell under the influence of a weak electrostatic field. As the ions migrate, they are impeded by collisions with a neutral drift gas, typically helium between 3-10 Torr. Larger ions experience more collisions than smaller ions, which results in a slower velocity through the cell. The separation of ions in a weak electrostatic field (E) is measured as the ion drift velocity (v_d) and is related by the proportionality constant, K, which is the mobility of the ion in a particular neutral gas:

$$v_d = KE \tag{1}$$

The drift cell is of a fixed length (L), and the velocity of the ion packet is determined by measuring the drift time (t_d) of the packet across the drift cell. In evaluating K, the drift velocity of the ion packet depends not only on the

electrostatic field strength, but also on the pressure (p, Torr) of the neutral drift gas and the temperature (T, Kelvin) of separation. Therefore, it is conventional practice to report K as the standard or reduced mobility (K_0), which normalizes the results to standard temperature and pressure conditions (*i.e.* 0 ^{o}C and 760 Torr):

$$K_0 = \frac{L}{Et_d}\frac{273.15}{T}\frac{p}{760} \tag{2}$$

where L is the length of the drift cell (13.9 cm), E is the electrostatic-field strength (~90-120 V cm^{-1}) and p and T are the pressure (~3 Torr) and temperature (~293 K), respectively. For applications where IM is used to obtain structural information about the ion, such as those in structural proteomics and biophysics, the IM separations are performed using weak electrostatic-fields (*ca*. 20-30 V cm^{-1} Torr^{-1}). When the IM separations are performed in low-field conditions, the mobility is related to the collision cross section of the ion-neutral pair:

$$K_0 = \frac{(18\pi)^{1/2}}{16}\frac{ze}{(k_B T)^{1/2}}\left[\frac{1}{m_i}+\frac{1}{m_n}\right]^{1/2}\frac{760}{p}\frac{T}{273}\frac{1}{N_0}\frac{1}{\Omega} \tag{3}$$

where these parameters include the charge of the ion (ze), the number density of the drift gas at STP (N_0, 2.69 x 10^{19} cm^{-3}), the reduced mass of the ion-neutral collision pair (ion and neutral masses of m_i and m_n, respectively), Boltzmann's constant (k_b), and the ion-neutral collision cross section (Ω). This is derived from the kinetic theory of gases.[36] Inspection of Equation (3) shows that the mobility of an ion is inversely related to its collision cross section, or apparent surface area. Substituting for K_0 in Equation (3) and rearranging to solve for the collision cross section yields:

$$\Omega = \frac{(18\pi)^{1/2}}{16}\frac{ze}{(k_b T)^{1/2}}\left[\frac{1}{m_i}+\frac{1}{m_n}\right]^{1/2}\frac{t_d E}{L}\frac{760}{p}\frac{T}{273.15}\frac{1}{N_0} \quad (4)$$

which is the typical functional form of the equation used to solve for collision cross sections from IM data. Conceptually, the ion-neutral collision cross section can be thought of as the radius of the orientationally averaged projection of the ion in combination with the drift gas, *i.e.*:

$$\Omega = (r_i + r_{He})^2 \quad (5)$$

where r_i and r_{He} are the radii of the ion of interest and the helium buffer gas, respectively, as depicted in Figure 1.4.[57]

In order to ensure our drift time measurements and collision cross section calculations for glycans were comparable to other IM-MS studies, the collision cross section for α-cyclodextrin was calculated to be 200.7±0.5Å^2 which is comparable to a previous measurement 204±5Å^2 within experimental error of 2%.[65]

Following the drift cell, ions are directed into an orthogonal time-of-flight mass spectrometer (TOFMS). By taking many time-of-flight (TOF) spectra (μs per spectra) across the IM elution profile (ms timescale), a two-dimensional plot of Å^2 (surface area) vs. *m/z* is obtained.[36] Details of the data acquisition strategy used to generate 2D plots of conformation space are analogous to those described elsewhere. [33]

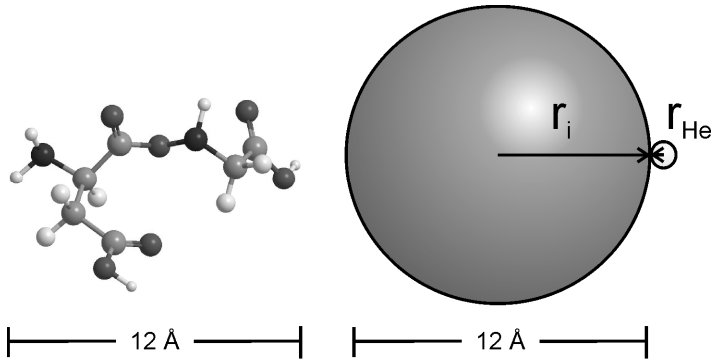

Figure 1.4 Visual representation of the collision cross section of a molecule that can be experimentally determined using IM. The radii of the ion (r_i) and the helium atom (r_{He}) can be used to approximate the collision cross section (Ω) using Equation (5).[57]

1.2.2 Types of ion mobility

The two time-dispersive methods of IM separation are DTIM and TWIM. DTIM facilitates absolute collision cross section calculations.[66-69] These data can then be compared to molecular simulation results to interpret analyte structural and conformational details. TWIM utilizes electrodynamic fields, which only provides estimated collision cross sections when measurements are compared to internal standards with previously measured DTIM absolute collision cross sections.[59,60] This is because gas-phase theory is insufficiently developed for the fundamental physical processes in TWIM separations, although recent efforts in this regard have been reported[70] along with reports comparing the values obtained from relative collision cross sections calculated by TWIM to the absolute values from DTIM.[71] Nevertheless, both DTIM and TWIM instrumentation are increasingly used for bioanalytical IM-MS applications.

1.2.2.1 Drift tube ion mobility

The first ion mobility instruments were developed on a drift tube design.[72] DTIM-MS instruments are conceptually analogous to typical MS instruments with the exception of inserting an IM drift cell between the source and mass analyzer. The DTIM instrument used for these experiments was an interchangeable source IM-TOFMS (Ionwerks Inc., Houston, TX).[73] It was equipped with a 13.9 cm ion mobility drift cell that is maintained at a pressure from 3-10 Torr helium and an orthogonal reflectron TOF-MS with a 1 m flight path maintained at 5 x 10^{-8} Torr (Figure 1.5). All collision cross section measurements were made using MALDI

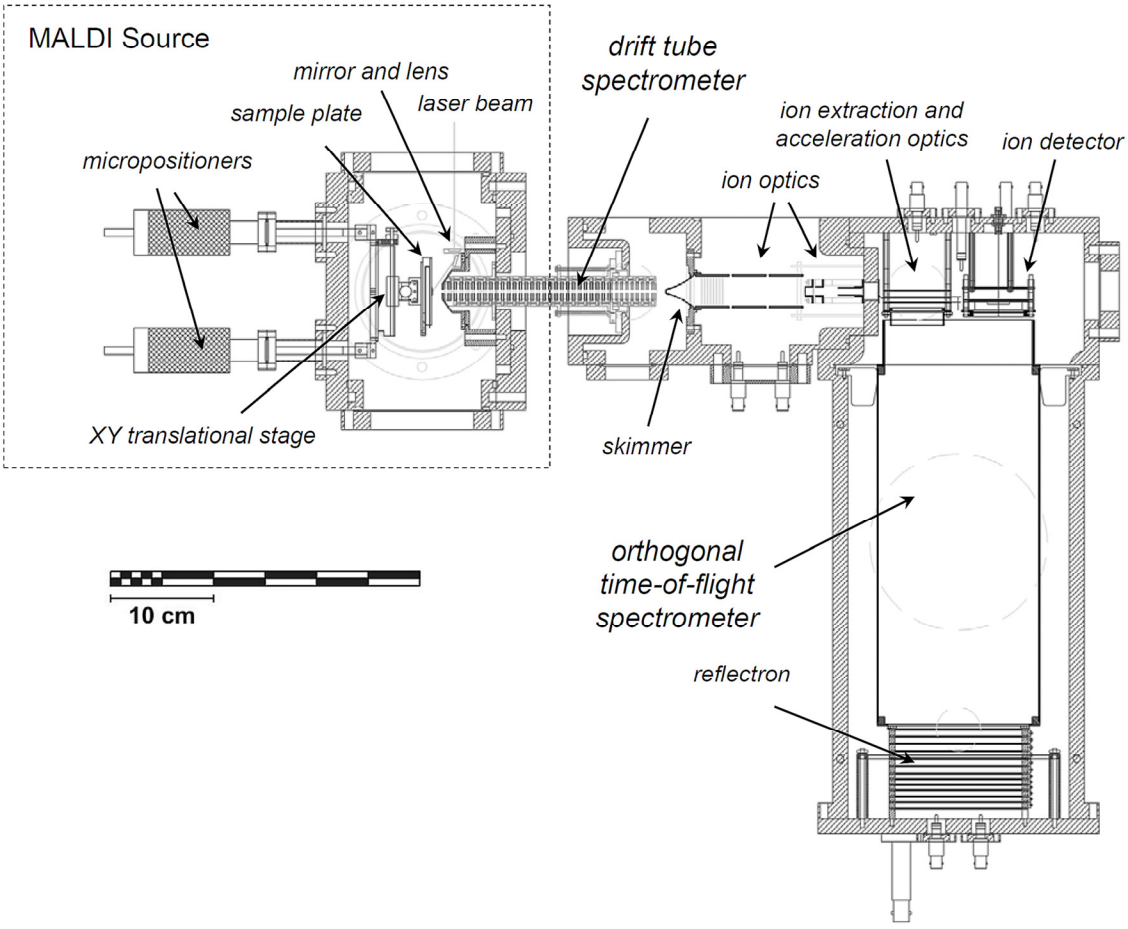

Figure 1.5 Schematic diagram of the MALDI-DTIM-TOFMS instrument used for absolute collision cross section measurements.[73]

which was performed using a high pulse repetition frequency Nd:YLF (frequency tripled, 349 nm) laser (Spectra-Physics, Mountain View, CA) operated at 300 Hz. Mass calibration of the instrument was performed externally using a mixture of C_{60} (720.0 amu) and C_{70} (840.0 amu), which was chosen due to the differing mobility-mass relationship when compared to peptides. Mobility resolution in the DTIM is typically >30 ($r=t/\Delta t$ at FWHM).

1.2.2.2 Traveling wave ion mobility

The recent commercial availability of traveling wave ion mobility (TWIM) instrumentation (Synapt HDMS, Waters Corp., Figure 1.6) has made IM-MS accessible to a large number of users. Similar to drift tube instruments, TWIM separates ions by time dispersion through collisions with a background buffer gas, but in contrast, it uses electrodynamic fields rather than electrostatic fields.[61,74] This is accomplished by transmitting voltage pulses sequentially across a stack of ring electrodes, which creates the travelling wave.[75] Conceptually, TWIM separations are performed based on the susceptibility of different ions to the influence of the specific wave characteristics and have been described as the ability of ions to "surf" on waves.[74] Adjustable wave parameters include: travelling wave pulse height, wave velocity, and ramping either of these variables. The Synapt is composed of a MALDI (200 Hz pulse repetition rate) or ESI source, a mass resolving quadrupole, a trapping region for injecting pulses of ions into the TWIM, the TWIM drift cell, an ion transfer region, and an orthogonal TOFMS ($r=m/\Delta m$ at FWHM of >17,500, Figure 1.6). CID can be performed in the

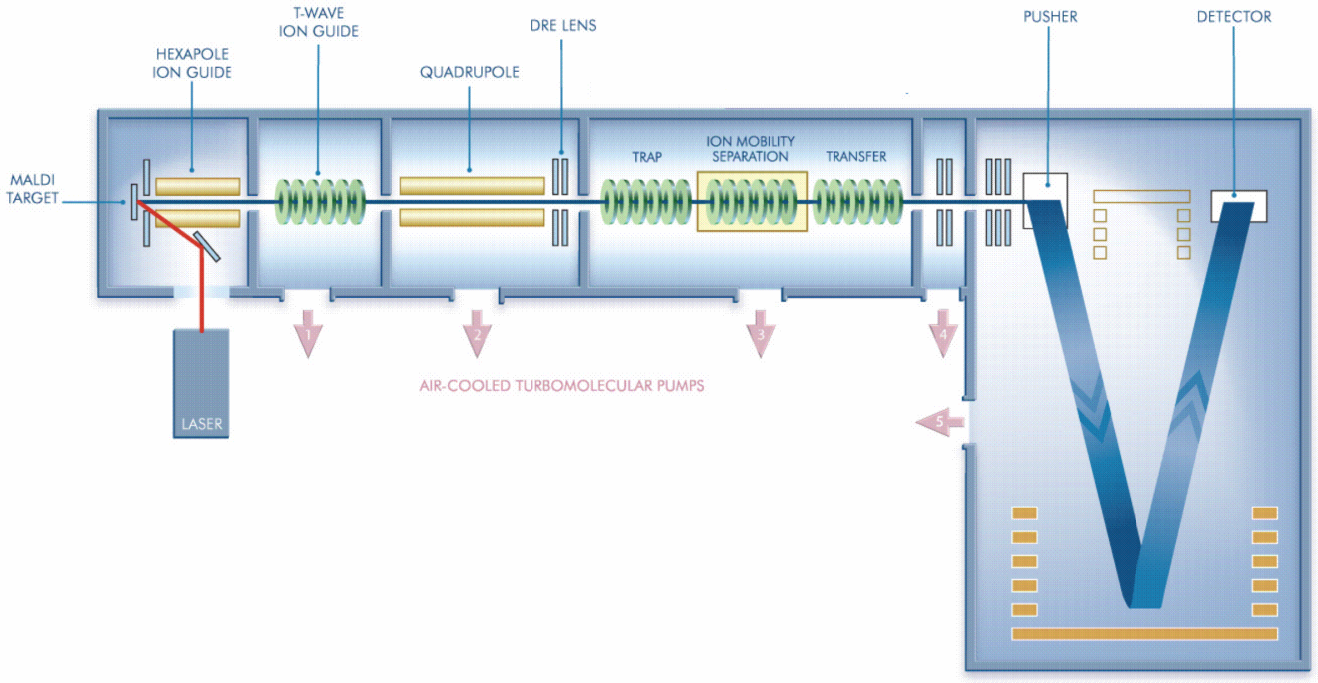

Figure 1.6 Schematic diagram of the MALDI-TWIM-TOFMS instrument (Synapt HDMS, Waters Corp., Manchester, UK).

regions before and after the TWIM drift cell. Generally resolution in the TWIM is <15 ($r=t/\Delta t$ at FWHM), but this is sufficient for the separation of many molecular classes of interest. In addition, an updated version of the instrument (Synapt G2) has been recently released that has improved mobility resolution <40. For example TWIM has been used to separate biomolecular signals from complex samples[76] and to study the structure of peptides following CID in the trapping region.[77] Although protocols have been proposed to approximate collision cross section values using TWIM experimental data, the calculations still rely on absolute values obtained using drift tube instruments.[59,60]

1.2.3 Data interpretation in conformation space

Data analysis in this research was performed using Data Explorer Version 4.3 (Applied Biosystems, Foster City, CA) software for the one-dimensional MALDI-TOFMS spectra and custom software (Ionwerks Inc.) for the two-dimensional MALDI-DTIM-TOFMS, which displays mobility drift time versus *m/z*. For the Synapt HDMS, MassLynx software was used for instrument control and data analysis (Waters Corp., Manchester, UK). All peaks are manually assigned. Instrument settings will be specified for each experiment performed.

Typical data for a 2D IM-MS separation is presented in Figure 1.7 for the separation of lipids and oligonucleotides. Conformation space data [Figure 1.7(a)] is termed such because it represents biomolecular structure, or conformation, as a function of *m/z*. Since IM-MS data is actually three dimensions (IM arrival time distribution, *m/z*, signal intensity) presented in two,

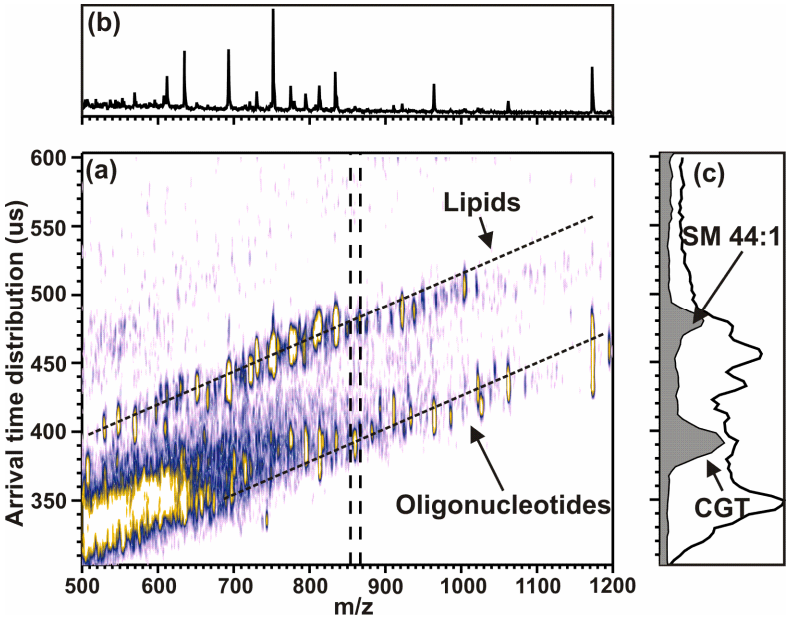

Figure 1.7 (a) IM-MS 2D plot of lipid and oligonucleotide standards show how the variation of the gas-phase packing efficiencies cause the separation of different biomolecules. Two peaks with similar masses were extracted to compare the different mobilities (lipid-[sphingomyelin 44:1+Na]$^+$, 866.7 Da; oligonucleotide- [CGT+H]$^+$, 860.2 Da). (b) The summed mass spectrum for all of the 2D data. (c) *White.* The IM chromatogram for the entire experiment. *Grey.* The IM arrival time distribution for the two selected peaks to demonstrate the separation provided by IM-MS.

the signal intensity is typically projected with false coloring or grey scale to project 3D data in a 2D plot. An integrated mass spectrum over all arrival time distributions is shown in Figure 1.7(b), which is what would be observed in the absence of IM. An integrated IM arrival time distribution is illustrated by the white curve of Figure 1.7(c) which would be obtained by placing the detector directly after the IM drift cell. By plotting the data in 2D conformation space two distinct correlations are observed, one for lipids and one for oligonucleotides, respectively. Note that either extracted mass spectra or arrival time distributions can be derived from conformation space data. For example, an extracted arrival time distribution over the *m/z* range of 860 to 870 is represented by the grey curve in Figure 1.7(c). The latter illustrates baseline resolution for a sodium-coordinated lipid (sphingomyelin 44:1, *m/z* = 866.7 Da) and a protonated oligonucleotide (CGT, *m/z* = 860.2 Da) of nearly the same *m/z*.

Structural interpretation of the experimentally derived collision cross section is afforded through comparing molecular dynamic simulations with these empirically derived values. In contrast with atomic structural resolution afforded by methods such as X-ray crystallography or NMR, IM provides a relatively low resolution structure consistent with the experimental results. However, IM-MS can provide this information for small quantities of sample (*e.g.* < ng) for many analytes directly from complex mixtures. Structural information notwithstanding, IM-MS provides extremely rapid 2D gas-phase separations in comparison with condensed-phase separations such as those encountered in LC-MS (μs-ms versus min-hrs, respectively).

1.3 Characterization of Carbohydrates by IM-MS

When this dissertation research commenced, only few studies had used IM-MS for the characterization of carbohydrates.[65,78-82] These include studies aimed at examining short linear oligosaccharides and cyclodextrins and comparing their collision cross sections to those obtained from molecular dynamic simulations.[65,82,83] The next studies examined simple sugars and sugar alcohols using IM-MS combined with HPLC[81] and variations in conformations of hexose complexes with zinc ligands.[80] More recent studies that have been published since I began my research have tried to determine stereochemical information about monomeric or small di- and trisaccharide structures using DTIM,[78,79,84-86] TWIM,[85,87,88] or another type of relative IM known as high-field asymmetric waveform ion mobility spectrometry (FAIMS).[89] N-linked and O-linked glycans removed from glycoproteins have also been characterized by IM-MS from purified samples[90,91] after separation and extensive purification from serum[46] or urine.[76] To date, all of the previous studies had been performed using ESI.

The first glycosylation studies performed by our lab looked at the intact ribonuclease B (RNAse B) protein (Figure 1.8). In the study, which was performed in a top-down approach,[92] the apo-protein without a glycan attached (RNAse A) and the glycoprotein with each of the five known high-mannose

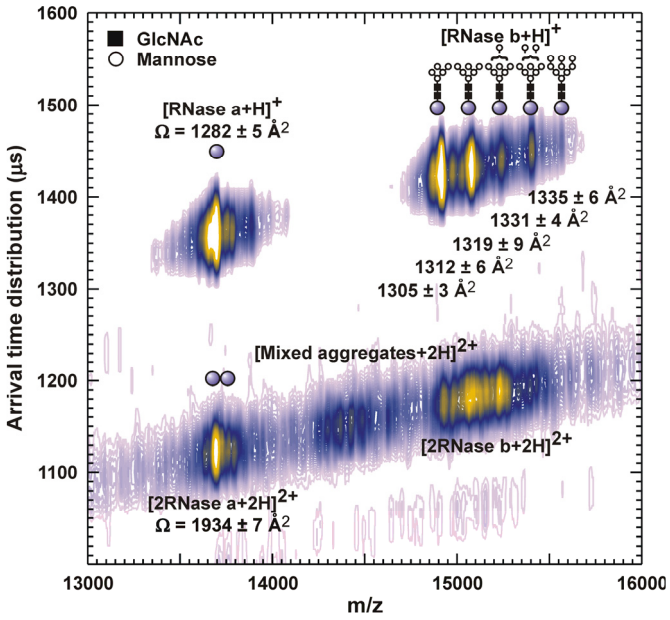

Figure 1.8 IM-MS conformation space for a mixture of ribonuclease A and B (bovine pancreatic). For +1 species, well-resolved signals are observed for individual protein glycoforms corresponding to differences in their pendant Asn-34 N-linked glycan.

glycans were identified. In order to further characterize the protein and attached glycans, additional research was needed in a more comprehensive approach.

1.4 Summary and Objectives

For my dissertation research, I aimed to simplify the analysis of glycoproteins and their associated glycans, specifically N-linked glycans, through the use of IM-MS. Whereas most protocols for the analysis of carbohydrates used derivatization and purification to enhance the ionization efficiency, one of my aims was to simplify this process and analyze the carbohydrates in their native form directly from complex mixtures. Even though this proved challenging, many of the protocols I developed for the characterization of carbohydrates and other associated biomolecules followed this goal. My research also used both ESI and MALDI with IM-MS which allowed the comparison of the two ionization sources for carbohydrate studies. Some of the specific objectives I proposed, and the chapters where each will be addressed, are:

1. Do different biomolecular classes (*i.e.* oligonucleotides, carbohydrates, peptides, and lipids) occupy different regions of conformational space? Can these regions be quantified? This is addressed in Chapter 2: Separation of biomolecular classes in ion mobility-mass spectrometry conformation for the analysis of complex biological samples.

2. Can IM-MS be used to differentiate positional and structural isomers which pose a significant challenge in glycomics? This is addressed in Chapter 3: Structural separations of positional and structural carbohydrate isomers based on gas-phase ion mobility-mass spectrometry.

3. Can IM-MS simultaneously differentiate carbohydrates, peptides, and lipids present in the same sample and in the same mass range? This is addressed in Chapter 4: Simultaneous glycoproteomics and glycolipidomics on the basis of structure using ion mobility-mass spectrometry.

4. Are there ion mobility shift reagents that can be used to further separate carbohydrates from other biomolecules and background present in a sample without the need for purification? Could these ion mobility shift reagents also be used to assist in the ionization of carbohydrates? This is addressed in Chapter 5: Enhanced carbohydrate structural selectivity in ion mobility-mass spectrometry analyses by boronic acid derivatization.

In this dissertation research, the primary goal was to use IM-MS to perform simultaneous glycomics, or separate carbohydrates and glycoconjugates from other biomolecules present in a complex biological sample without the necessity for time-consuming separation and purification. In order to characterize all biomolecules present in a sample, first the area occupied in 2D IM-MS space was determined for each biomolecular class. For carbohydrates, this consisted of creating the first collision cross section database for 303 species from over 3500

measurements. Then, IM-MS was used to separate positional and structural carbohydrate isomers. Since these isomers have the same mass, they cannot be separated using MS alone but were differentiated using IM-MS. These species pose a significant challenge to current glycomics research. After this separation was accomplished, IM-MS was used to perform simultaneous glycomics and separate carbohydrates from peptides and lipids present in complex mixtures such as digests and human milk. All previous IM-MS studies of carbohydrates used purified samples for characterization. This research was bench-marking for future glycomics research using IM-MS and was the first to study carbohydrates using MALDI-IM-MS.

CHAPTER II

SEPARATION OF BIOMOLECULAR CLASSES IN ION MOBILITY-MASS SPECTROMETRY CONFORMATION SPACE FOR THE ANALYSIS OF COMPLEX BIOLOGICAL SAMPLES

2.1 Introduction

Many contemporary biological studies center on broad-scale "omics" characterization of complex biological systems, *e.g.* genomics, glycomics, proteomics, lipidomics, and metabolomics. Typically, such studies are performed separately for each biomolecular class and then combined across classes to derive information about a system as a whole with the ultimate aim of incorporating the data into a systems biology understanding or knowledgebase.[93] Although this reductionist methodology is effective, it may underestimate the intricate relationships of the integrated processes.[94-97] For example, when carbohydrates are analyzed separately from their associated glycoconjugates, it can be challenging to assess the interaction between specific moieties and to derive accurate structural information.[5] Although difficult to realize experimentally, all biomolecular classes would ideally be characterized simultaneously to preserve biochemical interdependencies. There are four primary advantages to performing simultaneous "omics" measurements, including: 1) characterizing all biomolecular species simultaneously provides high

throughput and rapid analyses (*i.e.* comprehensive characterization of complex mixtures), 2) the ability to minimize sample losses and sample preparation artifacts from extensive purification procedures (*e.g*. in tissue imaging, characterizing cell exudates, lysates, etc), 3) preserving the biomolecular context, such as that encountered with conjugate species (*e.g.* biomolecular complexes, glycoproteins and glycolipids, etc.), and 4) ability to observe unpredicted biomolecular interdependencies or correlations.

High-throughput separations on the basis of IM-MS have demonstrated great utility in life sciences research due to IM-MS providing gas-phase separations in one dimension on the basis of structure and in a second dimension by mass-to-charge (*m/z*), respectively. Prior studies utilizing IM-MS have focused on the characterization of different biomolecular classes and structural interpretation via computational strategies, for example in the analyses of carbon clusters,[98,99] polymers,[44,100] peptides,[36] proteins,[101,102] carbohydrates,[65] and oligonucleotides.[103] IM-MS has more recently been used for the characterization of massive protein complexes,[54] imaging directly from thin tissue sections,[55,56] and performing comprehensive proteomics through combining LC-ESI-IM-MS.[47-49] Importantly, because IM-MS provides separations on the basis of structure, different biomolecular classes can be readily distinguished based on differences in their gas-phase packing efficiencies: lipids < peptides < carbohydrates < nucleotides. In the analysis of complex samples this results in the separation of chemical noise from the analytes of interest, *e.g*. the separation of isobaric non-peptidic signals from peptides in proteomics, which

results in enhanced signal-to-noise for peptide signals and higher confidence level protein identification. However, this also affords the possibility of performing simultaneous “omics” or combining the characterization of carbohydrates (*i.e.* glycomics), peptides (*i.e.* proteomics), lipids (*i.e.* lipidomics), etc., into a single analysis.

This thesis focuses on quantifying the conformation space, or structure versus mass space, occupied by different biomolecular classes. This was explored by characterizing the conformation space occupied by a suite of biologically relevant species corresponding to oligonucleotides, carbohydrates, lipids, and peptides. A statistical treatment of the data delineates where specific signals are predicted to occur and the breadth of where signals are expected about the specific structure versus mass correlation. To illustrate the information contained in the fine structure of these correlations, an example of using structural data combined with molecular dynamics simulations is provided for isobaric oligonucleotide tetramers.

2.2 Experimental

2.2.1 Samples and Preparation

2.2.1.1 Oligonucleotides

All oligonucleotide standards, matrix (2,4,6-trihydroxyacetophenone, THAP), and ammonium citrate were purchased from Sigma (St. Louis, MO) and used without further purification. Oligonucleotide standards (1 μM) were initially

dissolved in DDW (18 MΩ cm, Millipore). Matrix solutions were prepared fresh daily by mixing 50 mg/mL THAP and 50mg/mL ammonium citrate at a 9:1 ratio (v/v) in DDW. Samples were then prepared for MALDI by mixing 10 μL (10 nmol) of oligonucleotide solution with 30 μL (10,000 nmol) matrix solution. An aliquot of 3 μL of the mixture was then spotted onto a MALDI plate and vacuum-dried prior to MALDI-IM-MS analysis.

2.2.1.2 Carbohydrates

Lacto-N-fucopentaoses 1 (LNFP1) and LNFP2 from human milk were obtained from Dextra Laboratories (Reading, UK) and LNFP3, LNFP5, Lacto-N-difucohexaose 1 (LNDFH1), and LNDFH2 were obtained from V Labs, Inc. (Covington, LA). Synthetic glycans, Galα3-type1, P1, H-type2-LN-LN, P1 antigen, Di-Le^{A}, P1 penta, LNT, Lec-Lec, Tri-LacNAc, GNLNLN, and 3'SLN-Lec were obtained through the Carbohydrate Synthesis/Protein Expression Core of The Consortium for Functional Glycomics (CFG). 2,5-Dihydroxybenzoic acid (DHB), NaCl, and all other reagents were purchased from Sigma and used without further purification. The matrix used for MALDI-IM-TOFMS was saturated DHB in 50% ethanol. The matrix and analyte were combined in a 1:1 volume ratio (or 200:1 molar ratio). NaCl was added to make a final concentration of 0.1% for purposes of converting all signals to those corresponding to sodium-coordinated ions. The samples were prepared using the dried droplet method.[104]

2.2.1.3 Lipids

Five lipid extracts in powder form, two sphingolipids - sphingomyelins (SM, porcine brain), cerebrosides (CB, porcine brain) and three phospholipids - phosphatidylcholines (PC, chicken egg), phosphatidylserines (PS, porcine brain), phosphatidylethanolamines (PE, chicken egg), were obtained from Avanti Lipids, Inc. (Birmingham, AL). Each of these extracts were individually dissolved in a 2:1 v/v $CHCl_3$:MeOH mixture to yield 2 mM solutions. DHB was dissolved in 50% ethanol to yield a 200mM solution. The individual lipid extracts were premixed with DHB matrix solution in a 1:10 ratio (v/v) and manually spotted onto a 100 well steel MALDI plate and flash evaporated under vacuum.[104] Identification of lipid species was aided by information available from Avanti Lipids Inc., the LIPIDMAPS database,[105] and previously published identification of MALDI lipid spectra.[106]

2.2.2 Instrumentation

MALDI-DTIM-TOFMS measurements for collision cross section calculations were performed with the instrument as described in Chapter I, Section 1.2.2.1. To confirm the identities of various signals a MALDI–TOFMS (Voyager DE-STR, Applied Biosystems, Foster City, CA), operated in reflectron mode and a MALDI–TOF/TOFMS (Ultraflex III, Bruker Daltonics, Inc., Billerica, MA), operated in reflectron mode with a Smartbeam frequency-tripled Nd:YLF (349nm) 200 Hz laser were used to obtain high mass accuracy parent ion signals and MS/MS fragmentation data, respectively.

2.2.3 Molecular Dynamics Simulations

Computer structures of oligonucleotide tetramers were built in LEaP, from the Amber 9.0[107] suite of programs. Quantum mechanical (QM) minimization and electrostatic potential calculations were performed using Gaussian 2003.[108] Electrostatic potential output results of the QM minimized structures were used for atom point-charge parameterization in the molecular dynamics using the RESP (restrained electrostatic potential) algorithm.[109] Molecular dynamics were further performed in Sander (Amber 9.0). Protonated phosphate parameters not available in Amber 9.0 were derived using the molecular dynamics parameters published by Cornell et al.[110] Mobcal[98,99] was utilized to determine the collision cross section of oligonucleotide structures generated from molecular dynamics runs. The energy information obtained from molecular dynamics and the collision cross-section information produced by Mobcal were combined and low energy structures whose collision cross-section matched the experimental value were chosen for cluster analysis. Superposition and clustering programs available and partially developed at the Vanderbilt Center for Structural Biology were used to separate structures into clusters based on conformational similarity.[111,112]

2.3 Results and Discussion

Studies to date have predominately focused on the utility of IM-MS analyses of isolated molecular classes, such as those encountered in

proteomics,[49,113-116] glycomics,[46] and metabolomics.[117] The aim of this work is combining such studies in a common platform for performing integrated "omics" research. Prior research using IM-MS for the structural characterization of carbohydrates were discussed in Chapter I. For oligonucleotides and DNA, previous studies involved short single stranded (ss) oligonucleotides,[103,118] short DNA duplexes and helix stability,[119,120] DNA-metal coordination,[121] and the thermodynamics of G-quadruplex formation.[122-125] However, the preponderance of biological IM-MS research has focused on the study of peptide and protein ion structure.[49,113-116] For example, research has centered on the characterization of peptide and protein misfolding diseases, such as those implicated in Alzheimer's and Parkinson's diseases.[126-128] Furthermore, IM-MS studies on the retention of peptide secondary structure[62-64,129] and characterization of peptide post-translational modifications,[33,67,130] have been described. Relatedly, lipids have been characterized through the use of profiling and imaging IM-MS of brain lipids (human and rat),[55,56,131] and have been shown to have the least gas phase packing efficiency of all previously studied biomolecules, allowing reliable separation of their signals from peptides and other biomolecular signals.[132]

In accumulating a wide collection of the collision cross section versus *m/z* values for these isolated class systems, it has been observed that each individual biomolecular class, such as oligonucleotides, carbohydrates, peptides, and lipids, occupy a distinct region in the two-dimensional IM-MS plot also referred to as conformational space (*i.e.* arrival time distribution versus *m/z*). Understanding the positions and spread of these specific regions should give insights to predictive

capabilities that would be utilized for rapid molecular class identification of an unknown signal depending on its position in conformation space. Towards this aim, we have generated a large dataset (*ca*. 100, 200, and 60 for oligonucleotides, carbohydrates, and lipids, respectively) of the collision cross sections obtained for singly-charged species of standard materials in each molecular class. Details of how these collision cross sections were calculated is presented in Chapter I, Section 1.2.1. These data are then combined with previously reported values for singly-charged peptide species (*ca.* 600).[68] A summary of this data is illustrated in Figure 2.1 [See Appendix A, Tables A.1 (carbohydrates), A.2 (oligonucleotides) and A.3 (lipids) for numerical data]. Complementary to previous reports for a limited number of analytes[61,132] the different molecular classes clearly occupy different regions of conformation space over the *m/z* range of 200 to 2000, which is commensurate with what is typically used in omics measurements. The relative collision cross sections at a particular *m/z* increase in the order of oligonucleotides<carbohydrates<peptides <lipids. The positions where particular signals occur depend on the prevailing intramolecular folding forces for the particular molecular class. The distinct separation of signals therefore indicates that the average packing density, or gas-phase packing efficiency, differs for each class. It is important to recognize that for a specific average density, surface area (*i.e.* collision cross section) scales as length-squared and mass scales as length-cubed. At the limit of high mass, the incremental increase in collision cross section resulting from further increase in mass should approach zero at a decreasing rate. Mathematically, this

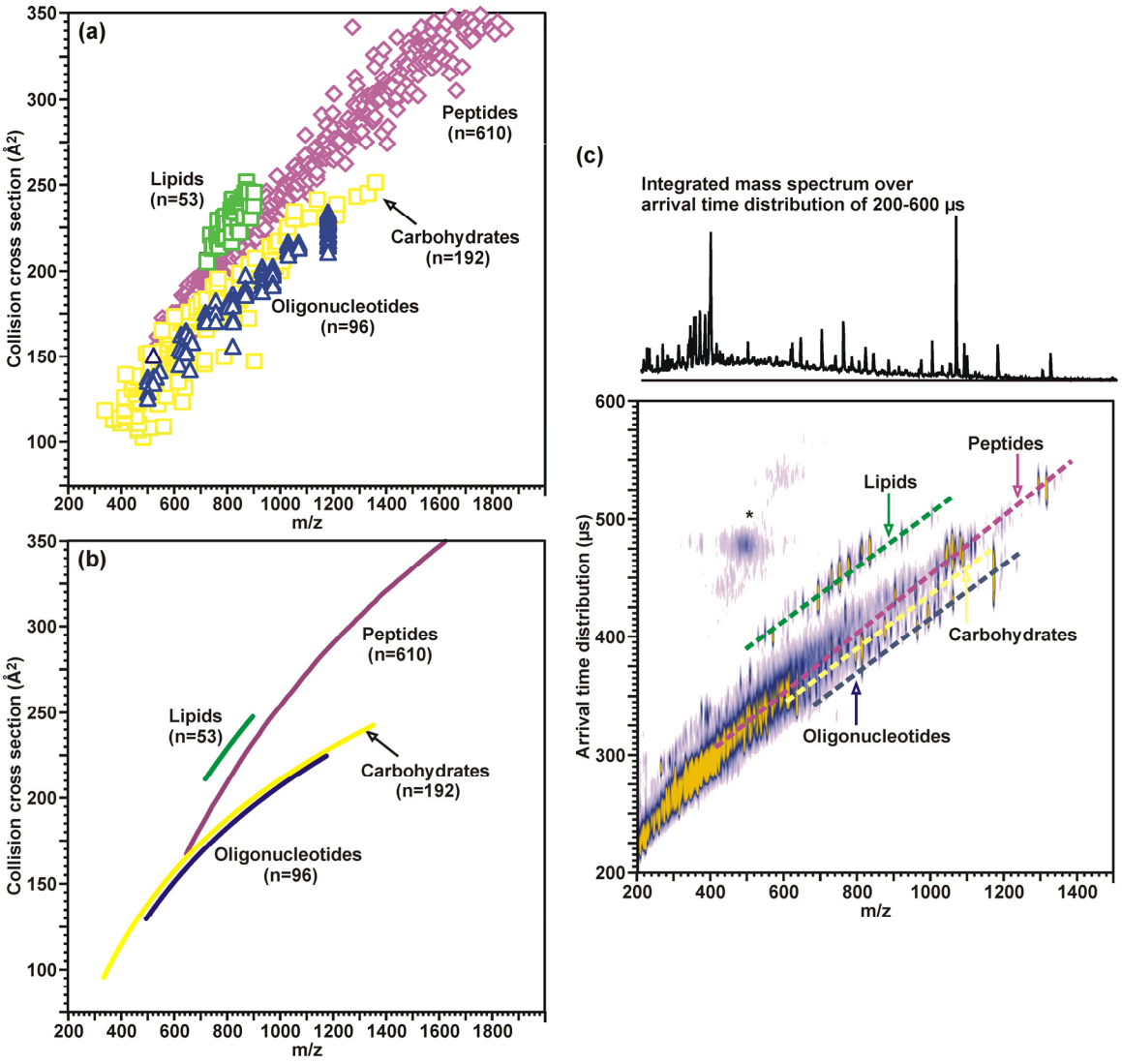

Figure 2.1 (a) A plot of collision cross section as a function of *m/z* for different biologically-relevant molecular classes, including: oligonucleotides (n = 96), carbohydrates (n = 192), peptides (n = 610), and lipids (n = 53). All species correspond to singly-charged ions generated by using MALDI, where error ±1σ is generally within the data point. Values for peptides species are obtained from a previous study.[68] (b) A plot of the average collision cross section versus *m/z* fitted to logarithmic regressions for the data corresponding to each molecular class. The specific equations for each class are: oligonucleotides y = 107.45 ln(x) - 535.34 (R^2 = 0.96), peptides y = 197.4 ln(x) - 1109.8 (R^2 = 0.96), carbohydrates y = 103.7 ln(x) - 507.22 (R^2 = 0.83), and lipids y = 164.59 ln(x) - 871.44 (R^2 = 0.70), respectively. (c) A plot of MALDI-IM-MS conformation space obtained for a mixture of model species representing each molecular class (ranging from 7 to 17 model species for each class, spanning a range of masses up to 1500 Da). Dashed-lines are for visualization purposes of where each molecular class occurs in conformation space. Signals in the vicinity of the asterisk arise from limited post-IM fragmentation of the parent ion species. With kind permission

Figure 2.1—cont. from Springer Science+Business Media: *Analytical and Bioanalytical Chemistry*, "Characterizing Ion Mobility-Mass Spectrometry (IM-MS) Conformation Space for the Analysis of Complex Biological Samples," 394, 2009, 235-244, L.S. Fenn, M. Kliman, A. Mahsut, S.R. Zhao, J.A. McLean, Figure 1.

behavior is best modeled and approximated with collision cross section as a logarithmic function of *m/z*. The average correlation for each dataset is shown in Figure 2.1(b) for clarity. Representative arrival time distribution (ATD) IM-MS spectra obtained for model species of all four classes is shown in Figure 2.1(c).

The distribution of cross section values about each of the average correlations is presented in Figure 2.2. Previous studies examining the peak capacity of conformation space for peptides (separated in He) exhibited a residual deviation from a linear regression with ±1σ of *ca*. 2.5%.[133] In contrast, residuals from a logarithmic regression of *ca.* 600 peptide signals used in this work resulted in a relative deviation of 7.33% (±1σ). A similar treatment of oligonucleotide, carbohydrate, and lipid signals resulted in deviations of 3.70, 8.81, and 2.64%, respectively. A relative ordering of these classes on the basis of increasing breadth of conformation space occupied is, therefore, lipids < oligonucleotides < peptides < carbohydrates. To rationalize the gross separation of these molecular classes, a basic examination of the compositional nature of each species is likely sufficient. For example, the narrowness of the lipid distribution may arise from the limited size of the dataset; however, the structural simplicity of the lipids examined (*i.e*. all possessing two relatively larger fatty acid moieties and a relatively smaller head group) naturally limits the distinct structural forms that the samples are able to adopt. Likewise, the narrowness of

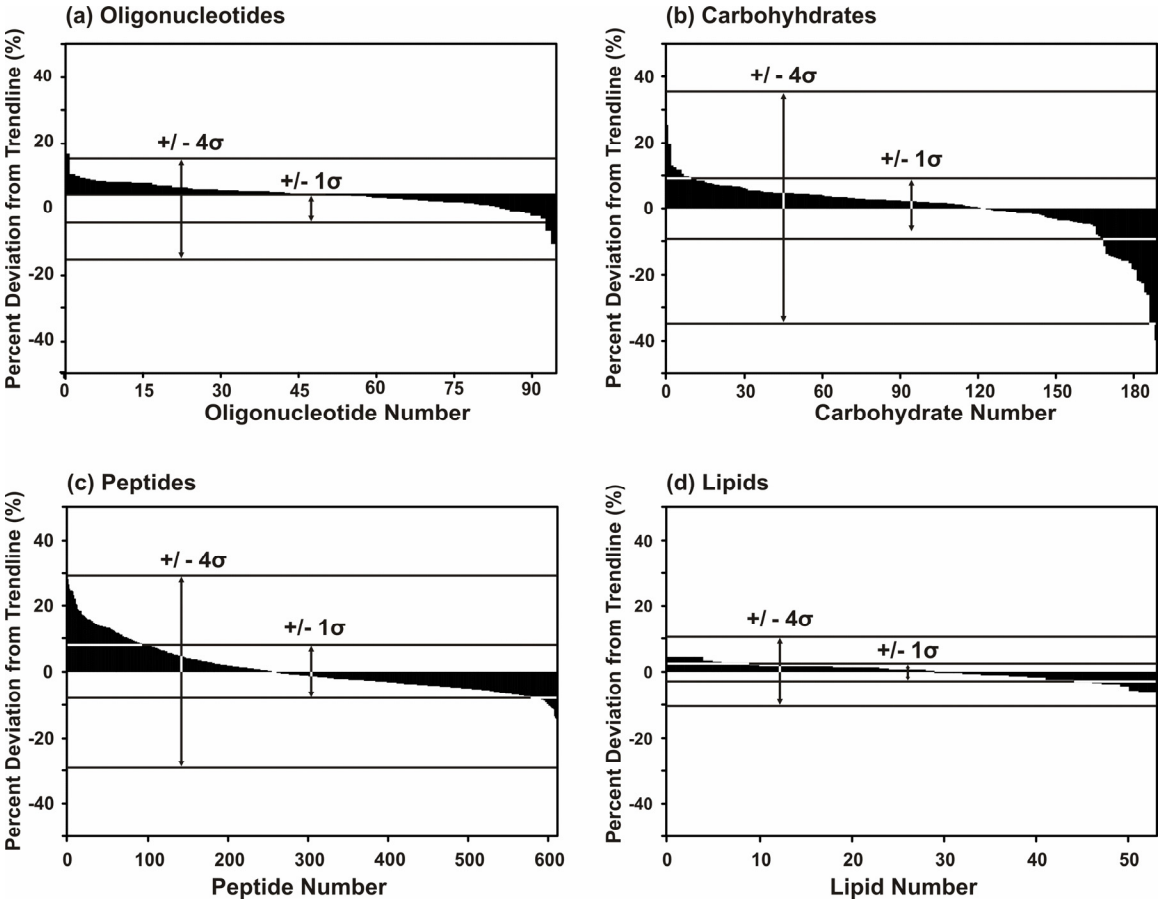

Figure 2.2 Residual plots of each molecular class for the data shown in Fig. 2.1(a), about the logarithmic regressions provided in Fig. 2.1(b). These plots illustrate the percent relative deviation (±) for all of the species reported. The abscissa axis is ordered by descending values of percent relative deviation. The calculated values of σ indicated in each of the plots are (a) 3.70, (b) 8.81, (c) 7.33, and (d) 2.64, respectively. With kind permission from Springer Science+Business Media: *Analytical and Bioanalytical Chemistry*, "Characterizing Ion Mobility-Mass Spectrometry (IM-MS) Conformation Space for the Analysis of Complex Biological Samples," 394, 2009, 235-244, L.S. Fenn, M. Kliman, A. Mahsut, S.R. Zhao, J.A. McLean, Figure 2.

oligonucleotide conformation space can be attributed to these molecules being made of a linear polymer with the potential ordering of a limited number (four) of monomeric units. In contrast, peptides and carbohydrates have potentially higher structural diversity arising from the larger number of monomeric units and the potential for significant branching. However, from a fundamental biophysical perspective, it is well understood that the prevailing intramolecular folding forces are what dictate the structural diversity observed for specific species (*i.e*. relative deviations within a specific class). Therefore, to better understand the structural diversities of a particular molecular class, in-depth molecular modeling studies to complement these data must be performed to assess the relative magnitude of the prevailing folding forces (*e.g.* van der Waals interactions, hydrogen bonding, π-π interactions, etc.), which are likely quite different both among and within classes, depending on the chemical composition of the molecule.

Figure 2.3 illustrates the residuals from each of the regressions grouped as histograms, to evaluate the distribution profiles. The two species with the smallest number of samples, oligonucleotides and lipids, appear to have more Gaussian distributions and exhibit the narrowest profiles. Conversely, the broadest profiles are observed for peptides and carbohydrates. Carbohydrates exhibit a larger number of signals of low collision cross section at small m/z values (i.e. 300-800 Da), which result in weighting of a larger number of signals with relatively large negative deviations. Similarly, there is a weighting bias for positive relative deviations in the distribution profile of peptides, *i.e.,* a greater

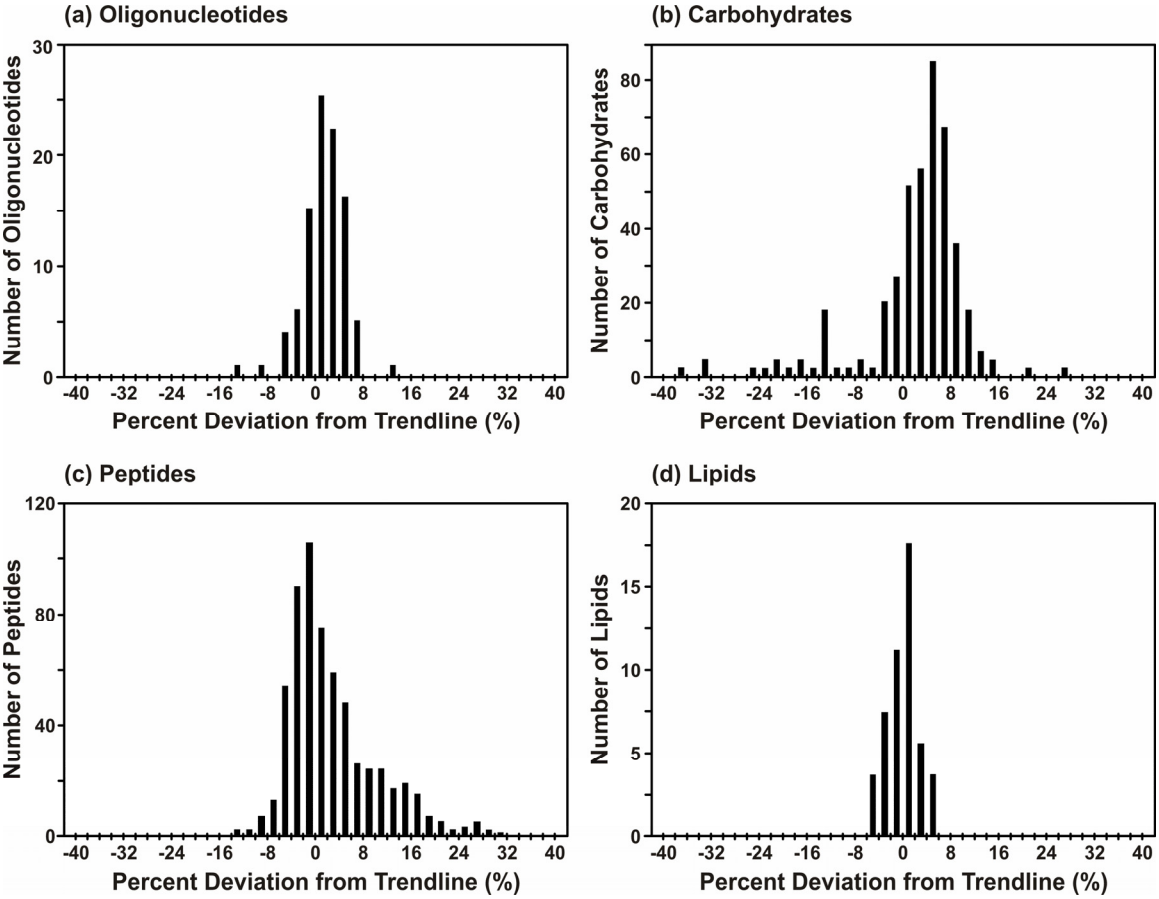

Figure 2.3 Histogram plots of the appearance frequency of analyte signals as a function of the percent relative deviation from the logarithmic regressions for each molecular class provided in Figure 2.1. With kind permission from Springer Science+Business Media: *Analytical and Bioanalytical Chemistry*, "Characterizing Ion Mobility-Mass Spectrometry (IM-MS) Conformation Space for the Analysis of Complex Biological Samples," 394, 2009, 235-244, L.S. Fenn, M. Kliman, A. Mahsut, S.R. Zhao, J.A. McLean, Figure 3.

number of peptides occur above the regression line in the lower m/z range (300-

700 Da). Thus although theoretically a logarithmic regression is most

appropriate, it overestimates the relative frequency of signals positively deviating from the average correlation for signals in the low *m/z* range. Fitting of this data to a polynomial expression results in more Gaussian histograms, but fails to capture the theoretical limit of surface area with increasing mass.

Although this data describes the regions of conformation space occupied for the molecular classes presented, caution should be exercised when applying this treatment to biomolecular signals outside the mass range presented. The regression lines are derived only for the range of *m/z* investigated. Thus, correlations presented can only be extrapolated beyond the limits of this study (<~2kDa) with caution. Currently, there is a lack of experimental data for the transition region from peptides to well ordered protein complexes (from 3kDa<*m/z*<200kDa). Therefore the difference between, for example, peptides (< 3kDa *m/z*) and well-ordered massive protein complexes (>200 kDa *m/z*) has yet to be characterized. It is unclear at this juncture how conformation space appears in this transition region.

Nevertheless, the correlations presented for each molecular class in Figures 2.1-2.3 provide a guide to characterize unknown signals in the analysis of complex biological samples. Although the histograms in Figure 2.3 suggest approximately normal distributions of signals centered about the average correlation, it is important to recognize that specific structural deviations within each class (e.g. retained secondary structure in peptides,[62-64,129] branching ratio and glycosidic linkage variation in carbohydrates,[46,117] backbone and headgroup differences in lipids, etc.) give rise to complex probability distribution profiles. For

example, there exist many examples of using IM-MS for separations of isomeric and/or isobaric species. To illustrate the complexity that can arise in the probability distribution profiles, Figure 2.4 shows the separation of two oligonucleotides composed of the same four bases, but of permuted sequence (*i.e*. CGAT and TGCA). Although the ion species are isobaric, they are nearly baseline resolved on the basis of structure in the collision cross section profile [Figure 2.4(a)]. As indicated in Figure 2.4(b), the average structures that these individual species preferentially adopt are strikingly different, *i.e*. CGAT adopts a more compact structure dominated by base-stacking, while the structure for TGCA is more extended with extensive hydrogen bonding. For each species *ca.* 21,000 structures were obtained that resulted in 666 and 1405 low-energy structures that correspond to within ± 2.5 $Å^2$ of the measured collision cross section for CGAT and TGCA, respectively. Then, a RMS analysis of the low-energy structures was used to determine the most representative structure which is shown in Figure 2.4(b). Thus, although this study delineates the expected region in which particular signals are predicted to occur, fine structure within these correlations provides a further level of information that can be used. Studies aimed at elucidating specific compositional motifs that give rise to distinct fine structure in conformation space are presently underway in our laboratories.

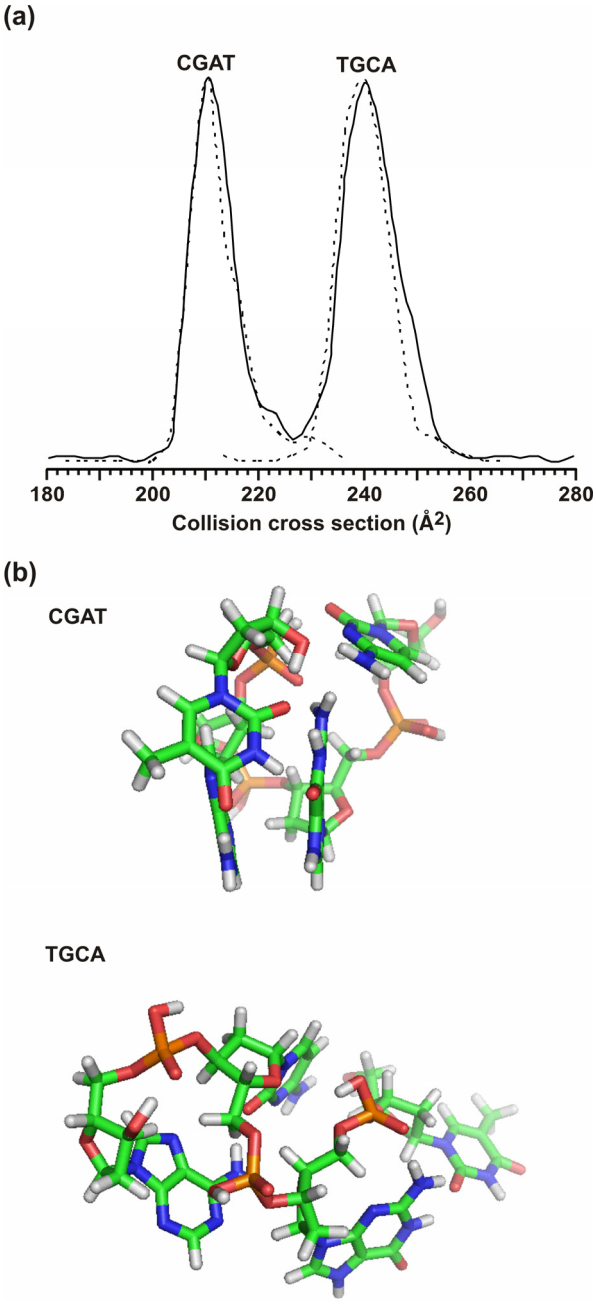

Figure 2.4 (a) A plot of the collision cross section profile obtained in the separation of a mixture of two isobaric tetranucleotide species: CGAT and TGCA, respectively ($[M+H]^+$ = 1174.3). The solid line corresponds to a mixture of the two components. Dashed-lines correspond to collision cross section profiles obtained for each ssDNA species analyzed separately with signal intensity normalized to the height of the major feature in the profile for the mixture. (b) Molecular dynamics simulations for each of the two ssDNA species. With kind permission from Springer Science+Business Media: *Analytical and Bioanalytical Chemistry*, "Characterizing Ion Mobility-Mass Spectrometry (IM-MS) Conformation Space for

Figure 2.4—cont. the Analysis of Complex Biological Samples," 394, 2009, 235-244, L.S. Fenn, M. Kliman, A. Mahsut, S.R. Zhao, J.A. McLean, Figure 4.

2.4 Conclusions

The data presented in this chapter allows for a broad view of the conformational landscape for different classes of biomolecules. This provides a general metric for assigning signals to particular molecular classes based on where the unknown signals occur in conformation space. Further understanding of the fine structures within conformation space might be achieved through utilizing computational strategies, such as molecular dynamics, to predict where sub-class populations would appear. These sub-class separations could be due to post-translational modifications to peptides, retained secondary structure, preferential folding owing to metal coordination, etc. The characterization of conformation space for complex biological samples opens new avenues for life sciences research, such as rapid and integrated "omics" analysis necessary for the advancement of fields such as systems biology.

2.5 Acknowledgements

I would like to acknowledge Sophie Zhao and Ablatt Mahsutt for the oligonucleotide work and Michal Kliman for the lipid and computational analyses.

CHAPTER III

STRUCTURAL RESOLUTION OF POSITIONAL AND STRUCTURAL CARBOHYDRATE ISOMERS BASED ON GAS-PHASE ION MOBILITY-MASS SPECTROMETRY

3.1 Introduction

This study describes the rapid characterization of positional and structural carbohydrate isomers based on structural separations provided by ion mobility-mass spectrometry (IM-MS). To chart the structural variation observed in IM-MS, the ion-neutral collision cross sections for over 300 carbohydrates are reported. This diversity can also be varied through the utility of using different alkali metals to tune separation selectivity via alkali metal-carbohydrate coordination. Furthermore, the advantages of combining either pre- and/or post-IM fragmentation prior to MS analysis is demonstrated for enhanced confidence in carbohydrate identification.

The characterization of glycans using mass spectrometry (MS) techniques is challenging due to the potential for isobaric glycan isomers that increases with higher numbers of carbohydrate monomers. Even with the addition of HPLC to MS and MS^n, a high-throughput and less time-consuming methodology for carbohydrate structure elucidation is desired. We applied gas-phase ion mobility-mass spectrometry (IM-MS) to the study of

carbohydrates with particular attention to 3 sets of isomers, both positional and structural.

In this report we examine the utility of IM-MS for the separation of isobaric positional and strucutral isomers. Benchmarking studies were first performed for a large series of carbohydrate standards by determining their collision cross sections and the collision cross sections of in-source decay fragments. A total of over 300 carbohydrate collision cross sections are reported. Studies were then focused on a series of positional and structural carbohydrate isomers, the utility of utilizing different alkali metals to vary carbohydrate collision cross section, and the utility of increasing confidence in carbohydrate characterization through in-source fragmentation.

3.2 Experimental

3.2.1 Samples and preparation

Synthetic glycans, Galβ1-4GlcNAcβ-Sp (LacNAc), Galβ1-3GlcNAcβ-Sp (Le^c), Galβ1-4Glcβ-Sp (Lac), Galα1-3[Fucα1-2]Galβ1-3GlcNAcβ-Sp (B tetra type 1), Galα1-3[Fucα1-2]Galβ1-4[Fucα1-3]GlcNAcβ-Sp (2'F-B type 2), Galβ1-3[Fucα1-4]GalNAcβ1-3Galβ1-4[Fucα1-3]GlcNAcβ-Sp (Le^ALe^x), Galβ1-3[Fucα1-4]GlcNAcβ1-3Galβ1-3[Fucα1-4]GlcNAcβ-Sp (Di-Le^A), Galβ1-4GlcNAcβ1-3Galβ1-4Glcβ-Sp (LNnT), Galα1-3Galβ1-4GlcNAcβ-Sp (B2-tri), Galα1-4Galβ1-4Glcβ-Sp (Pk), $(Galβ1\text{-}4GlcNAcβ1\text{-}3)_3β$-Sp (Tri-LacNAc), $Fucα1\text{-}2(Galβ1\text{-}4GlcNAcβ1\text{-}3)_3β$ -Sp (H-type2-LN-LN), Galb1-3GalNAcβ1-3Galα1-4Galβ1-4GlcNAcβ-Sp (P1

penta), Galα1-4Galβ1-4GlcNAcβ1-3Galβ1-4Glcβ-Sp (P1 antigen), GlcNAcβ1-3(Galβ1-4GlcNAcβ1-3)$_2$β-Sp (GNLNLN), Neu5Acα2-3Galβ1-4GlcNAcβ1-3Galβ1-3GlcNAcβ-Sp (3'SLN-Lec), Galα1-3Galβ1-3GlcNAcβ-Sp [Galα3-type1(1)], Galα1-4Galβ1-4GlcNAcβ-Sp [P1 tri (2)], Galβ1-3GlcNAcβ1-3Galβ1-4GlcNAcβ-Sp [LNT (3)], and Galβ1-3GlcNAcβ1-3Galβ1-3GlcNAcβ-Sp [Di-Le^c (4)] were obtained through the Carbohydrate Synthesis/Protein Expression Core of The Consortium for Functional Glycomics (Sp was an azide spacer not used in current studies). Fucα1-2Galβ1-3GlcNAcβ1-3Galβ1-4Glc [Lacto-*N*-fucopentaose (LNFP) 1 (5)] and Galβ1-3[Fucα1-4]GlcNAcβ1-3Galβ1-4Glc [LNFP2 (6)] from human milk were obtained from Dextra Laboratories (Reading, UK) and Galβ1-4[Fucα1-3]GlcNAcβ1-3Galβ1-4Glc (LNFP3), Galβ1-3GlcNAcβ1-3Galβ1-4[Fucα1-3]Glc (LNFP5), Fucα1-2Galβ1-3[Fucα1-4]GlcNAcβ1-3Galβ1-4Glc [lacto-*N*-difucohexaose (LNDFH) 1], and Galβ1-3[Fucα1-4]GlcNAcβ1-3Galβ1-4[Fucα1-3]Glc (LNDFH2) from human milk were obtained from V-Labs, Inc. (Covington, LA). Galβ1-4Glc (lactose), Galβ1-4GlcNAc (*N*-acetyl-lactosamine, LN), Glcα1-4Glc (maltose), α-cyclodextrin, β-cyclodextrin, 2,5-dihydroxybenzoic acid (DHB), LiCl, NaCl, KCl, RbCl, and CsCl were purchased from Sigma (St. Louis, MO).

3.2.2 MALDI-IM-TOFMS

Both the MALDI-DTIM-MS and MALDI-TWIM-MS instruments were used in these experiments as described in Chapter I. Fragmentation of the carbohydrates after the IM drift cell was performed on the TWIM-MS. IM was performed using travelling wave separation through nitrogen gas. The ion

guide T-wave was operated at 300 m/s and linearly ramped in amplitude from 5-20 V over each experiment. The Transfer guide T-wave was operated at 248 m/s and with a constant 3 V amplitude. For IM acquisitions with no fragmentation, ion injection voltages into the Trap and Transfer were set at 4 and 6 V, respectively. With fragmentation in the Transfer region, the voltage was set between 25 and 45 V.

To perform MALDI, the sample preparation procedure was the same for both instrumental arrangements. The matrix used was saturated DHB in 50% ethanol. The matrix and analyte were combined in a 1:1 volume ratio (or 200:1 molar ratio) and then spotted on a MALDI stainless steel target and allowed to dry. Note that in contrast with high vacuum MALDI, both of the IM-MS instruments utilized in this work are combined with moderate pressure MALDI. Specifically, on the uniform field instrument MALDI is performed at the pressure of the IM drift cell or 3-5 Torr, while on the travelling wave instrument MALDI is performed at *ca.* 200-300 Torr. This is significant in the analysis of carbohydrates, because following ionization the ions are collisionally cooled, which typically results in less extensive fragmentation than MALDI performed at high vacuum.

3.3 Results and discussion

Clearly the structural information afforded by IM separations coupled with MS provides a key advantage over MS alone. Initial studies were

performed to characterize the conformation space, or region in ion mobility-*m/z* space, in which carbohydrates preferentially occur. This was accomplished using a series of 31 carbohydrate standards ranging from simple disaccarides to branched glycans. Collision cross sections were determined for these carbohydrate standards and carbohydrate fragment species arising from in-source decay. In total this resulted in obtaining collision cross section values for 303 carbohydrates, which are shown in Figure 3.1. Through the determination of the collision cross sections, the region of conformational space (plot of cross section versus *m/z*). Tabulated values for the specific carbohydrates and their associated masses and collision cross sections are provided in Appendix A, Table A.1. In Chapter II, we presented collision cross sections for a smaller suite of 192 carbohydrates. A comparison of the collision cross sections previously reported with those measured in this work reveals minor variations that are largely within measurement error. A distinction between the previously reported values and those in this work are that precision for many species is significantly improved owing to a significantly larger number of measurements. For the 303 carbohydrate species reported, the number of collision cross section measurements for individual species ranges from 4 to 181. The average number of measurements for an individual carbohydrate in this data is *ca.* 12. Thus, the total number of carbohydrate collision cross section measurements in this report is in excess of 3,500 for the data reported herein. From this suite of carbohydrates three pairs of positional and structural isomers were

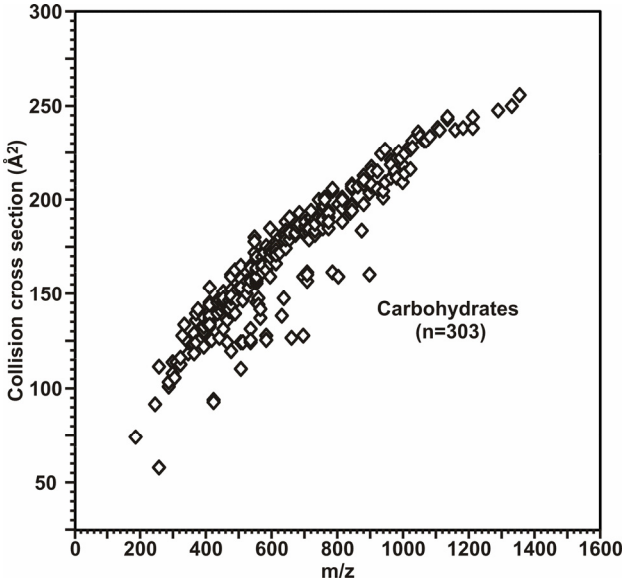

Figure 3.1 A plot of collision cross section as a function of *m/z* for carbohydrates (n = 303). All species correspond to singly-charged species generated by using MALDI, where error ±1σ is within the data point. For identifications of carbohydrates, masses, and associated collision cross sections, see Appendix A, Table A.1.

examined further to determine the utility of IM-MS to separate these types of isobaric isomers.

3.3.1 Characterization of positional and structural carbohydrate isomers

Structures for the positional and structural isomers selected are presented in Figure 3.2, representing trisaccharides to pentaoses. Carbohydrates 1 and 2 both contain the same three monomers but differ in that 1 contains two 1→3 glycosidic linkages whereas 2 has two 1→4 linkages. Carbohydrates 3 and 4 contain the same four monomers, but vary by a difference in only one glycosidic linkage. Specifically, carbohydrate 3 contains three 1→3 glycosidic linkages, while 4 contains two 1→3 and a single 1→4 glycosidic linkage. In contrast with these positional isomers, both carbohydrates 5 and 6 contain the same five monomers and glycosidic linkages between them, with the exception of the placement of a single fucose, from the non-reducing end in 5 to the secondary GlcNAc in 6, resulting in two non-reducing ends and a branching pattern in 6 versus a linear pentaose in 5. Thus, 5 and 6 represent isobaric structural isomers.

3.3.2 Drift time profile comparison

MALDI-IM-MS measurements were taken for all carbohydrates to simultaneously obtain the drift time profile and *m/z* for each species. The drift time for each carbohydrate relates to its structure through the ion-neutral collision cross section. As a result, the drift time was used to differentiate

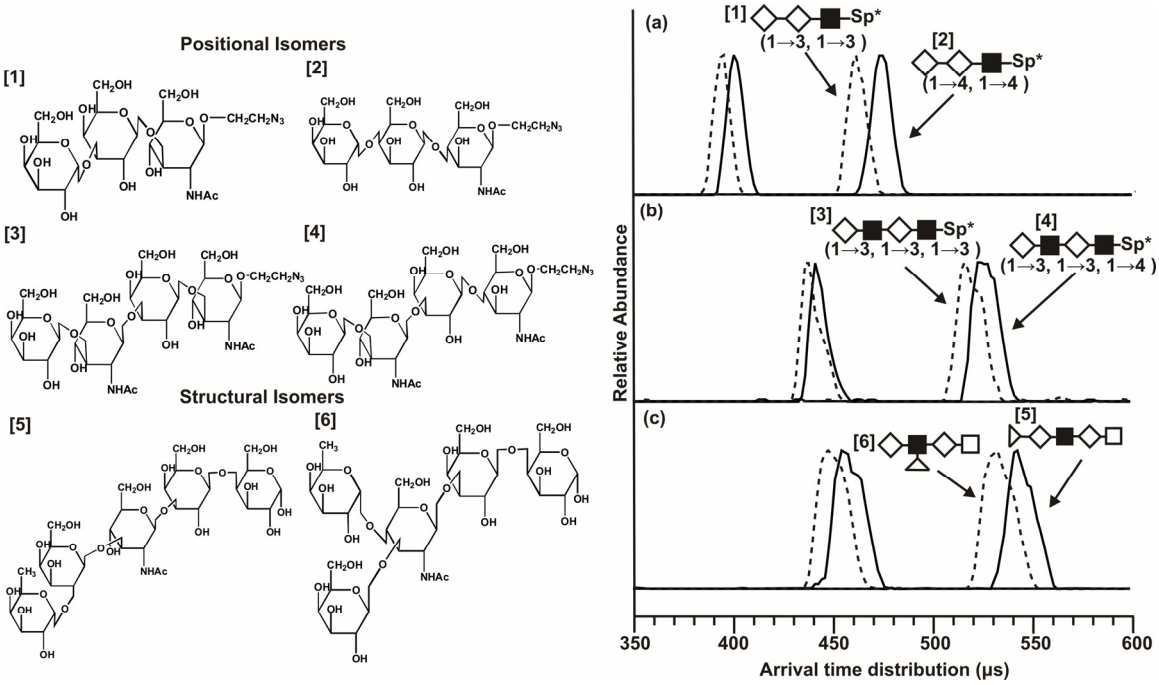

Figure 3.2 Structures of the isobaric sets of positional and structural isomers (*left*) and the associated drift time profiles (*right*). (*Left*) Notice the change in structure from glycans 1 to 2 being accounted to two 1→3 linkages being replaced with 1→4 linkages. Glycans 3 and 4 have one linkage variation, and glycans 5 and 6 (LNFP1 and LNFP2) vary in the location of fucose from galactose to N-acetylglucoseamine. (*Right*) Drift time profiles at lower (*right*- 20.6 volts cm^{-1} Torr) and higher (*left*- 27 volts cm^{-1} Torr) electrostatic field strengths which pull the ions through the ion mobility drift cell. Structures of the oligosaccharides are replaced with shape representations. Drift times are related to the ion structure in that larger, more elongated ions experience more collisions with the neutral buffer gas present in the drift cell causing a longer drift time than more compact structures. (a) In the comparison between glycans 1 (dotted line) and 2 (solid line), the 1→3 linkages of glycan 1 cause it to have a shorter drift time which indicates a more compact structure that glycan 2, which is more elongated or linear. (b) Glycans 3 (dotted line) and 4 (solid line) have differing drift times due to the change in one glycosidic linkage. The 1→3 linkages allow glycan 3 to adopt a compressed conformation when compared to its positional isomer, which has one 1→4 linkage. (c) Drift times for glycans 5 (solid line) and 6 (dotted line), or LNFP1 and LNFP2, respectively, are compared. LNFP2 has a shorter drift time than LNFP1 at both voltages. This can be accounted to the slight branching pattern in LNFP2 that allows the glycan to conform into a more compact structure. Glycan representations are as follows: ◇- galactose; ■-N-acetylglucoseamine; △-fucose; with linkage information below.

isobaric positional and structural isomers that cannot be separated on the basis of mass alone. The drift time profiles for the six carbohydrates were compared at two different electrostatic field strengths (Figure 3.2). At both higher (27 V cm^{-1} Torr) and lower (21 V cm^{-1} Torr) field strengths each set of isobaric isomers exhibited IM separation selectivity. As the electrostatic field strength is decreased, the relative difference between the glycan drift times remained the same while the absolute difference in the drift time increased. Because the resolution is largely unchanged (ca. 35-40), this results in higher resolving power and hence a slightly better separation of the isomer pairs as the field strength is reduced. This is observed as the deeper valley between the two species at longer drift times than at shorter drift times.

In the drift time profiles, the smaller or more compact carbohydrates transversed through the drift cell at a higher velocity, or shorter drift time, than the larger or more elongated carbohydrates. In the drift time profiles for positional isomers (1) and (2), carbohydrate (1) displayed a drift time shorter than that of carbohydrate (2). For the positional isomers (3) and (4), carbohydrate (3) resulted in shorter drift time than that for carbohydrate (4). The commonality between these two isomer pairs is that the carbohydrates containing a higher proportion of 1→3 glycosidic linkages yielded a subsequently more compact structure than the carbohydrates containing 1→4 glycosidic linkages. Therefore, this suggests a relationship between different glycosidic linkages between carbohydrate monomers and the prevailing influence of specific glycosidic bonding on the resulting carbohydrate

structure. In the drift time profiles for the structural isomer carbohydrates (5) and (6), the species containing a site of branching (6) resulted in a more compact structure than that for the linear species (5). All of these ions correspond to sodium-coordinated species. Owing to the oxyphilicity of sodium, the more compact structure for the structural isomer with increased branching is attributed to the ability of the branching flexibility to coordinate more strongly to sodium, which likely resides at the position where branching occurs. This is consistent with the conclusions of Lebrilla and colleagues in tandem MS fragmentation studies of similar carbohydrate species.[134]

It is important to note that the extent of structural selectivity with IM is enhanced when the relative differences between the two species is greatest. For example, the relative IM resolving power is greater for the positional isomers (1) and (2) than it is between isomers (3) and (4), because the magnitude of differences in the glycosidic connectivity is greater. Namely, (1) contains two 1→3 linkages, (2) contains two 1→4 linkages, while (3) and (4) contain three 1→3 linkages and two 1→3 linkages/one 1→4 linkage, respectively. At the present IM resolution, it may be challenging to differentiate small differences in carbohydrates that are greater than *ca.* 1000 *m/z*. This upper limit was increased substantially through the use of higher resolution IM separations. Difference between the glycan drift times stayed the same while the absolute difference in the drift time increased. This accounted for the drift time profiles appearing further apart at the lower field strength.

3.3.3 Collision Cross Section Determination

The drift times for the isomeric carbohydrates were used to calculate their collision cross sections using theory outlined in Chapter I, Section 1.2.1, which relates the drift time to the apparent surface area ($Å^2$). The aforementioned isobaric carbohydrate isomers cannot be differentiated through MS alone, but were separated through the determination of their gas phase collision cross section (Table A.1). For example, the difference in the drift time of the sodium-coordinated ions of (5) and (6), which are used to calculate collision cross section, was experimentally obtained from conformational plots to be 473 and 465 μs respectively at 27 V cm^{-1} Torr (Figure 3.2). This corresponds to a difference in the collision cross sections of the two species of *ca.* 3 $Å^2$ and is likely attributed to the alakli metal coordination with the carbohydrate.

Using the same methodology, the collision cross sections of the positional isomers (1-4) were found to differ from their respective conjugate isomer by *ca.* 6-9 $Å^2$. The magnitude of these differences is significant due to being greater than the cumulative error in the individual cross section values.

3.3.4 Alkali Metal Coordination

Carbohydrates are typically ionized as the sodium-coordinated species, however, all of the alkali metals are strongly oxyphilic. Thus, other alkali metals of differing ionic radii can be used for ionization and can assist in structure stabilization and controlling the extent of fragmentation.[134-138]

Accordingly, we examined the extent of structural selectivity that would be afforded through the use of other alkali metals as the ionizing cation. Other alkali metals are known to affect the folding and conformation of carbohydrates, which would consequently impact the measured collision cross section. This was investigated by adding to the matrix 0.1% of the chloride salts of Li, Na, K, Rb, and Cs to shift the base peak in the spectrum to that of the specific alkali metal coordinated with the carbohydrate.

The carbohydrates (5) and (6) were coordinated to Li, Na, K, Rb, and Cs in separate experiments and analyzed by IM-MS to obtain drift times for each species at different electrostatic field strengths (Figure 3.3, Table 3.1). Collision cross sections varied for these two isomers with the addition of each different alkali metal. The difference in the collision cross section measured between the two isomers, *i.e.* resolving power, are more pronounced upon the addition of Li, Na, and Cs (*ca.* 3-4 $Å^2$) in comparison with those observed for K and Rb coordination. Note however that the absolute change in collision cross section for each isomer across the series of alkali metals is rather small ranging from *ca*. 198-205 $Å^2$ for (5) and *ca*. 197-202 $Å^2$ for (6). There also appears to be anomalous behavior for the two largest ionic radii alkali metals, namely Rb and Cs, in that the collision cross section does not monotonically increase with alkali metal size. This may reflect differences in the preferred coordination of these metals combined with the structural flexibility of the carbohydrate monomers comprising these species. This premise is reinforced by the studies of Lebrilla and colleagues, where they concluded that the minimum number of carbohydrate

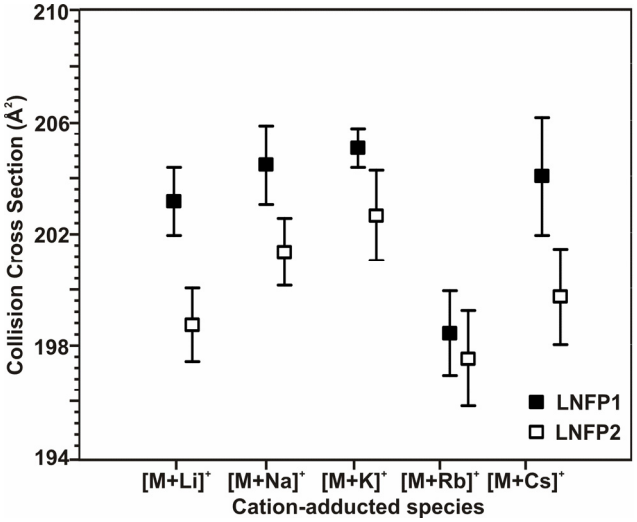

Figure 3.3 Plot of alkali metal-coordinated LNFP1 and LNFP2. 0.1% LiCl, NaCl, KCl, RbCl, or CsCl was added to each glycan before MALDI analysis. Although the two glycans are isobaric, the addition of various metals was investigated to optimize their structural separation. Collision cross section differences for the addition of lithium, sodium, and cesium are more pronounced. Note however than in all cases the collision cross sections are smaller for higher branching ratio glycans. This is like attributed to the metal coordinating with the glycan at the branching site for more efficient intramolecular coordination and subsequently smaller structures. Error bars represent ± 1σ (n ≥ 20) measured over multiple days.

Table 3.1 Carbohydrate collision cross sections with various alkali metal coordination.

Carbohydrate Name	species	*m/z* (Da)	Ω (Å^2)	σ (# of measurements)
LNFP1	$[M+Li]^+$	859.0	203.1	1.2(20)
LNFP2	$[M+Li]^+$	859.0	198.7	1.3(20)
LNFP1	$[M+Na]^+$	875.0	204.4	1.4(162)
LNFP2	$[M+Na]^+$	875.0	201.3	1.2(181)
LNFP1	$[M+K]^+$	891.0	205.0	0.7(23)
LNFP2	$[M+K]^+$	891.0	202.6	1.6(20)
LNFP1	$[M+Rb]^+$	937.5	198.4	1.5(20)
LNFP2	$[M+Rb]^+$	937.5	197.5	1.7(20)
LNFP1	$[M+Cs]^+$	985.0	204.0	2.1(20)
LNFP2	$[M+Cs]^+$	985.0	199.7	1.7(20)

monomers that were necessary to form a full coordination sphere for Rb and Cs was five. This is the same number of monomer units in (5) and (6), such that these species are at the minimum limit to stablize the coordination with these large alkali metals.[134] Further investigations will examine the structure of larger carbohydrates with the coordination to these alkali metals and potentially other cationizing species.

3.3.5 Carbohydrate fragmentation in IM-MS

Carbohydrates are known to fragment readily in MS owing to the labililty of glycosidic linkages. This is mitigated in these experiments through collisional cooling that occurs at moderate pressure MALDI. However, pre- and post-IM fragmentation can provide additional information for carbohydrate characterization. For example, by promoting in-source fragmentation through using elevated laser fluence results in diagnostic peaks in the IM-MS conformation space plot that can be used to confirm the structure of the glycan and also yields collision cross section data for the fragment ion species. In the conformation space plot for (5) and (6), the sodium-coordinated molecular ion was the base peak, followed by additional peaks that are identified as in-source decay products (Figure 3.4). These fragment peaks are labeled according to the nomenclature developed by Domon and Costello and corresponded to previously published CID fragments of (5) and (6).[27] These fragment ions include cleavage across carbohydrate rings (X and A ions) as well as internal fragments (indicated using a / between two fragments).[20] In this particular case, the fragmentation

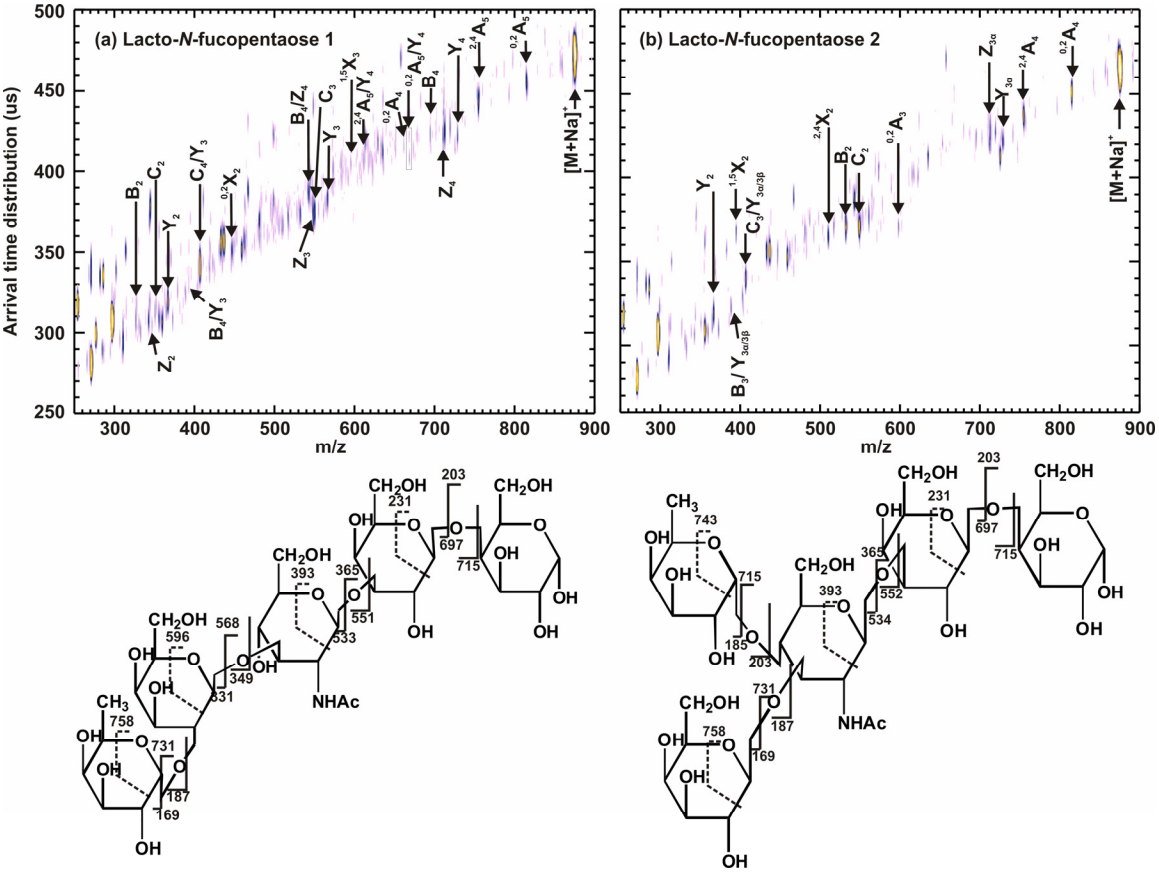

Figure 3.4 IM-MS conformation space for glycans 5 (LNFP1, a) and 6 (LNFP2, b) from human milk doped with NaCl (0.1%). The in-source decay fragment ions correlate to those that have been identified using collision-induced dissociation (CID) and post-source decay using a MALDI-TOFMS. The fragments are identified using Domon and Costello's nomenclature.[27]

pattern is sufficient to differentiate the two carbohydrates, but these assignments are reinforced through the differences in the IM separation. Specifically, enhanced internal fragmentation was observed for the branched structure of (6) relative to the linear structure of (5) as illustrated in Figure 3.5, which shows comparative MS data for each of the isobaric positional and structural isomer pairs.

In-source fragmentation was seen using IM-MS for all glycans analyzed in this study (Figure 3.5). The differences in the fragments seen and intensity of those fragments was compared using the one-dimensional *m/z* spectra. Due to the azide moiety on the spacer of the synthetic glycans, removal of N_2 is common which was seen in the prominent loss of 28 Da from the sodium-coordinated molecular ion.[139] Generally, cross-ring cleavages are less frequent and far less intense when using positive ion mode CID MS. This was also true in our study in that cross-ring cleavages were seen, but glycosidic bond cleavages were by far the most abundant. Glycan 2 has more identified peaks than glycan 1 which could be due to the 1→4 linkages in glycan 2 not providing as much stabilization as the 1→3 linkages in glycan 1 (Figure 5A). These A and X fragments were not as intense as cleavages of the glycosidic bond, but are required to differentiate glycans that differ only by a variation in linkage when using MS^n alone. When comparing glycans 3 and 4, more internal cleavages are seen for glycan 4. This again could be due to the presence of the 1→4 linkage which causes glycan 4 to form a more elongated or less stable structure. The fragmentation data can be used complementary

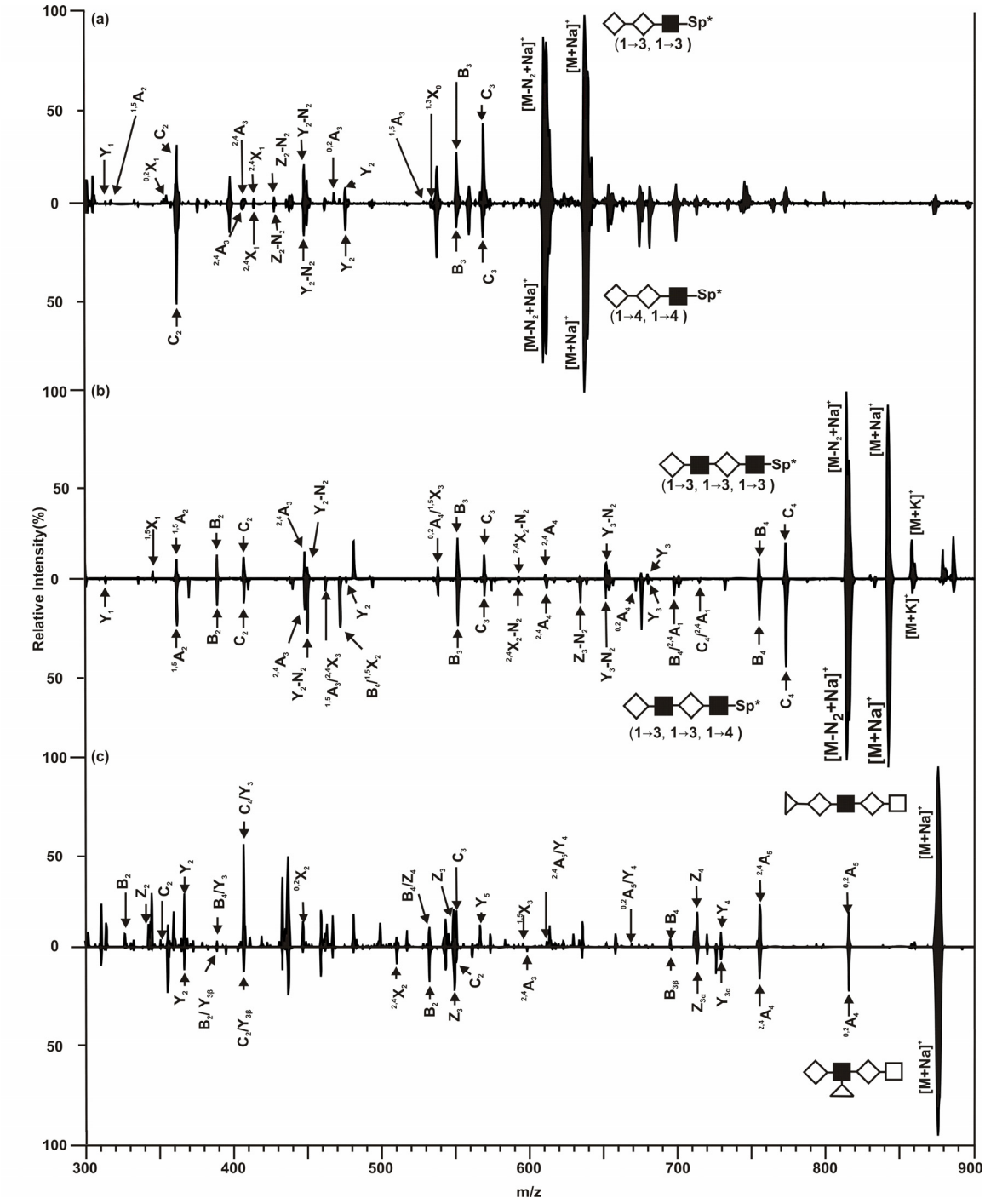

Figure 3.5 In-source fragmentation was abundant in the MALDI-IM-MS. Peaks were identified using Domon and Costello nomenclature for carbohydrate fragmentation. (a) Glycans 1 (top) and 2 (bottom) fragmentation patterns are compared. (b) Glycans 3 (top) and 4 (bottom) fragmentation patterns are compared. (c) Fragmentation spectra for LNFP1 (top) and LNFP2 (bottom) are presented. Patterns differ between the two glycans in the type of fragmentation seen as well as the intensity of certain fragment peaks.

to the calculated collision cross section for confident and complete structural elucidation of glycans using IM-MS.

A future direction in the use of IM-MS to characterize isobaric positional and structural isomers is fragmentation of the carbohydrate after the ion mobility drift cell. Fragmentation in this means is after IM separation which leaves the fragments correlating with the drift time of the parent ion. An example of this can be seen using LNFP1 and LNFP2 (Figure 3.6). This method leaves the possibility to fragment many peaks simultaneously in a complex sample with correlation to the parent ion through the drift time.

3.4 Conclusion

IM-MS is a rapid and efficient technique in differentiating carbohydrate positional and structural isomers. Three sets of isobaric isomers were differentiated based on their structure through the calculation of their collision cross sections. Carbohydrate branching and 1→3 versus 1→4 linkages are seen to cause lower values for drift time and collision cross section signifying branching and 1→3 linkages cause more compact carbohydrate structure. Also, the addition of some alkali metals is seen to further set apart the collision cross sections of LNFP1 and LNFP2. Additional studies will apply these findings to larger, more branched carbohydrates to attempt to discriminate isobaric ions based on their structure and determine which carbohydrate linkages lead to a reduction in collision cross section.

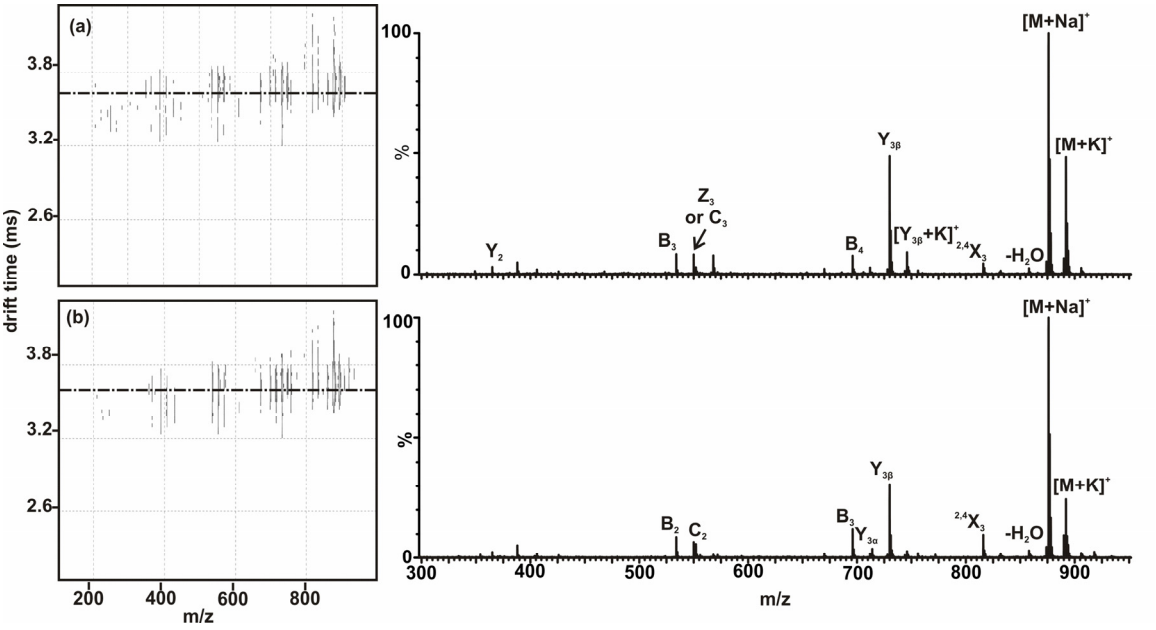

Figure 3.6 Fragmentation after the ion mobility drift cell but before TOF mass detection for (a) LNFP1 and (b) LNFP2. The fragmentation took place after separation in the ion mobility drift cell causing the peaks to be related back to the parent through the IM drift time. This opens the possibility of fragmenting many peaks present in a complex mixture at one time with correlation back to the parent without having to isolate and fragment each peak of interest. (*Right*) The 1D spectra labels the carbohydrates fragments present using Domon and Costello nomenclature. All peaks are sodium-adducted unless specified otherwise.

CHAPTER IV

SIMULTANEOUS GLYCOPROTEOMICS AND GLYCOLIPIDOMICS ON THE BASIS OF STRUCTURE USING ION MOBILITY-MASS SPECTROMETRY

4.1 Introduction

Contemporary MS techniques for studying glycoproteins and other glycoconjugates are intricate and time consuming, most requiring carbohydrates, peptides, and lipids to be analyzed in separate experiments for the same sample.[6] For example, most MS techniques to characterize glycoproteins involve extensive carbohydrate purification followed by MS/MS fragmentation studies to interpret glycan structure (Figure 4.1, Scheme A). It is important to recognize that separating the protein from the carbohydrate analysis removes the context in which the two are integrated. This chapter describes a new strategy to combine glycomic, proteomic, and lipidomic analyses in the same experiment, without the need for extensive sample preparation. This is accomplished on the basis of 2D separations by IM-MS (Figure 4.1, Scheme B).

Earlier chapters have demonstrated the utility of IM-MS separations on the basis of shape and *m/z* in biomolecular studies. IM-MS is performed with ions produced by MALDI or ESI and then introduced into the ion mobility drift cell. The ions are separated by structure by IM and this separation readily distinguishes the biomolecular class of a given signal due to their differences in gas-phase

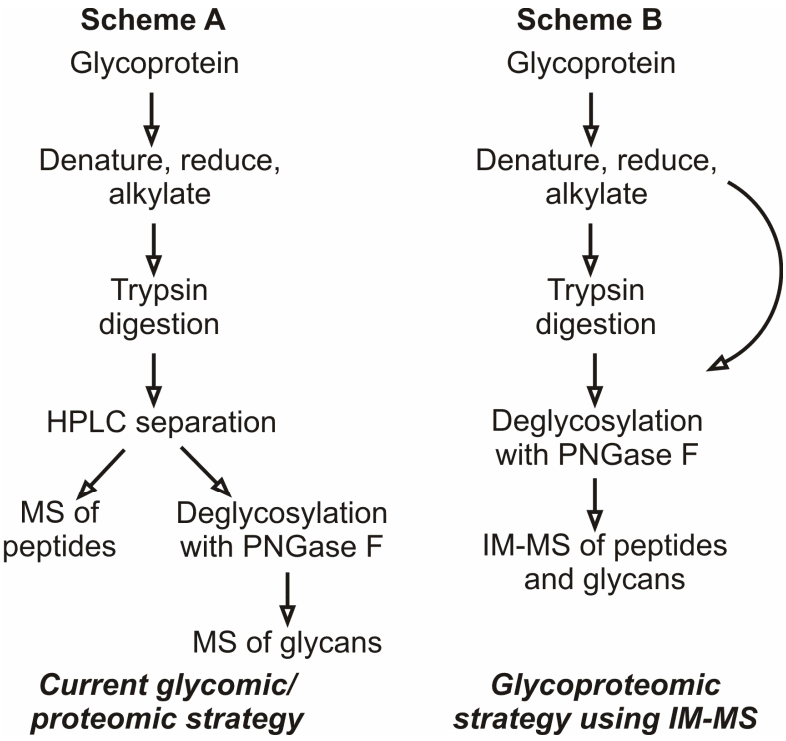

Figure 4.1 Comparison of current glycomic and proteomic protocols (Scheme A) versus the proposed glycoproteomic strategy using IM-MS (Scheme B). L.S. Fenn, J.A. McLean, *Molecular BioSystems* **2009**, 5, 1298-1302. – Reproduced by permission of The Royal Society of Chemistry (RSC).

packing efficiencies.[61,140] Previous work studying carbohydrates using IM-MS either analyzed carbohydrate standards[65,79,89] or carbohydrates separated from complex samples.[46,76,91] In this chapter, we describe the potential of IM-MS for simultaneous characterization of carbohydrates, peptides, and lipids directly. The model glycoprotein ribonuclease B was first characterized as a proof-of-concept experiment using both ESI and MALDI. Then, more complex glycoproteins were characterized using MALDI. Finally, the lipids and glycans present in a complex sample, human milk, were detected using IM-MS. All experiments were performed without any type of purification before IM-MS analysis. This study demonstrates the potential IM-MS has as a high throughput methodology for the characterization of carbohydrates and glycans in the presence of other biomolecules within complex mixtures.

4.2 Experimental

Bovine ribonuclease B (RNAse B), ovalbumin from chicken egg white, fetuin from fetal calf serum, and α1-acid glycoprotein from human plasma (HGP) was purchased from Sigma (St. Louis, MO) and used without further purification. Sequencing grade modified trypsin was purchased from Promega (Madison, WI) and peptide-N4-(acetyl-ß-glucosaminyl)-asparagine amidase F (PNGase F) was purchased from Prozyme Glyko (San Leandro, CA). All other solvents, reagents, and salts used were purchased from Sigma unless otherwise specified.

The proteins were digested and deglycosylated using the following methodology. Briefly, the lyophilized glycoprotein was dissolved in 50 mM ammonium acetate solution and an aliquot (1 nmol) was thermally denatured at 90°C for 15 minutes. The samples were then proteolytically digested with trypsin (approximately 20:1 wt of substrate/wt of trypsin) at 37°C for 24 hours. After cooling, the N-linked glycans are removed from the glycopeptides by adding PNGase F and incubating for 12 hours. As a control, the glycoprotein was digested with only PNGase F (no trypsin digestion) in the same procedure as above, which yields only N-linked glycans in the mass range of < 3000 Da without peptides due to the protein being left intact (M_r ~ 13,700 Da for RNAse B). The matrix used for MALDI-IM-TOFMS was saturated DHB dissolved in 1:1 (v/v) ethanol and DDW. The matrix and analyte were combined in a 1:1 volume ratio (or 200:1 molar ratio). The samples were then prepared using the dried droplet method. For ESI analyses, the glycoprotein digest was dissolved in 50:50 (v/v) water: methanol to a final concentration of 25 μM.

The human milk sample analyzed was post-term and was stored in -20°C. For analysis, the milk was diluted 1:10 (v/v) with DDW and then mixed 1:1 (v/v) with saturated DHB matrix dissolved in 1:1 ethanol and DDW then spotted on a stainless steel plate and allowed to air dry.

IM-MS experiments were performed on a Synapt HDMS instrument (Waters Corp., Manchester, UK) equipped with an interchangeable MALDI or ESI source which was further described in Chapter I. IM was performed using travelling wave separation through nitrogen gas that has been described in detail

elsewhere.[74] The ion guide T-wave was operated at 300 m/s and linearly ramped in amplitude from 5-20 V over each experiment. The transfer guide T-wave was operated at 248 m/s and with a constant 3 V amplitude. Ion injection voltages in the Trap and Transfer were set at 4 and 6 V, respectively. For instrument control and data analysis, MassLynx software was used (Waters Corp., Manchester, UK). Peak identification was assisted by Glycomod[141,142] and PeptideMass[143-145] from ExPASy.

4.3 Results and discussion

Standard glycoproteins were studied using MALDI- and ESI-IM-MS for the characterization of the associated glycans and deglycosylated tryptic peptides. Also, lipids and glycans present in human milk were detected without prior purification. Whereas most current glycoprotein methodologies separate glycan, proteomic, lipidomic characterization into different steps, we present the ability to simultaneously characterize these signals in one IM-MS plot of conformation space. The advantages from each ionization method are used in a complimentary way to increase the information content in glycoproteomics data.

4.3.1 RNAse B Characterization by MALDI and ESI-IM-MS

RNAse B was selected for the first benchmarking studies because it only has one site of glycosylation (Asn34) with the possibility of five high-mannose glycans (MAN5-9) being attached at this site.[146] After the sequential digestion

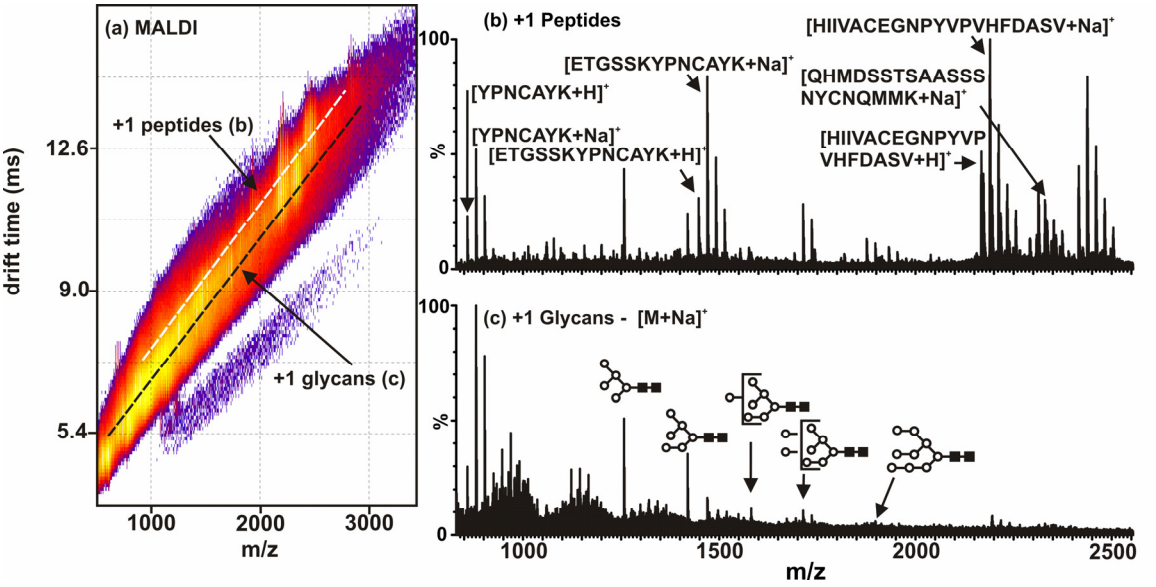

Figure 4.2 MALDI-IM-MS plot and extracted mass spectra from RNAse B digested and deglycosylated with trypsin and PNGase F, respectively. (a) A 2D IM-MS plot of conformation space. Structural separations are observed for peptides [labeled (b)] and glycans [labeled (c)]. Since MALDI is used, all identified peaks correspond to singly-charged species as sodium-coordinated glycans and protonated peptides. (b) An extracted mass spectrum corresponding to peptides [along white dashed-line in (a)]. (c) An extracted mass spectrum corresponding to glycans [along black dashed-line in (a)]. Carbohydrate structure representations are as follows: ○-mannose and ■-*N*-acetylglucosamine. Unidentified peaks seen at lower masses in (c) are due to in-source fragmentation of the glycans present. L.S. Fenn, J.A. McLean, "*Molecular BioSystems* **2009**, 5, 1298-1302. – Reproduced by permission of The Royal Society of Chemistry (RSC).

and deglycosylation of the glycoprotein using a combination of trypsin and PNGase F, the resulting samples were analyzed using MALDI-IM-MS (Figure 4.2) and ESI-IM-MS (Figure 4.3) along with the PNGase F control digest (Figure 4.4). The latter is used to validate signals in the combined conformation space plots. For a detailed list of identified peptides and glycans, see Appendix B, Tables B.1 and B.2.

In Figure 4.2(a), a MALDI-IM-MS plot of conformation space is presented for the trypsin and PNGase F digestion of RNAse B and demonstrates the simultaneous analysis of glycans and peptides present in the mixture. In this conformation space plot, the mobility-mass correlations for singly-charged tryptic peptides and singly-charged glycans are illustrated with white and black dashed-lines, respectively. Carbohydrates adopt more compact structures than those observed for peptides and result in shorter IM drift times at a given *m/z* (as described in Chapter II). Thus, in a single analysis, both peptide and glycan analytes are observed in different regions of conformation space owing to structure, despite isobaric overlap in the *m/z* dimension. In comparison with MS-only results, chemical noise is separated from the analytes of interest in IM-MS, which facilitates identification of low abundance glycan signals not observed in MS-only approaches. The one dimensional mass spectra for these mobility-*m/z* correlations are extracted from the conformation space plot and the peaks are subsequently identified. In the glycan mass spectrum [Fig. 4.2(c)], all five glycans present on RNAse B are identified and the tryptic peptide mass spectrum [Fig. 4.2(b)] results in a 43.5% coverage of the amino acid sequence of the protein.

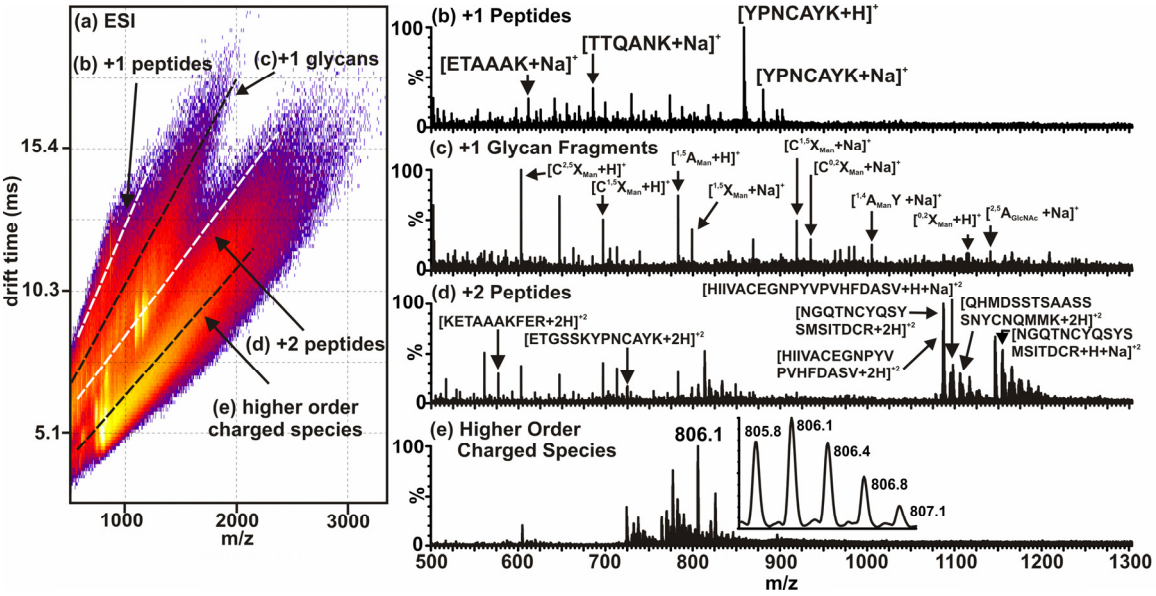

Figure 4.3 ESI-IM-MS plot and extracted mass spectra from RNAse B digested and deglycosylated with trypsin and PNGase F, respectively. (a) A 2D IM-MS plot of conformation space. Structural separations are observed for singly-charged peptides [labeled (b)], singly-charged glycans [labeled (c)], doubly-charged peptides [labeled (d)], and higher order charged species [labeled (e)]. (b) An extracted mass spectrum corresponding to singly-charged peptides [along top white dashed-line in (a)]. (c) An extracted mass spectrum corresponding to singly-charged glycans with identification of fragments by Domon and Costello nomenclature [along top black dashed-line in (a)].[27] (d) An extracted mass spectrum corresponding to doubly-charged peptides [along bottom white dashed-line in (a)]. (e) An extracted mass spectrum corresponding to higher order charged species [along bottom black dashed-line in (a)]. The inset illustrates the isotopic pattern for a triply-charged analyte. L.S. Fenn, J.A. McLean, "*Molecular BioSystems* **2009**, 5, 1298-1302. – Reproduced by permission of The Royal Society of Chemistry (RSC).

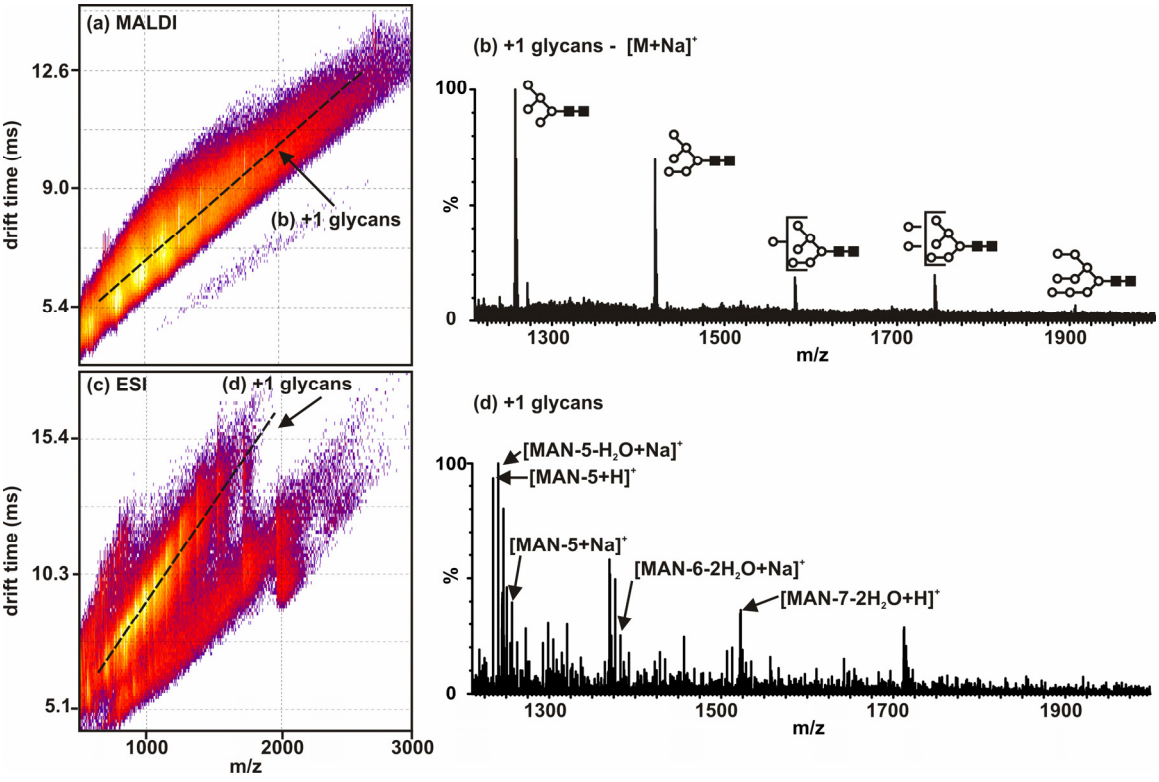

Figure 4.4 Plots and extracted mass spectra from intact RNAse B that has been deglycosylated with PNGase F and analyzed using MALDI-IM-MS (a,b) and ESI-IM-MS (c,d). Note that the protein was not proteolytically digested and remained intact (Mr ~ 13,700 Da). (a) A 2D MALDI-IM-MS plot of conformation space. Structural separations are observed for singly-charged glycans [labeled (b)] which are then compared to those identified in Figure 4.2. (b) An extracted mass spectrum corresponding to singly-charged glycans [along dashed-line in (a)]. (c) A 2D ESI-IM-MS plot of conformation space. Structural separations are noted for singly-charged glycans [labeled (d)] which are then compared to those identified in Figure 4.3. (d) An extracted mass spectrum corresponding to singly-charged glycans [along dashed-line in (c)]. Carbohydrate structure representations are as follows: ○-mannose and ■-*N*-acetylglucosamine. L.S. Fenn, J.A. McLean, "*Molecular BioSystems* **2009**, 5, 1298-1302. – Reproduced by permission of The Royal Society of Chemistry (RSC).

The mobility-*m/z* correlation occurring below that for glycans is possibly from higher charge-state species which were not identified in this study.

In Figure 4.3, an ESI-IM-MS plot of conformation space is presented for RNAse B digested with trypsin and PNGase F to remove the N-linked glycans. In this plot [Figure 4.3(a)], four correlations are readily identified. Similar to that using MALDI, singly-charged peptide and singly-charged glycan correlations are noted along with doubly-charged peptides which were unique to the ESI data. The singly-charged peptides are annotated in the extracted mass spectrum [Fig. 4.3(b)], but in the extracted singly-charged glycan mass spectrum [Fig. 4.3(c)], only fragments of the N-linked glycans are observed. In the extracted doubly-charged peptide mass spectrum, larger peptide sequences are indentified and when combined with those obtained from the singly-charged peptide data this results in a 71.8% amino acid sequence coverage of the protein. Furthermore, additional data can be extracted from a correlation of higher order charged species (> doubly-charged) as illustrated in the extracted mass spectrum of Figure 4.3(e). These species exhibit isotope patterns characteristic of higher charge-state species as indicated for a triply-charged analyte in the inset.

A comparison of the MALDI and ESI data highlight the unique analytical aspects of both techniques and underscore the importance of combining data sets obtained by both MALDI (Fig. 4.2) and ESI (Fig. 4.3). Owing to the high propensity for glycan fragmentation, glycan fragments are observed in the lower mass range (<1000 Da) in both MALDI [Fig. 4.2(c)] and ESI [Fig. 4.3(c)] data, which include subsequent H_2O and small neutral losses from the glycans. While

glycans were amenable to ionization by both MALDI and ESI, only MALDI produced intact sodium-coordinated glycan signals (1200 - 1900 Da) whereas ESI produced few signals corresponding to glycans > 1000 Da. The ESI glycan fragments that were observed are labeled using Domon and Costello nomenclature for CID fragmentation of carbohydrates in Fig. 4.3(c).[27] A second difference in the glycan data is that while MALDI produced primarily sodium-coordinated glycans, ESI produced glycan species as both protonated and sodium-coordinated ions and additionally as combinations of protonated and sodium coordinated species which could be due in part to the solvent choice and ion source focusing conditions. Although it is an advantage to observe intact glycans using MALDI, there exist many ESI glycan protocols using chemical derivatization (*e.g.* permethylation, etc.) prior to analysis to assist in reducing glycan fragmentation. No attempt was made here to chemically derivatize the glycans, A primary advantage to using ESI is the structural separation of different charge states as well as through structure. This can be seen by obtaining protein sequence coverages of 43.5 and 71.8%, using MALDI and ESI, respectively.

4.3.2 Ovalbumin, Fetuin, and HGP Characterization by MALDI-IM-MS

After the first proof-of-concept experiments detecting simultaneously the peptides and glycans from digests of RNAse B using MALDI and ESI-IM-MS, we then pursued the characterization of more complex glycoproteins. Previously purified glycoproteins, ovalbumin, fetuin, and HGP, were chosen for analysis

since they are well-characterized[11-13,147-158] and have more complex glycans than the five high-mannose species present on RNAse B. Due to the glycans being detected as intact species using MALDI in the previous experiments, this ionization source was used for the continuing studies.

For comparison purposes, the glycoproteins were first deglycosylated using PNGase F as a control experiment (Figure 4.5). This would leave only glycans in the mass range of interest (<3000 Da). In Figure 4.5 (a,c,e), the IM-MS conformation space plot is presented for each glycoprotein digest, ovalbumin, fetuin, and HGP, respectively. The carbohydrate mass/mobility correlation is represented with a black dotted line. Below this correlation shows a band from higher ordered species which do not have enough signal to be identified. In Figure 4.5 (b,d,f), the mass spectrum along each carbohydrate mass/mobility correlation is extracted in order to identify the carbohydrates present. Only the most abundant glycans are depicted (For a full list of identified glycans and their associated masses, see Appendix B, Table B.2). The glycans are labeled according to previously published structures at each mass. In Table B.2, carbohydrates are listed as general hexose and N-acetylhexoseamine (other than the trimannosyl-chitobiose core) due to MS/MS not being performed for each peak. In order to further characterize the glycans, MS/MS would have to be performed to determine each specific monomer along with the glycosidic linkages. Some of the identified peaks may be fragments of larger glycans caused by the MALDI process. This is also evident in the abundance of peaks below 1000 Da in all of the glycan spectra.

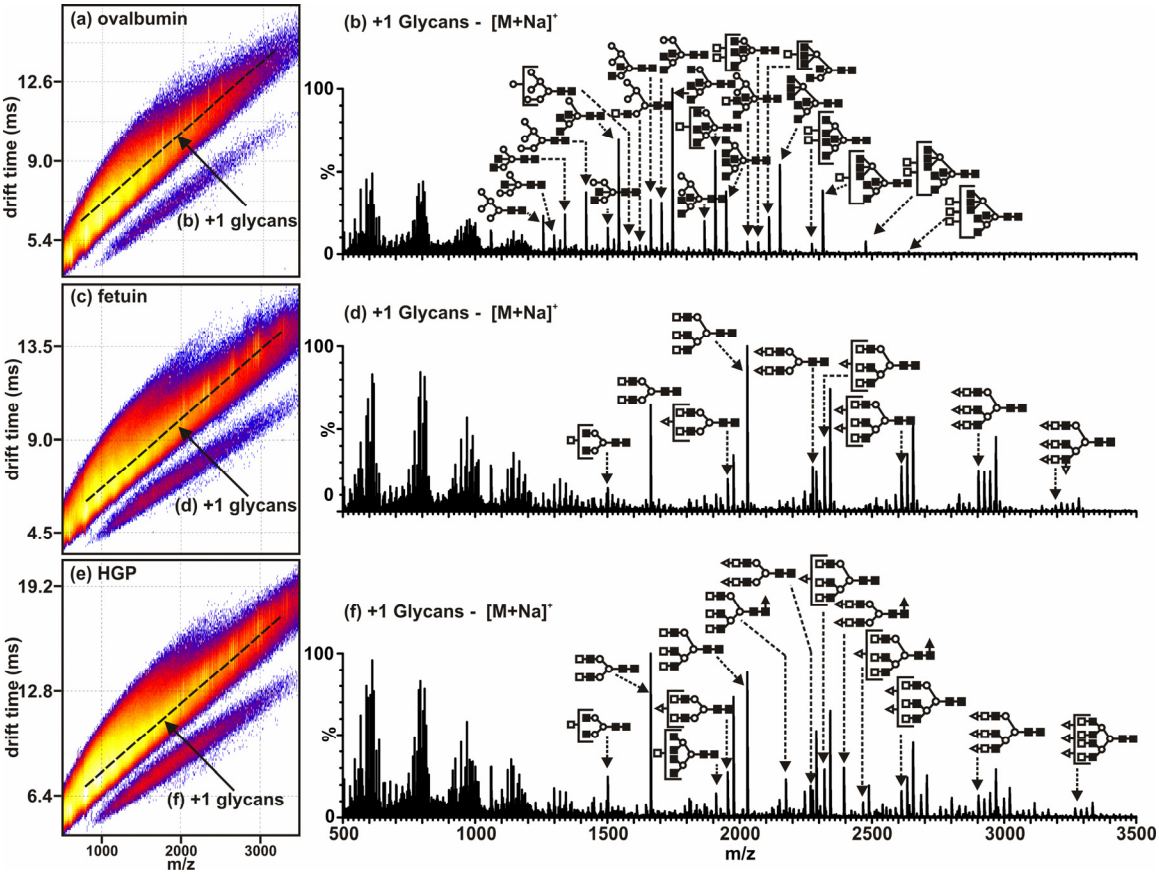

Figure 4.5 Plots and extracted mass spectra for the glycans from ovalbumin (a,b), fetuin (c,d), and HGP (e,f) analyzed using MALDI-IM-MS. The protein was deglycosylated with PNGase F to remove N-linked glycans. Note that the protein was not proteolytically digested and remained intact. (a) A 2D MALDI-IM-MS plot of conformation space for ovalbumin. Structural separations are observed for singly-charged glycans [labeled (b)] which are then compared to those identified in Figure 4.6(c). (b) An extracted mass spectrum corresponding to singly-charged glycans from ovalbumin [along dashed-line in (a)]. (c) A 2D MALDI-IM-MS plot of conformation space for fetuin. Structural separations are observed for singly-charged glycans [labeled (d)] which are then compared to those identified in Figure 4.6(f). (d) An extracted mass spectrum corresponding to singly-charged glycans from fetuin [along dashed-line in (c)]. (e) A 2D MALDI-IM-MS plot of conformation space for HGP. Structural separations are observed for singly-charged glycans [labeled (f)] which are then compared to those identified in Figure 4.6(i). (f) An extracted mass spectrum corresponding to singly-charged glycans from HGP [along dashed-line in (e)]. Carbohydrate structure representations are as follows: ○-mannose, ●-glucose, △-sialic acid, ■-*N*-acetylglucosamine, □-galactose, and ▲-fucose.

While ovalbumin had all 3 types of N-linked glycans identified (high-mannose, hybrid, and complex, Figure 1.1), fetuin and HGP had only complex glycans present. They also had sialic acids on many of their glycans which are known to readily dissociate from the glycan in the ionization process. This could be due to the differences between the ionization process in MALDI-IM-MS compared to conventional MALDI-MS. Ionization in MALDI-IM-MS is done at or slightly below the pressure of the drift cell (3-8 Torr) which creates the ability for "collisional cooling" of the ions preventing some in-source fragmentation. However, ionization in MALDI-MS is performed at high vacuum (~10^{-8} Torr) which does not have the buffer gas present to cool the ions and can cause fragmentation to labile carbohydrates especially those with sialic acid.

Another interesting phenomenon due to the sialic acids is the presence of peaks from sequential addition of sodium and loss of a proton up to one more than the number of sialic acids. This was seen for all glycans which had a sialic acid present. After the glycans in the PNGase F control digests were identified, they were compared with the glycans present in digests with tryptic peptides.

Tryptic peptides and released N-linked glycans from ovalbumin, fetuin, and HGP were detected simultaneously in digests using MALDI-IM-MS as demonstrated in Figure 4.6. In Figure 4.6 (a,d,g), the IM-MS conformation space plot for each glycoprotein digest shows separate mass/mobility correlations for singly-charged peptides and glycans. The correlations can then be extracted to form the mass spectra where the peptides and glycans can be identified. As in the PNGase F only digests, only the most abundant peptides and glycans are

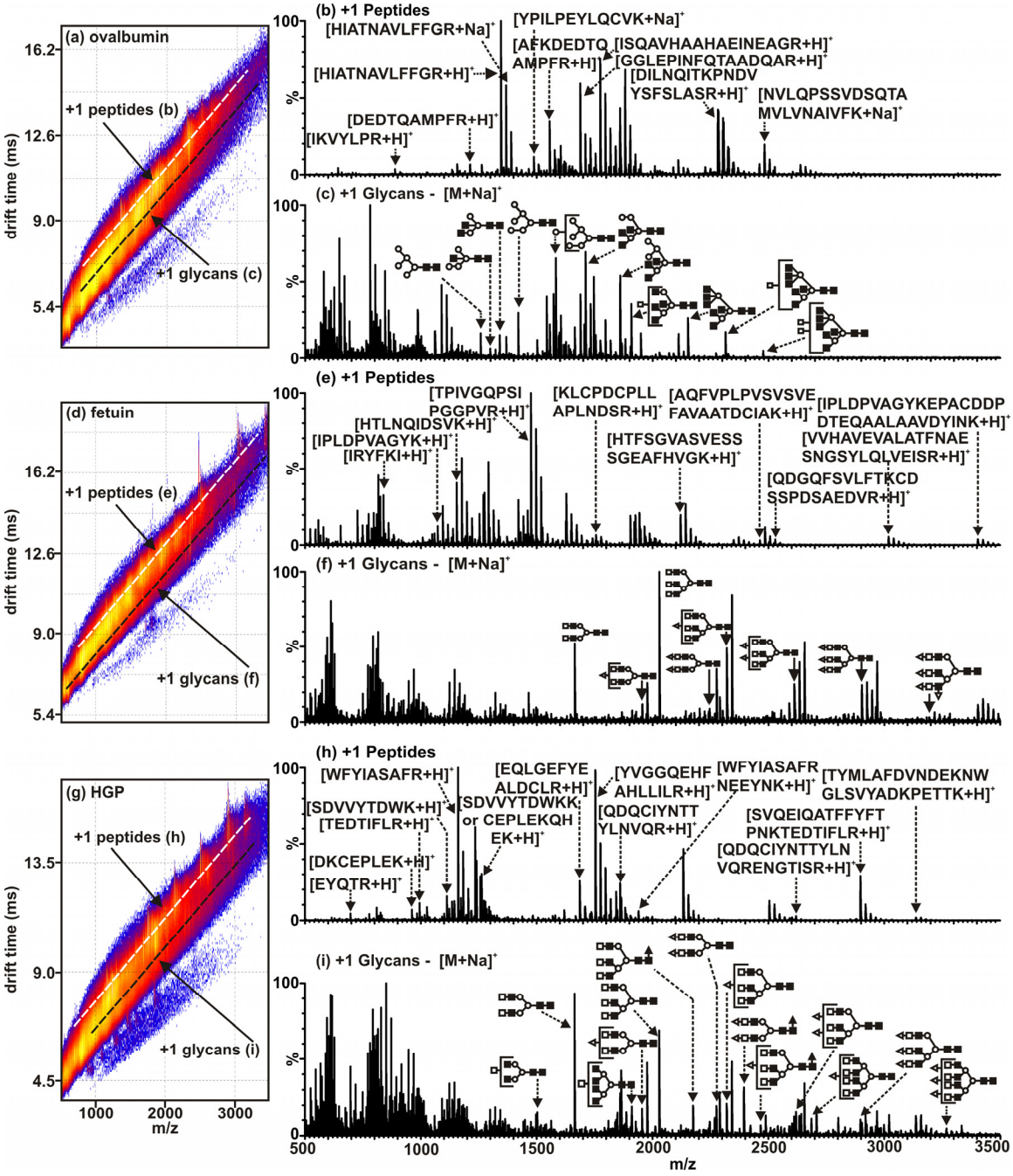

Figure 4.6 MALDI-IM-MS plot and extracted mass spectra from ovalbumin (a,b,c), fetuin (d,e,f), and HGP (g,h,i) digested and deglycosylated with trypsin and PNGase F, respectively. Since MALDI is used, all identified peaks correspond to singly-charged species as sodium-coordinated glycans and protonated or sodium-coordinated peptides. Unidentified peaks seen at lower masses in glycan mass spectra are due to in-source fragmentation of the glycans present. (a) A 2D IM-MS plot of conformation space for ovalbumin. Structural separations are observed for peptides [labeled (b)] and glycans [labeled (c)]. (b) An extracted mass spectrum corresponding to peptides [along white dashed-line

Figure 4.6—cont. in (a)]. (c) An extracted mass spectrum corresponding to glycans [along black dashed-line in (a)]. (d) A 2D IM-MS plot of conformation space for fetuin. Structural separations are observed for peptides [labeled (e)] and glycans [labeled (f)]. (e) An extracted mass spectrum corresponding to peptides [along white dashed-line in (d)]. (f) An extracted mass spectrum corresponding to glycans [along black dashed-line in (d)]. (g) A 2D IM-MS plot of conformation space for HGP. Structural separations are observed for peptides [labeled (h)] and glycans [labeled (i)]. (h) An extracted mass spectrum corresponding to peptides [along white dashed-line in (g)]. (i) An extracted mass spectrum corresponding to glycans [along black dashed-line in (g)]. Carbohydrate structure representations are as follows: ○-mannose, ●-glucose, △-sialic acid, ■-*N*-acetylglucosamine, □-galactose, and ▲-fucose.

identified in the figure, but a complete list of peptides and glycans are listed in Appendix B, Tables B.1 and B.2. Even though the glycan signal is slightly suppressed in the presence of the peptides, most of the glycans identified in the control PNGase F digests can still be identified in the mixture of peptides and glycans. Due to the peptides and glycans being simultaneously detected within these digests, the next experiment aimed to detect glycans in the presence of lipids within a more complex mixture, human milk.

4.3.3 Simultaneous glycolipidomics by MALDI-IM-MS of human milk

Human breast milk research is growing in prominence due to the unique components comprising the milk and how each component assists in the development of infants. Human milk is primarily made up of lipids and oligosaccharides, and the lipids form globules and lactosomes which assist in the absorption of nutrients.[159] The oligosaccharides cannot be digested by the infants but are a food source to bacteria present in the digestive tract.[160] These bacteria are thought to assist in breast milk-fed infants having an improved immune

system compared to formula-fed infants.[161] As with most current analysis techniques, the two biomolecular classes present in human milk are usually separated and purified before characterization. In this experiment, human milk was diluted and analyzed without any prior purification or separation using MALDI-IM-MS to analyze the lipids and oligosaccharides present.

In Figure 4.7, lipids and glycans present in human milk are separated by their structures in the IM dimension. In the 2D conformation space plot, a mass/mobility correlation is seen for both biomolecular classes [Figure 4.7(a)]. In Figure 4.7(b), the integrated mass spectrum over all of conformation space is shown to demonstrate the results that would be obtained if using MS alone to characterize human milk. In this spectrum, the lipids overpower the oligosaccharide signal causing even the most abundant carbohydrates to be lost. However, when IM is used, the structural separation differentiates the two biomolecular classes. From the correlations seen in Figure 4.7(a), mass spectra corresponding to each class can be extracted and particular species can be identified. In Figure 4.7(c), the mass spectrum for lipids is extracted. For the lipids present in the sample, the most likely identifications from previous human milk studies are given in Appendix B, Table B.3.[159] In Figure 4.7(d), the oligosaccharide signals are extracted and identified. It is known that human milk glycans are composed of D-glucose, D-galactose, *N*-acetylglucosamine, L-fucose, and *N*-acetylneuraminic acid.[162] The glycans depicted have been identified previously in numerous publications and for a list of these identifications, see Appendix B, Table B.4.[160-165] Similar to the glycoprotein

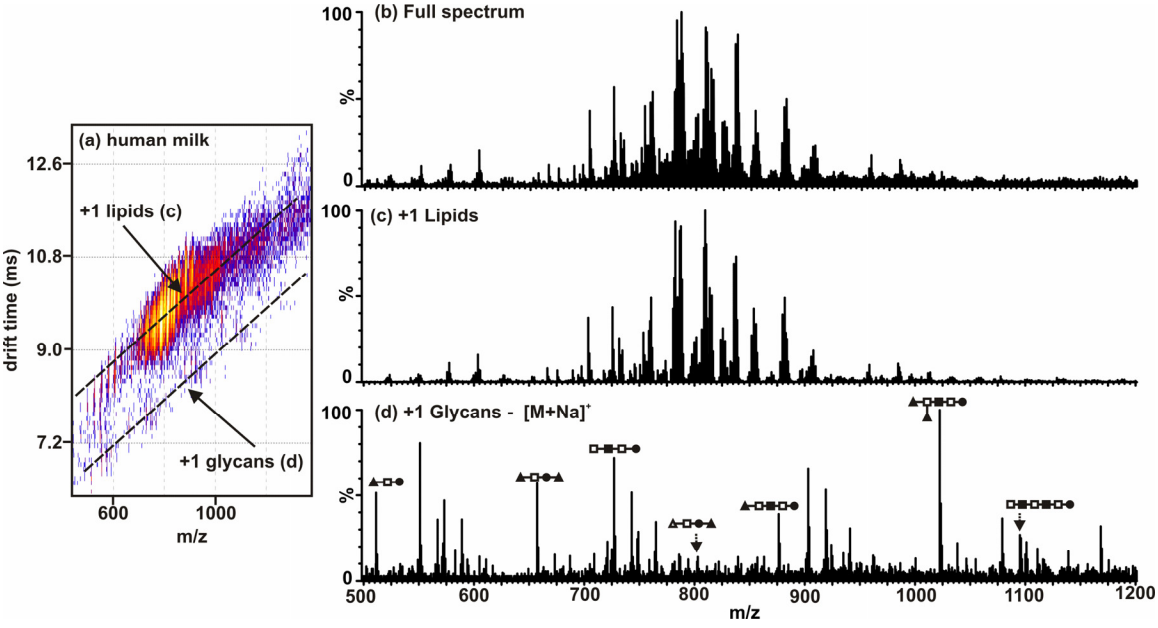

Figure 4.7 MALDI-IM-MS plot and extracted mass spectra from human milk with no prior purification. (a) A 2D IM-MS plot of conformation space. Structural separations are observed for lipids [labeled (c)] and glycans [labeled (d)]. Since MALDI is used, all identified peaks correspond to singly-charged species. (b) An integrated mass spectrum for all of conformation space. This is what would be seen if using MS alone to characterize the human milk sample. (c) An extracted mass spectrum corresponding to lipids [along top dashed-line in (a)]. (d) An extracted mass spectrum corresponding to glycans [along bottom dashed-line in (a)]. Carbohydrate structure representations are as follows: ●-glucose, △-sialic acid, ■-*N*-acetylglucosamine, □-galactose, and ▲-fucose.

identifications, the glycan structure is given but the stereochemistry is not confirmed due to MS/MS not being performed. Even though the lipid signal overpowers the combined mass spectrum for the sample, with the added dimension of separation from IM, the carbohydrates are differentiated and identified.

4.4 Conclusion

Current bottom-up methodologies for studying glycans and their associated glycoconjugates involve complex and time-consuming protocols with extensive purification and derivatization techniques prior to MS analysis. After using standard proteolytic digestion protocols and removal of the pendant glycans, we demonstrate the use of IM-MS to characterize standard glycoproteins by structurally separating and identifying peptides and glycans simultaneously without sample purification. Using both MALDI and ESI, a clear and distinct structural separation is observed for both peptides and glycans present in a digest of RNAse B. The advantages of each ionization method suggests the utility of combining MALDI and ESI data sets to encompass the unique glycoprotein information from each technique. Using MALDI alone, the more complex glycans present on ovalbumin, fetuin, and HGP are detected in the presence of tryptic peptides for complete characterization of each glycoprotein. Glycans and lipids present in the same complex sample, human

milk, were also detected for simultaneous glycolipidomics. These strategies should greatly facilitate high throughput glycomics in future studies.

4.5 Acknowledgements

I would like to acknowledge Michal Kliman for the identifications of the lipids present in the human milk sample and Viera Kliman for her generous donation of the milk sample.

CHAPTER V

ENHANCED CARBOHYDRATE STRUCTURAL SELECTIVITY IN ION MOBILITY-MASS SPECTROMETRY ANALYSES BY BORONIC ACID DERIVATIZATION

5.1 Introduction

In the previous chapters, the combination of IM-MS has been used for the characterization of carbohydrates and glycoconjugate mixtures due to it providing two-dimensional separations on the basis of both analyte ion structure and mass-to-charge (*m/z*). Chapter II demonstrated that for singly-charged ions, the correlation of collision cross section versus mass is strongly dependent on the specific class of biomolecule. This was further demonstrated in a more complex sample in Chapter IV where carbohydrates and peptides were separated from one another in the same glycoprotein digest mixture. Another example of this is given in Figure 5.1 which illustrates results for the separation of singly-charged peptides and N-linked glycans for a model glycoprotein (ribonuclease B, pancreatic bovine), which was proteolytically digested with trypsin followed by release of N-linked glycans via PNGase F. The difference between this figure and those from Chapter IV is that Figure 5.1 was obtained from a DTIM-MS, whereas the examples in Chapter IV were from a TWIM instrument. As discussed in Chapter I, the DTIM instrument has a higher mobility resolution and

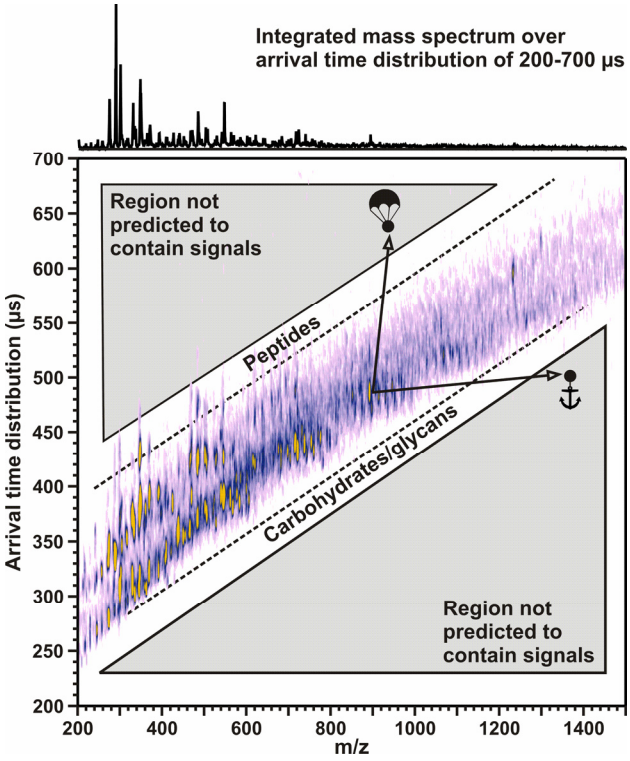

Figure 5.1 A plot of conformation space in the MALDI-IM-MS analysis of the glycoprotein ribonuclease B. The protein was first proteolytically digested with trypsin followed by N-glycan release using PNGase F. The carbohydrates present are from in-source decay fragmentation of the intact glycans. Dashed-lines are to visualize qualitatively where peptide and glycan signals occur. Ion mobility shift agents are used to shift specific analytes into regions of conformation space not expected to contain signals as hypothetically illustrated by the parachute and the anchor. L.S. Fenn, J.A. McLean, *Chemical Communications*, **2008**, *43*, 5505-5507. – Reproduced by permission of The Royal Society of Chemistry (RSC).

should be able to more efficiently separate the classes. However, as illustrated in Figure 5.1, in the analysis of complex biological samples the correlations of molecular class in conformation space can sometimes be insufficient to distinguish to which class of molecule a particular signal corresponds. To further increase the information derived in IM-MS carbohydrate analyses, the feasibility of a new ion mobility shift reagent strategy is demonstrated.

Ion mobility shift reagents consist of coordinating or covalently modifying a selected chemical functionality. For example, the shift reagent could be lower or higher density than the type of molecule to be derivatized to structurally shift the desired signals to regions of conformation space above or below the predicted molecular class correlation. Noncovalent ion mobility shift strategies have been demonstrated for selectively shifting isomeric amines and peptides by using crown ethers,[166,167] and shifting carbohydrates through coordination with different metals and metal acetates.[79] In contrast with noncovalent tagging, covalently attached ion mobility shift reagents offer several potential advantages, including: (i) quantitative derivatization of the analytes of interest, (ii) relative quantitation using isotopically labeled tags, (iii) potential for adding affinity capture moieties on the tag itself, and (iv) potential for inclusion of a permanent charge carrier for enhanced ionization efficiencies. Boronic acid based functionalization was selected for carbohydrate derivatization because of its demonstrated utility in spectroscopic measurements.[168-170]

The use of boronic acids (BA) to covalently modify saccharides was known for many years prior to the first quantitative evaluation of BA chemistry

published by Lorand and Edwards in 1959.[171] In this work they determined equilibrium constants for the reaction of benzene BA with various polyols including a suite of monosaccharides, for the latter these values ranged from 110-4400. Thus, although the reaction of BAs with cis-diols on carbohydrates is slightly reversible, the selective reaction is nearly quantitative and can be tuned by optimizing pH.

A suite of carbohydrates including 3 disaccharides, 2 trisaccharides, 2 tetraoses, and 2 pentaoses (Table 5.1 and Figure 5.2) were derivatized using two structurally distinct boronic acids under the reaction conditions depicted in Figure 5.3. The collision cross sections for underivatized and derivatized species were calculated to evaluate the effect of derivatization on the position of the resulting structural shift appears in IM-MS conformation space.

5.2 Experimental

The carbohydrates lacto-N-fucopentaose 1 (LNFP1) and lacto-N-fucopentaose 2 (LNFP2) from human milk were obtained from Dextra Laboratories (Reading, UK); N-acetyl-D-lactoseamine, maltose, and lactose were obtained from Sigma (St. Louis, MO). Synthetic glycans, Galα1-3Galβ1-3GlcNAcβ-Sp, Galα1-4Galβ1-4GlcNAcβ-Sp, Galβ1-3GlcNAcβ1-3Galβ1-4GlcNAcβ-Sp, and Galβ1-3GlcNAcβ1-3Galβ1-3GlcNAcβ-Sp (Sp=$CH_2CH_2N_3$) were obtained from the Carbohydrate Synthesis/Protein Expression Core of The Consortium for Functional Glycomics. Each carbohydrate was derivatized with

Table 5.1 Common names, systematic names, average molecular weights, and derivatized mass of the carbohydrates. Abbreviations are as follows: Glc-Glucose; Gal-Galactose; GlcNAc-N-acetylglucosamine; Fuc-fucose.

Common name	Systematic name	Molecular weight (M_r, Da)	$[M+Na]^+$ (Da)	$[M+FBA+Na]^+$ (Da)	$[M+PBA+Na]^+$ (Da)
Maltose	4-α-D-Glc-D-Glc	342.3	365.3	559.1	641.5
Lactose	β-D-Gal-(1→4)-α-D-Glc	342.3	365.3	559.1	641.5
LN	β-D-Gal-(1→4)-D-GlcNAc	383.4	383.4	600.2	682.5
Gala3-type1	Gal-α-(1→3)-Gal-β-(1→3)-GlcNAc-β-azide	614.6	637.6	831.4	913.7
P1	Gal-α-(1→4)-Gal-β-(1→4)-GlcNAc-β-azide	614.6	637.6	831.4	913.7
Lec-Lec	Gal-β-(1→3)-GlcNAc-β-(1→3)-Galβ-(1→3)-GlcNAc-β-azide	817.8	840.8	1034.6	1116.9
LNT	Gal-β-(1→3)-GlcNAc-β-(1→3)-Gal-β(1→4)-GlcNAc-β-azide	817.8	840.8	1034.6	1116.9
LNFP1	Fuc-α-(1→2)-Gal-β-(1→3)-GlcNAc-β-(1→3)-Gal-β -(1→4)-Glc	853.8	876.8	1070.6	1152.9
LNFP2	Gal-β-(1→3)-[Fuc-α-(1→4)]-β-GlcNAc-β-(1→3)-Gal-(1→4)-Glc	853.8	876.8	1070.6	1152.9

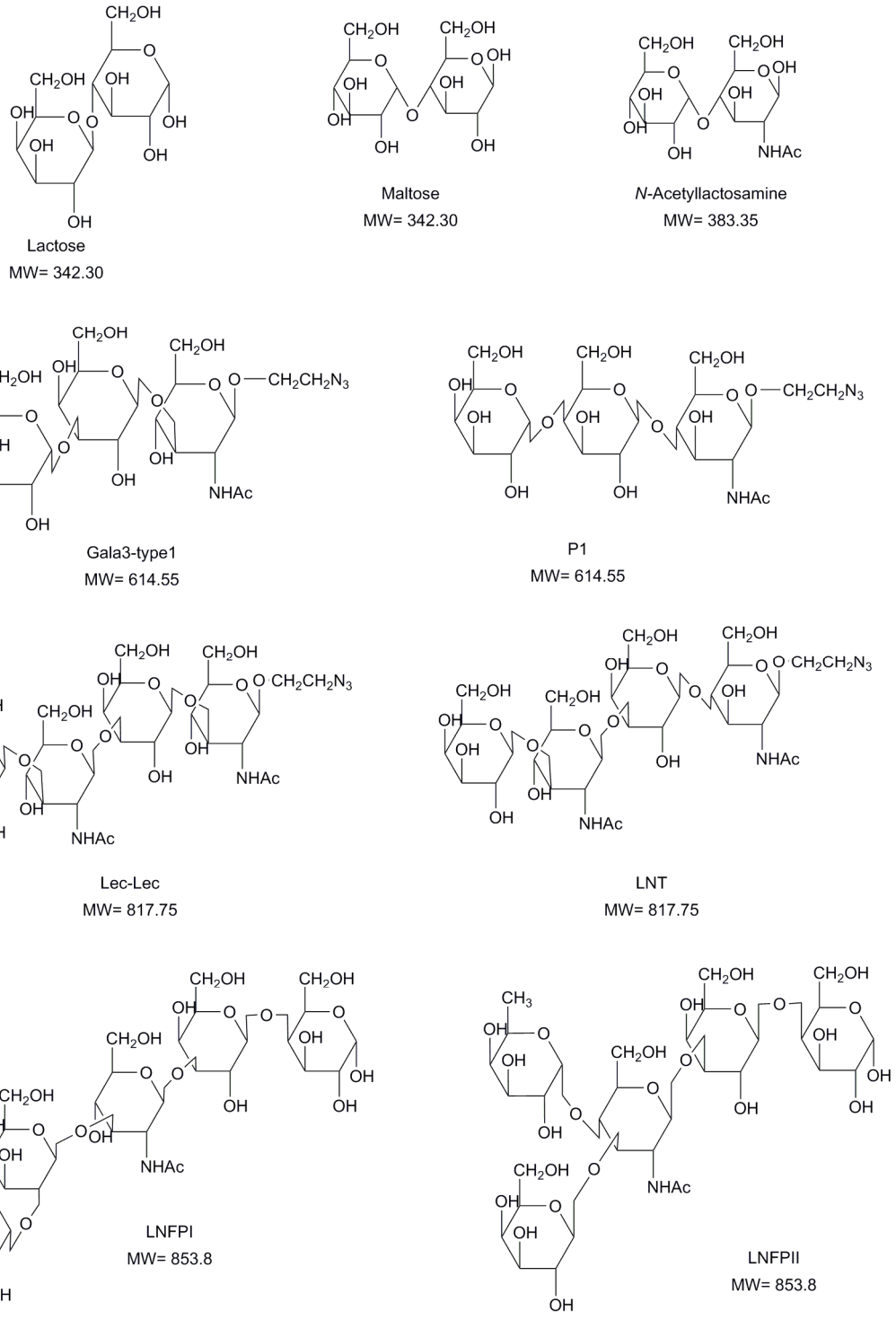

Figure 5.2 Structures of the underivatized carbohydrates. L.S. Fenn, J.A. McLean, *Chemical Communications*, **2008**, *43*, 5505-5507. – Reproduced by permission of The Royal Society of Chemistry (RSC).

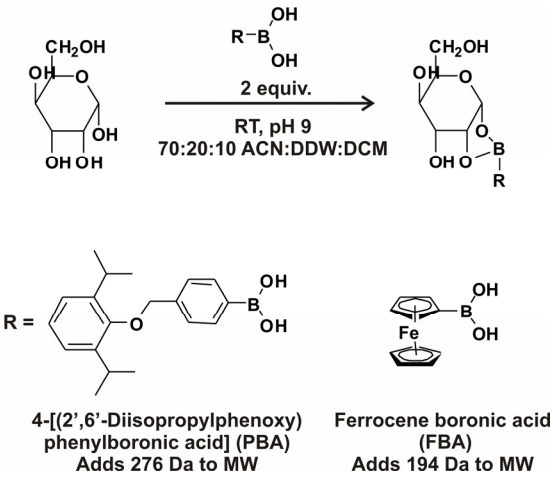

Figure 5.3 A generalized scheme for the reaction of carbohydrates with substituted boronic acids used in these studies. BA prefers to attach to the reducing end of cis-diols forming a stable five-membered ring. The structures and molecular weights of the 9 carbohydrates investigated, ranging from disaccharides to pentaoses, are provided in Figure 5.2. L.S. Fenn, J.A. McLean, *Chemical Communications*, **2008**, *43*, 5505-5507. – Reproduced by permission of The Royal Society of Chemistry (RSC).

both ferrocene boronic acid (FBA) and 4-[(2',6'-iisopropylphenoxy)phenylboronic acid] (PBA) obtained from Sigma. Solutions of BA were prepared in DMSO to final concentrations of 10-50 mM. Carbohydrate solutions were prepared in 70:20:10 ACN:DDW:DCM to a final concentration of 0.03 mM and were adjusted to the optimized pH for each BA (7.5 and 9.0 for PBA and FBA, respectively).[170] The BA solution was added to the carbohydrate solution resulting in molar ratio of approximately 2:1 BA to carbohydrate. The reaction was then allowed to proceed for 12 hours, or alternatively sonicated for 5 minutes at room temperature.[172]

To determine collision cross sections, MALDI ionization was performed by mixing analytes in a 200:1 molar ratio of saturated 2,5-dihydroxybenzoic acid in 50% ethanol with analyte. Samples were spotted onto a stainless steel plate, and dried under vacuum. The IM measurements were performed on the drift tube MALDI-IM-TOFMS as described in Chapter I, Section 1.2.2.1. The collision cross sections were calculated using the procedure outlined in Chapter I, Section 1.2.1.

5.3 Results and discussion

In order to determine the affect of the BA derivitization with carbohydrates, collision cross sections where determined for both protonated and/or sodium-coordinated species. For FBA derivatized species, both $[M+H]^+$ and $[M+Na]^+$ species were observed in nearly equal abundance; however, for PBA derivatized species the preponderance (>98%) of signal was for sodium-coordinated

species, so protonated cross sections are not reported for comparison purposes. The collision cross sections of the underivatized carbohydrates are provided as well (Table 5.2).

The affect of derivatization on the collision cross sections of carbohydrates is illustrated in Figure 5.4. FBA was selected to serve as a high density tag (*i.e.* to serve as an anchor in Figure 5.1), owing to the addition of Fe and tightly coordinated cyclopentadienyl groups. However, the increase in surface area and mass upon FBA derivatization appears to shift signals along the carbohydrate correlation. PBA was selected to perform as a low density tag (*i.e.* to serve as a parachute in Figure 5.1), owing to the sterically bulky diisopropylphenyl moiety. In this case, the desired shift in conformation space is achieved for most species as indicated by a greater increase in surface area than that predicted for a commensurate increase in underivatized carbohydrate mass. Furthermore, the carbohydrates studied also contain 4 pairs of isomeric carbohydrates, which is a serious complication when using mass spectrometry alone. However, using IM-MS, these isobaric carbohydrates are separated on the basis of structure as was demonstrated in Chapter III.

It should be noted that there exists a diverse collection of commercially available BAs exhibiting a range of chemical functionality. Thus it should be feasible to select specific BAs to promote different but particular anhydrous folding forces, which in turn should result in ion mobility shift tuneability. Furthermore, in contrast with underivatized carbohydrates derivatization described herein provide three distinct advantages, which include: (i) tuneability

Table 5.2 Collision cross sections determined for protonated and/or sodium coordinated carbohydrates prior to and following boronic acid derivatization.

	Collision cross section ($Å^2$)[a]		
Carbohydrate	$[M+Na]^+$	$[M+FBA+Na]^+$	$[M+PBA+Na]^+$
Maltose	103.1 ± 4.1 (21)	140.3 ± 7.7 (5)	156.3 ± 5.7 (16)
Lactose	106.8 ± 5.1 (35)	151.5 ± 8.4 (16)	163.7 ± 3.4 (30)
LN	117.4 ± 1.8 (23)	156.7 ± 3.4 (15)	195.0 ± 1.5 (30)
Gala3-type1	160.2 ± 2.1 (26)	197.9 ± 4.4 (31)	229.8 ± 7.3 (18)
P1	166.9 ± 1.2 (70)	200.5 ± 2.8 (39)	255.4 ± 2.3 (40)
Lec-Lec	183.2 ± 1.6 (51)	220.0 ± 2.6 (15)	252.2 ± 2.1 (21)
LNT	195.9 ± 1.4 (42)	217.9 ± 2.8 (19)	254.8 ± 8.3 (19)
LNFP1	204.3 ± 1.4 (147)	222.5 ± 3.4 (9)	230.2 ± 6.1 (26)
LNFP2	201.4 ± 1.0 (166)	226.1 ± 2.3 (11)	233.7 ± 3.1 (21)

a. Error represents ± 1σ for *n* measurements indicated in parenthesis. The protonated form of PBA derivatized carbohydrates is not included as the relative abundance for $[M+PBA+H]^+$ species was <2% of the base peak ($[M+PBA+Na]^+$) in the spectra.

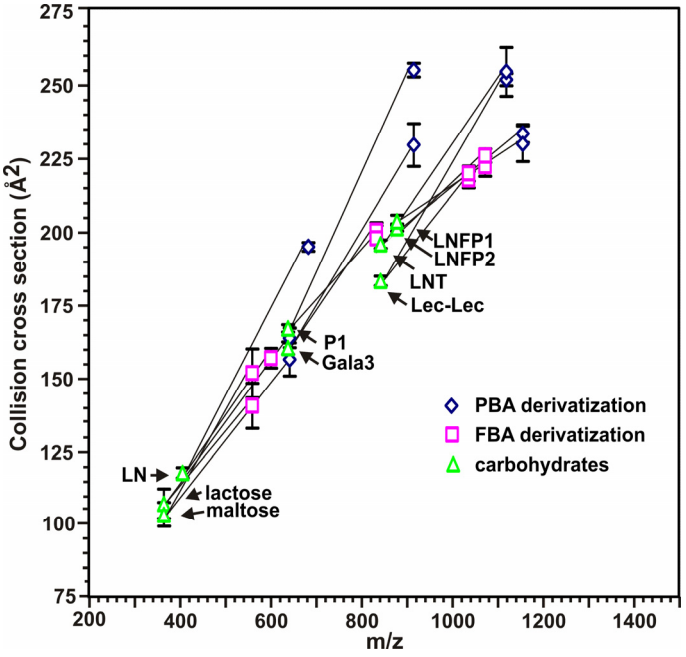

Figure 5.4 A plot of collision cross section vs. *m/z* for underivatized carbohydrate species, FBA, and PBA (all present as $[M+Na]^+$) derivatized carbohydrates. Error bars on the derivatized species represent ± 1σ. Refer to Table 5.2 for tabulated values. L.S. Fenn, J.A. McLean, *Chemical Communications*, **2008**, *43*, 5505-5507. – Reproduced by permission of The Royal Society of Chemistry (RSC).

in the separation of isobaric species, (ii) enhanced ionization efficiency (*e.g.* upon FBA derivatization an ca. 2x enhancement in sensitivity is observed), and (iii) potential to serve as fragment labels in CID,[173,174] and IR active species in IRMPD,[172] in tandem MS studies. Owing to covalent derivatization, new classes of BAs incorporating moieties for affinity purification, isotopic enrichment for relative expression determination, and inclusion of structural standards (*e.g.* fullerenes) provide new avenues for further characterization, identification, and quantification of carbohydrate species in glycomics and glycoproteomics.

5.4 Conclusion

This chapter has demonstrated the potential of ion mobility shift reagents in the detection and characterization of carbohydrates. As a specific example, BAs were used to attach specific moieties in order to shift them structurally either above or below the predicted correlation for carbohydrates. The shift reagents can be used for other purposes as well including enhancing ionization efficiency or attaching tags for quantitative measurements.

CHAPTER VI

CONCLUSIONS AND FUTURE DIRECTIONS

6.1 Summary and Conclusions

In this dissertation, the detection and characterization of carbohydrates while in the presence of other biomolecular classes through the structural separations provided by IM-MS was described. There are currently many complications when determining the carbohydrates present on glycoproteins and in complex mixtures. Current methodologies remove and purify the carbohydrates from the original sample which disturbs the intricate natural environment such as the glycan location on a glycoprotein. There are also complications when using MS to characterize positional and structural carbohydrate isomers. Even though these carbohydrates have different structures, they cannot be differentiated using MS alone due to having the same mass. Throughout this report, IM-MS was used to characterize glycans and their associated glycoconjugates from complex samples. This work also reviewed the first reported utilization of MALDI-IM-MS in the study of carbohydrates whereas all other published reports use ESI-IM-MS.

First, IM-MS was used to separate and survey the area of IM-MS conformation space occupied by different biomolecular classes. The conformation space occupied by carbohydrates lies between the more elongated

classes of lipids and peptides and the more compact class of oligonucleotides This is due to the nature of the carbohydrate itself, the types of atoms that they are composed of, the oxophilic interaction with alkali metals, and their preference for branching as their size increases. They also have the highest deviation from the average mass/mobility correlation which means they occupy a larger area of conformation space than other biomolecules. This can be attributed to the higher structural diversity of carbohydrates.

Even though carbohydrates have a high structural diversity, they form many for positional and structural isomers which IM-MS was able to differentiate due to the differences in collision cross section. The limited number of monomers and glycosidic linkages between these monomers cause carbohydrates to have a high probability for positional and structural isomerization. These isomers are isobaric in nature and are unable to be resolved by MS alone. In this regard, it is desirable to have a rapid method for differentiation for which IM-MS was used. IM-MS was able to differentiate three pairs of carbohydrate isomers that, even though they have the same mass, vary in structure.

The primary aim of this dissertation research was to differentiate carbohydrates simultaneously from other biomolecular classes in complex mixtures. This was demonstrated for glycoprotein digests with a range of complexity and in the separation of glycans from lipids in human milk. Even though the peptides and lipids dominate the MS spectra, the additional dimension of separation provided by IM-MS distinguished the glycan signals. All three types of N-linked glycans were detected along with sialic acids still

attached, which are known to readily dissociate in conventional MS. The ability to separate glycans, lipids, and peptides simultaneously will greatly assist in future characterizations of glycans in complex mixtures where rapid analysis time is needed.

Even though the peptides, glycans, and lipids were differentiated in IM-MS conformation space, in some situations, additional separation or ionization efficiency is needed. This was addressed through the use of IM shift reagents based on BA interactions with the cis-diols present on carbohydrates. A structural shift and ionization enhancement was seen for the carbohydrates and BAs tested.

Overall, this dissertation describes the first experiments to simultaneously characterize different biomolecules from the same sample with particular attention to carbohydrates. All previous studies of carbohydrates and glycoconjugates using IM-MS separated and purified the biomolecules of interest before analysis. In this dissertation research, carbohydrates were differentiated from peptides and lipids in the same sample without the need for time-consuming separation and purification. In addition, IM-MS was able to differentiate positional and structural carbohydrate isomers which is a significant challenge to current glycomics research. Since these isomers have the exact same mass, they cannot be separated my MS alone, no matter the resolution. The first carbohydrate collision cross section database with over 3500 measurements for 303 carbohydrate species was also created. This research has made a

significant contribution to carbohydrate characterization using IM-MS, an area which will only gain attention in future endeavors.

6.2 Future Directions

Through these studies, great progress was made in characterizing glycans within complex mixtures using IM-MS, but there are many opportunities for further research. The positional and structural isomer study along with determining the area of conformation space occupied by carbohydrates used low molecular weight standards (<1300 Da). For future studies, the mass/mobility correlation for carbohydrates could be extended for higher masses to determine how the glycans' structure would change with the addition of more monomers along with the increasing branching probability.

Higher mass positional and structural isomers could also be characterized to determine the level of structural deviation that IM-MS can be used to differentiate. As is seen in the current studies, as the mass increases and amount of structural deviation decreases (*i.e.* comparing glycans with many glycosidic bond variations to glycans with only one bond variation), the differences in collision cross section decrease. This could be used to explore which isomers IM-MS would be the most effective at separating. The use of ESI-IM-MS could also be explored to see how the addition of more charges would affect the difference in collision cross section and possibly enhance separation.

For the characterization of glycoprotein digests, these studies concentrated predominantly on characterization of N-linked glycans and purified glycoproteins. For ongoing studies, O-linked glycans could be pursued using MALDI-IM-MS. Glycoproteins present in samples with growing complexity could also be explored to determine how well IM-MS will separate the glycans within the mixture.

For future studies, IM-MS would be of great use characterizing glycan-containing species such as glycopeptides or glycans complexed with other biomolecules. This type of study could probe the structure of the species without interrupting the interactions within the natural environment, unlike conventional methods using separation and purification before analysis.

The full utility of IM shift reagents for the study of carbohydrates has not been realized. The use of BA-based tags could be continued with other moieties attached to shift the carbohydrate signal in different directions. Also, since the BA reaction is slightly reversible, other tagging strategies could be investigated that are not reversible and could be used for quantitative measurements.

APPENDIX A

TABULAR DATA FOR COLLISION CROSS SECTIONS OF BIOMOLECULAR STANDARDS

Table A.1 Collision cross sections for carbohydrate standards in Chapter II (denoted with *) and Chapter III.[1]

Name (parent name if fragmented)	species	*m/z* (Da)	Ω (Å^2)	σ (# of measurements)
B_1 (P1 tri)	$[M+Na]^+$	185.1	53.6	3.8(5)
$^{2,4}A_2$ (P1 tri)	$[M+Na]^+$	245.0	72.5	1.2(5)
$^{2,4}X_0$ (Le^ALe^x)	$[M+Na]^+$	253.0	35.9	2.0(5)
$^{2,4}X_0$ (Di-Le^A)	$[M+Na]^+$	253.0	94.0	0.8(7)
Y_1-N_2 (B tetra type 1)	$[M+Na]^+$	285.0	82.3	1.1(5)
Y_1-N_2 (P1 tri)	$[M+Na]^+$	285.3	85.3	2.8(5)
Z_1 (LacNAc)	$[M+Na]^+$	295.0	96.3	7.4(5)
Z_1 (B2-tri)	$[M+Na]^+$	295.3	89.7	2.1(5)
Z_1 (P1 tri)	$[M+Na]^+$	295.3	88.2	7.1(5)
$^{0,2}A_2$ (Pk)	$[M+Na]^+$	305.0	96.6	4.6(5)
$^{1,5}A_2$ (P1 tri)	$[M+Na]^+$	319.3	95.7	3.1(5)
$^{1,5}A_2$ (Galα3-type1)	$[M+Na]^+$	319.3	99.0	3.2(5)
$^{0,2}X_1$-N_2 (Galα3-type1)	$[M+Na]^+$	327.3	111.6	4.7(9)
*B_2 (LNFP1)	$[M+Na]^+$	331.0	118.6	0.5(7)
B_2 (Lac)	$[M+Na]^+$	347.0	108.4	3.5(7)
B_2 (P1 tri)	$[M+Na]^+$	347.3	101.4	6.6(5)
$^{0,2}X_1$ (P1 tri)	$[M+Na]^+$	355.3	106.6	1.8(5)
$^{1,5}A_2$ (LNnT)	$[M+Na]^+$	360.0	106.9	2.1(5)
*Y_2 (LNFP2)	$[M+Na]^+$	362.3	113.5	1.3(8)
*Y_2 (LNFP1)	$[M+Na]^+$	365.0	112.8	1.3(12)
C_2 (P1 tri)	$[M+Na]^+$	365.3	102.0	3.1(5)
lactose	$[M+Na]^+$	365.3	121.1	6.4(16)
maltose	$[M+Na]^+$	365.3	124.6	2.0(8)
C_2 (Lac)	$[M+Na]^+$	365.4	107.5	1.4(7)
$^{2,4}X_1$ (Pk)	$[M+Na]^+$	374.0	127.3	2.8(8)
$^{2,4}X_1$-N_2 (P1 tri)	$[M+Na]^+$	387.4	117.6	3.2(8)
$^{2,4}X_1$-N_2 (B2-tri)	$[M+Na]^+$	387.4	105.7	1.4(5)
B_2 (Di-Le^c)	$[M+Na]^+$	388.0	111.1	1.1(7)
B_2 (LNnT)	$[M+Na]^+$	388.0	113.6	0.9(5)
B_2 (LNT)	$[M+Na]^+$	388.0	115.8	2.3(10)
*B_2 (P1 penta)	$[M+Na]^+$	388.0	114.2	0.8(5)
B_2 (LacNAc)	$[M+Na]^+$	390.0	116.9	1.7(7)
*$^{2,4}A_3$ (H-type2-LN-LN)	$[M+Na]^+$	391.0	122.3	0.5(5)
C_2 (Le^c)	$[M+Na]^+$	405.0	124.9	3.4(7)
LN	$[M+Na]^+$	405.0	129.2	2.1(23)

C_2 (LacNAc)	$[M+Na]^+$	405.0	130.6	3.0(5)
$*C_2$ (P1 penta)	$[M+Na]^+$	406.0	118.3	2.1(9)
$*C_2$ (Di-Le^c)	$[M+Na]^+$	406.0	125.3	5.6(5)
$*C_2$ (GNLNLN)	$[M+Na]^+$	406.0	118.0	4.0(5)
M-N_2 (Lac)	$[M+Na]^+$	406.0	122.3	2.8(11)
$*C_2$ (LNT)	$[M+Na]^+$	406.0	119.4	1.5(5)
$^{2,4}A_3$ (Pk)	$[M+Na]^+$	407.0	116.4	1.4(5)
$*^{2,4}A_3$ (P1 antigen)	$[M+Na]^+$	407.0	123.0	3.4(10)
$^{2,4}A_3$ (P1 tri)	$[M+Na]^+$	407.3	119.5	2.1(5)
$*^{2,4}A_3$ (Galα3-type1)	$[M+Na]^+$	407.3	118.5	0.6(8)
$*C_4/Y_3$ (LNFP1)	$[M+Na]^+$	409.4	129.8	1.1(17)
$*Y_{3\beta}/C_2$ (LNFP2)	$[M+Na]^+$	409.4	139.5	2.6(9)
$Z_{1\alpha}$-N_2 (Le^ALe^x)	$[M+Na]^+$	413.0	108.7	4.7(5)
Z_2 (LNnT)	$[M+Na]^+$	416.0	74.7	1.1(5)
$Y_{1\alpha}$-N_2 (2'F-B type 2)	$[M+Na]^+$	431.0	125.0	3.0(5)
$*Y_2$ (P1 antigen)	$[M+Na]^+$	434.0	131.0	1.4(5)
Y_2 (LNnT)	$[M+Na]^+$	434.0	110.5	1.6(5)
Lac	$[M+Na]^+$	434.4	130.3	3.5(15)
$*^{0,3}A_3$ (P1 tri)	$[M+Na]^+$	437.0	133.0	1.2(7)
$*Z_{1\alpha}$ (Di-Le^A)	$[M+Na]^+$	441.4	132.1	2.7(13)
$*Y_2$-N_2 (H-type2-LN-LN)	$[M+Na]^+$	447.0	133.4	1.1(5)
$*Y_2$-N_2 (Di-Le^c)	$[M+Na]^+$	447.0	131.3	1.8(25)
$*Y_2$-N_2 (LNT)	$[M+Na]^+$	447.0	127.9	8.1(26)
M-N_2 (LacNAc)	$[M+Na]^+$	447.0	137.2	0.9(17)
M-N_2 (Le^c)	$[M+Na]^+$	447.0	136.4	1.0(10)
$*Y_2$-N_2 (P1 penta)	$[M+Na]^+$	447.0	134.1	0.3(8)
Y_2-N_2 (Galα3-type1)	$[M+Na]^+$	447.4	125.6	1.4(5)
Y_2-N_2 (B2-tri)	$[M+Na]^+$	447.4	137.7	0.8(9)
$*Y_2$-N_2 (P1 tri)	$[M+Na]^+$	447.4	133.6	0.8(17)
$*^{2,4}A_3$ (GNLNLN)	$[M+Na]^+$	448.0	115.1	0.5(8)
$^{0,2}X_2$-N_2 (Pk)	$[M+Na]^+$	448.0	137.8	1.6(8)
$^{2,4}A_3$ (LNnT)	$[M+Na]^+$	448.0	132.7	2.6(5)
$*^{1,3}A_3$ (Galα3-type1)	$[M+Na]^+$	448.4	128.0	2.0(5)
$*^{0,2}A_{2\alpha}$ (Di-Le^A)	$[M+Na]^+$	451.0	132.2	3.1(5)
$*^{0,2}A_3$ (H-type2-LN-LN)	$[M+Na]^+$	451.0	130.6	0.6(5)
$*Z_2$ (P1 tri)	$[M+Na]^+$	457.0	122.1	1.3(12)
$*Z_2$ (Galα3-type1)	$[M+Na]^+$	457.0	122.3	1.0(7)
$*Z_2$ (GNLNLN)	$[M+Na]^+$	457.0	108.3	1.3(5)
$Y_{1\alpha}$ (Le^ALe^x)	$[M+Na]^+$	459.0	107.5	1.4(5)
$*Y_{1\alpha}$ (Di-Le^A)	$[M+Na]^+$	459.4	126.6	1.8(12)
$*^{1,5}X_2$ (P1 antigen)	$[M+Na]^+$	462.0	121.2	0.7(9)
$^{0,2}A_3$ (Pk)	$[M+Na]^+$	467.0	127.0	2.8(5)
$*^{0,2}A_3$ (Galα3-type1)	$[M+Na]^+$	467.4	131.8	1.1(6)
$^{0,2}A_3$ (P1 tri)	$[M+Na]^+$	467.4	125.4	2.4(5)
$*Y_2$ (LNT)	$[M+Na]^+$	475.0	102.5	0.5(5)
$*Y_2$ (Di-Le^c)	$[M+Na]^+$	475.0	138.0	1.3(5)
$*Y_2$ (P1 penta)	$[M+Na]^+$	475.0	135.3	3.5(7)
$*Y_2$ (P1 tri)	$[M+Na]^+$	475.4	130.0	0.5(11)

LacNAc	$[M+Na]^+$	475.4	146.9	2.2(17)
$^*Y_2$ (Galα3-type1)	$[M+Na]^+$	475.4	133.8	0.6(7)
Le^c	$[M+Na]^+$	475.4	138.9	2.0(14)
Y_2 (B2-tri)	$[M+Na]^+$	475.4	145.6	1.7(7)
$^{*1,5}X_{1\alpha}$ (Di-Le^A)	$[M+Na]^+$	487.4	125.0	2.3(12)
$^{*0,2}X_2$-N_2 (P1 antigen)	$[M+Na]^+$	489.0	150.6	3.4(5)
$^{0,2}X_2$-N_2 (P1 tri)	$[M+Na]^+$	489.5	139.1	3.3(5)
B_2 (B tetra type 1)	$[M+Na]^+$	493.0	132.3	1.9(8)
$^{1,5}X_{2\alpha}$ (B tetra type 1)	$[M+Na]^+$	503.0	93.0	1.4(5)
$^{*1,5}X_2$ (Di-Le^c)	$[M+Na]^+$	503.0	152.0	3.4(5)
$^{*1,5}X_2$ (GNLNLN)	$[M+Na]^+$	503.0	138.5	1.5(5)
$^{*1,5}X_2$ (LNT)	$[M+Na]^+$	503.0	108.1	0.7(5)
$^{*1,5}X_2$ (H-type2-LN-LN)	$[M+Na]^+$	503.0	139.3	2.4(8)
$^{*1,5}X_2$ (Galα3-type1)	$[M+Na]^+$	503.4	144.8	3.5(8)
$^{1,5}A_{2\alpha}$ (Le^ALe^x)	$[M+Na]^+$	506.0	107.9	2.0(5)
$^{0,2}A_3$ (LNnT)	$[M+Na]^+$	508.0	107.8	2.2(5)
B_3 (Pk)	$[M+Na]^+$	509.0	132.1	1.3(5)
$^{*1,5}A_3$ (P1 tri)	$[M+Na]^+$	522.5	136.0	0.7(4)
$^{*1,5}A_3$ (Galα3-type1)	$[M+Na]^+$	522.5	143.9	2.5(9)
C_3 (Pk)	$[M+Na]^+$	527.0	139.4	1.8(12)
$^{0,2}X_2$-N_2 (Di-Le^c)	$[M+Na]^+$	531.0	109.1	1.5(5)
$^{*0,2}X_2$-N_2 (LNT)	$[M+Na]^+$	531.0	115.3	1.6(6)
$^*B_3$ (LNFP1)	$[M+Na]^+$	533.0	151.5	0.7(9)
$^{2,4}X_{1\alpha}$-N_2 (B tetra type 1)	$[M+Na]^+$	534.0	108.6	1.1(5)
$B_{2\alpha}$ (Le^ALe^x)	$[M+Na]^+$	534.0	109.0	1.6(5)
$^*B_3$ (H-type2-LN-LN)	$[M+Na]^+$	534.0	143.6	1.7(8)
$^*B_2$ (LNFP2)	$[M+Na]^+$	534.0	152.2	0.6(5)
$^*B_{2\alpha}$ (Di-Le^A)	$[M+Na]^+$	534.5	143.2	2.4(22)
$^{*3,5}X_1$-N_2 (Galα3-type1)	$[M+Na]^+$	535.0	145.5	1.8(5)
$^*Y_{3\beta}/Z_{3\alpha}$ (LNFP2)	$[M+Na]^+$	547.3	169.1	5.8(5)
$^{*0,3}X_1$ (Galα3-type1)	$[M+Na]^+$	547.5	160.3	3.4(10)
$^{2,4}X_2$-N_2 (B2-tri)	$[M+Na]^+$	549.5	166.3	6.2(9)
$^*B_3$ (Di-Le^c)	$[M+Na]^+$	550.0	147.7	1.8(33)
$^*B_3$ (LNT)	$[M+Na]^+$	550.0	142.4	1.9(9)
$^*B_3$ (P1 penta)	$[M+Na]^+$	550.0	150.6	0.3(13)
$^*B_3$ (P1 antigen)	$[M+Na]^+$	550.0	145.2	4.0(10)
B_3 (LNnT)	$[M+Na]^+$	551.0	157.9	1.0(6)
$^*C_3$ (LNFP1)	$[M+Na]^+$	551.0	134.1	1.6(9)
$^*C_3$ (H-type2-LN-LN)	$[M+Na]^+$	552.0	129.8	3.2(8)
$^*B_3$ (Galα3-type1)	$[M+Na]^+$	552.5	144.0	2.0(9)
B_3 (B2-tri)	$[M+Na]^+$	552.5	144.3	1.2(5)
$^*C_{2\alpha}$ (Di-Le^A)	$[M+Na]^+$	552.5	146.0	1.7(25)
$^*C_3$ (LNFP2)	$[M+Na]^+$	552.5	151.3	0.9(5)
$^*B_3$ (P1 tri)	$[M+Na]^+$	552.5	130.7	2.1(13)
$C_{2\alpha}$ (Le^ALe^x)	$[M+Na]^+$	553.0	146.4	1.4(8)

$^{2,4}X_{1\alpha}$ (Di-Le^A)	$[M+Na]^+$	561.5	121.5	2.0(5)
$^{*3,5}X_1$ (Galα3-type1)	$[M+Na]^+$	563.0	126.8	0.7(5)
$^*C_3$ (LNT)	$[M+Na]^+$	568.0	150.7	1.9(5)
$^*C_3$ (P1 antigen)	$[M+Na]^+$	568.0	148.6	1.2(6)
$^*C_3$ (Di-Le^c)	$[M+Na]^+$	568.0	152.8	2.3(31)
$^*Y_3$ (LNFP1)	$[M+Na]^+$	568.0	157.4	0.4(5)
$^*C_3$ (P1 penta)	$[M+Na]^+$	568.0	153.4	0.8(5)
C_3 (B2-tri)	$[M+Na]^+$	568.5	157.7	1.3(8)
$^*C_3$ (P1 tri)	$[M+Na]^+$	568.5	157.8	1.1(11)
M-N_2 (Pk)	$[M+Na]^+$	568.5	148.8	1.1(17)
$^*C_3$ (Galα3-type1)	$[M+Na]^+$	568.5	152.2	2.5(12)
$Z_{2\alpha}$-N_2 (Di-Le^A)	$[M+Na]^+$	575.5	150.2	3.2(5)
$^{*2,4}X_2$ (P1 antigen)	$[M+Na]^+$	577.0	161.9	5.6(5)
$^{*2,4}X_2$ (P1 penta)	$[M+Na]^+$	577.0	160.5	0.8(11)
$^{*2,4}X_2$ (Galα3-type1)	$[M+Na]^+$	577.5	164.1	4.6(8)
$^{2,4}X_2$ (P1 tri)	$[M+Na]^+$	577.5	112.2	1.9(5)
$^{2,4}X_2$ (LNnT)	$[M+Na]^+$	578.0	108.8	1.2(5)
$^{*2,4}X_2$-N_2 (LNT)	$[M+Na]^+$	591.0	153.7	1.8(7)
$^{*2,4}X_2$-N_2 (Di-Le^c)	$[M+Na]^+$	591.0	157.2	1.7(5)
$^*Z_3$-N_2 (P1 penta)	$[M+Na]^+$	591.0	145.9	0.9(5)
$^*B_3$ (GNLNLN)	$[M+Na]^+$	591.5	155.8	0.4(5)
$^*Y_{2\alpha}$-N_2 (Di-Le^A)	$[M+Na]^+$	593.6	157.3	1.8(24)
$Y_{2\alpha}$-N_2 (Le^{A}Le^x)	$[M+Na]^+$	594.0	162.3	2.6(13)
$Y_{2\alpha}$-N_2 (B tetra type 1)	$[M+Na]^+$	594.0	159.7	2.0(18)
$^{*2,4}A_4/Y_{3\alpha}$ (LNFP2)	$[M+Na]^+$	594.6	174.5	2.2(5)
Pk	$[M+Na]^+$	596.5	160.3	1.6(16)
$^*Y_3$-N_2 (P1 penta)	$[M+Na]^+$	609.0	160.1	1.7(10)
$Y_{2\beta}$-N_2 (B tetra type 1)	$[M+Na]^+$	609.6	163.2	0.9(14)
M-N_2 (B2-tri)	$[M+Na]^+$	609.6	170.6	1.4(18)
*M-N_2 (Galα3-type1)	$[M+Na]^+$	609.6	154.1	2.2(24)
*M-N_2 (P1 tri)	$[M+Na]^+$	609.6	161.9	1.2(30)
Y_3-N_2 (LNnT)	$[M+Na]^+$	610.0	165.9	2.0(12)
$^*C_3$ (GNLNLN)	$[M+Na]^+$	610.0	161.7	0.2(5)
$^{*2,4}A_4$ (Di-Le^c)	$[M+Na]^+$	611.0	160.4	1.5(6)
$^{*2,4}A_4$ (LNT)	$[M+Na]^+$	611.0	163.4	1.3(7)
$^{*2,4}A_4$ (P1 antigen)	$[M+Na]^+$	611.0	158.8	4.1(9)
$^{*2,4}X_2$ (LNT)	$[M+Na]^+$	619.0	169.2	2.4(5)
$Y_{2\alpha}$ (B tetra type 1)	$[M+Na]^+$	622.0	160.4	3.3(5)
$^{*3,5}A_4$ (LNT)	$[M+Na]^+$	624.0	123.6	0.7(5)
$^*Z_3$-N_2 (GNLNLN)	$[M+Na]^+$	633.0	169.9	1.9(5)
$^*Z_3$-N_2 (Di-Le^c)	$[M+Na]^+$	633.0	166.0	1.9(5)
$^*Z_3$-N_2 (LNT)	$[M+Na]^+$	633.0	132.9	2.8(5)
$^*Y_3$ (P1 penta)	$[M+Na]^+$	637.0	170.1	1.4(8)

B2-tri	$[M+Na]^+$	637.6	177.8	3.7(18)
*Galα3-type1	$[M+Na]^+$	637.6	162.9	3.2(63)
*P1 tri	$[M+Na]^+$	637.6	169.3	1.2(88)
$Y_{2\beta}$ (B tetra type 1)	$[M+Na]^+$	637.6	172.6	1.7(8)
Y_3 (LNnT)	$[M+Na]^+$	638.0	168.4	3.4(5)
Y_3 (P1 antigen)	$[M+Na]^+$	638.0	168.2	1.4(7)
$^{1,5}X_{2\alpha}$ (Di-Le^A)	$[M+Na]^+$	649.6	168.1	2.6(5)
*Y_3-N_2 (LNT)	$[M+Na]^+$	651.0	180.3	2.5(6)
*Y_3-N_2 (GNLNLN)	$[M+Na]^+$	651.0	173.0	1.8(9)
*Y_3-N_2 (Di-Le^c)	$[M+Na]^+$	651.0	172.7	1.9(28)
$^{0,2}X_{2\beta}$-N_2 (B tetra type 1)	$[M+Na]^+$	651.6	171.5	3.4(5)
*Z_3 (GNLNLN)	$[M+Na]^+$	661.0	110.4	2.2(5)
*$^{0,2}A_4$ (P1 penta)	$[M+Na]^+$	670.0	171.4	1.1(5)
*$^{0,2}A_4$ (LNT)	$[M+Na]^+$	671.0	170.1	1.6(7)
$^{0,2}X_{2\alpha}$-N_2 (Di-Le^A)	$[M+Na]^+$	676.6	183.3	3.3(8)
$^{0,2}X_{2\alpha}$-N_2 (Le^ALe^x)	$[M+Na]^+$	677.0	175.6	2.5(5)
*Y_3 (GNLNLN)	$[M+Na]^+$	679.0	177.2	5.5(5)
*Y_3 (Di-Le^c)	$[M+Na]^+$	679.0	176.5	1.9(8)
*$^{1,5}A_4$ (P1 penta)	$[M+Na]^+$	684.0	176.9	3.4(5)
*$^{0,2}X_3$-N_2 (P1 penta)	$[M+Na]^+$	692.0	145.8	1.0(5)
*$^{0,2}X_3$-N_2 (LNT)	$[M+Na]^+$	693.0	111.8	2.2(5)
*$B_{3\alpha}$ (Di-Le^A)	$[M+Na]^+$	696.6	175.9	1.9(27)
$B_{3\alpha}$ (Le^ALe^x)	$[M+Na]^+$	697.0	172.0	2.7(11)
*B_4 (LNFP1)	$[M+Na]^+$	697.0	180.4	0.5(10)
*B_3 (LNFP2)	$[M+Na]^+$	697.0	180.1	1.5(5)
*B_4 (H-type2-LN-LN)	$[M+Na]^+$	697.0	178.5	1.7(12)
B_3 (B tetra type 1)	$[M+Na]^+$	697.6	170.8	1.4(10)
*$^{1,5}X_3$ (Di-Le^c)	$[M+Na]^+$	707.0	144.0	5.6(5)
*$^{1,5}X_3$ (LNT)	$[M+Na]^+$	707.0	148.1	0.5(5)
*$^{1,5}X_3$ (GNLNLN)	$[M+Na]^+$	707.0	147.1	2.1(5)
*B_4 (P1 penta)	$[M+Na]^+$	712.0	171.4	1.9(5)
*B_4 (P1 antigen)	$[M+Na]^+$	713.0	167.2	3.0(5)
C_3 (B tetra type 1)	$[M+Na]^+$	714.6	179.6	1.3(14)
*$C_{3\alpha}$ (Di-Le^A)	$[M+Na]^+$	715.0	176.0	1.6(18)
$C_{3\alpha}$ (Le^ALe^x)	$[M+Na]^+$	715.0	173.7	2.1(8)
*C_4 (LNFP1)	$[M+Na]^+$	715.0	180.5	1.9(8)
*C_3 (LNFP2)	$[M+Na]^+$	715.0	183.8	1.2(5)
*C_4 (P1 antigen)	$[M+Na]^+$	731.0	169.8	1.5(5)
C_4 (LNnT)	$[M+Na]^+$	731.0	173.3	1.8(11)
*Y_4 (LNFP1)	$[M+Na]^+$	731.0	179.7	0.6(5)
*$Y_{3\beta}$ (LNFP2)	$[M+Na]^+$	731.0	176.5	0.9(5)
$Z_{1\beta}$-N_2 (2'F-B type 2)	$[M+Na]^+$	737.7	180.7	2.9(14)
*$^{1,5}X_{3\alpha}$ (LNFP2)	$[M+Na]^+$	742.0	191.3	1.1(5)

$*^{2,4}X_3$-N_2 (P1 penta)	$[M+Na]^+$	752.0	174.1	3.1(5)
$*B_4$ (GNLNLN)	$[M+Na]^+$	753.0	183.9	0.9(5)
$*^{2,4}X_3$-N_2 (H-type2-LN-LN)	$[M+Na]^+$	753.0	179.3	1.6(8)
$*B_4$ (LNT)	$[M+Na]^+$	754.0	180.0	2.9(16)
$*B_4$ (Di-Le^c)	$[M+Na]^+$	754.0	182.7	3.2(30)
$Y_{1\beta}$-N_2 (2'F-B type 2)	$[M+Na]^+$	755.7	187.5	1.6(23)
M-N_2 (B tetra type 1)	$[M+Na]^+$	755.7	187.1	0.8(19)
$*^{0,2}X_{3\alpha}$ (LNFP2)	$[M+Na]^+$	756.7	190.3	0.7(5)
$*^{1,5}X_4$ (LNFP1)	$[M+Na]^+$	758.6	192.4	0.6(7)
$Y_{2\alpha'}$ (2'F-B type 2)	$[M+Na]^+$	768.0	183.8	3.3(8)
$*C_4$ (LNT)	$[M+Na]^+$	772.0	180.5	1.6(27)
$*C_4$ (Di-Le^c)	$[M+Na]^+$	772.0	180.2	2.1(32)
M-N_2 (LNnT)	$[M+Na]^+$	772.0	182.8	1.0(22)
$*^{2,4}A_5$ (P1 penta)	$[M+Na]^+$	772.0	173.6	1.6(5)
$*^{2,4}A_5$ (P1 antigen)	$[M+Na]^+$	773.0	177.5	1.6(5)
$*Z_4$ (P1 antigen)	$[M+Na]^+$	782.0	149.1	2.1(4)
B tetra type 1	$[M+Na]^+$	783.7	195.6	1.9(27)
$Y_{1\beta}$ (2'F-B type 2)	$[M+Na]^+$	783.7	196.4	4.4(10)
LNnT	$[M+Na]^+$	799.7	188.0	1.3(28)
$*Y_4$ (P1 antigen)	$[M+Na]^+$	800.0	146.7	3.3(8)
$*Y_4$-N_2 (P1 penta)	$[M+Na]^+$	812.0	178.3	0.7(13)
*M-N_2 (Di-Le^c)	$[M+Na]^+$	812.8	185.2	1.6(45)
*M-N_2 (LNT)	$[M+Na]^+$	812.8	190.7	0.8(41)
$*Y_4$-N_2 (GNLNLN)	$[M+Na]^+$	813.0	191.5	0.9(8)
$*Y_4$-N_2 (H-type2-LN-LN)	$[M+Na]^+$	813.0	191.0	1.6(7)
$*^{0,2}A_5$ (P1 penta)	$[M+Na]^+$	832.0	183.2	0.7(5)
$*^{0,2}A_5$ (P1 antigen)	$[M+Na]^+$	833.0	185.0	3.1(5)
$*Y_4$ (P1 penta)	$[M+Na]^+$	840.0	184.1	0.6(13)
*3'SLN-Lec	$[M+Na]^+$	840.8	188.0	0.9(5)
*Di-Le^c	$[M+Na]^+$	840.8	187.3	1.5(76)
*LNT	$[M+Na]^+$	840.8	196.4	1.4(67)
Y_4 (GNLNLN)	$[M+Na]^+$	841.0	200.1	2.1(10)
$*Y_4$ (H-type2-LN-LN)	$[M+Na]^+$	841.0	198.7	2.2(6)
B_3 (2'F-B type 2)	$[M+Na]^+$	844.0	198.0	4.1(9)
C_3 (2'F-B type 2)	$[M+Na]^+$	861.0	198.5	2.4(15)
$*^{0,2}A_5$ (GNLNLN)	$[M+Na]^+$	874.0	172.6	2.0(8)
*LNFP1	$[M+Na]^+$	875.0	204.4	1.4(162)
*LNFP2	$[M+Na]^+$	875.0	201.3	1.2(181)
*LNFP3	$[M+Na]^+$	875.0	199.2	1.0(17)
$*B_5$ (P1 antigen)	$[M+Na]^+$	875.0	187.8	1.8(5)
*LNFP5	$[M+Na]^+$	875.0	201.8	0.7(18)
$*C_5$ (P1 antigen)	$[M+Na]^+$	893.0	194.4	0.8(7)
$*^{0,2}X_4$-N_2 (GNLNLN)	$[M+Na]^+$	896.0	147.4	0.6(5)

*B_5 (H-type2-LN-LN)	$[M+Na]^+$	900.0	209.3	2.9(12)
M-N_2 (2'F-B type 2)	$[M+Na]^+$	902.0	207.3	1.7(24)
$^{2,4}A_4$ (Di-Le^A)	$[M+Na]^+$	903.0	198.7	5.2(5)
$^{2,4}A_4$ (Le^ALe^x)	$[M+Na]^+$	903.0	199.2	4.5(5)
*B_5 (P1 penta)	$[M+Na]^+$	915.0	197.0	2.1(8)
*C_5 (H-type2-LN-LN)	$[M+Na]^+$	918.0	206.6	2.5(12)
2'F-B type 2	$[M+Na]^+$	929.8	217.3	2.7(27)
*C_5 (P1 penta)	$[M+Na]^+$	933.0	192.3	0.7(8)
*M-N_2 (P1 antigen)	$[M+Na]^+$	933.8	195.8	1.3(15)
$Z_{3\alpha'}$-N_2 (Di-Le^A)	$[M+Na]^+$	941.0	219.6	2.7(5)
$Y_{3\alpha'}$-N_2 (Le^ALe^x)	$[M+Na]^+$	948.0	200.8	7.0(5)
*$^{2,4}X_4$-N_2 (GNLNLN)	$[M+Na]^+$	956.0	213.3	2.6(5)
$Y_{1\beta \text{ or } 3\alpha''}$-$N_2$ (Le^ALe^x)	$[M+Na]^+$	959.0	211.0	1.6(20)
*$Y_{3\alpha'}$-N_2 (Di-Le^A)	$[M+Na]^+$	959.0	211.0	1.8(30)
*P1 antigen	$[M+Na]^+$	961.8	203.4	0.9(18)
$Y_{3\alpha''}$ (Di-Le^A)	$[M+Na]^+$	971.0	206.3	1.4(5)
$Y_{3\alpha'}$ (Le^ALe^x)	$[M+Na]^+$	971.0	206.9	1.6(13)
*M-N_2 (P1 penta)	$[M+Na]^+$	974.4	202.9	0.7(15)
*C_5 (GNLNLN)	$[M+Na]^+$	975.0	215.3	1.3(11)
*$^{0,2}X_{3\alpha''}$-N_2 (Le^ALe^x)	$[M+Na]^+$	985.0	218.3	2.2(10)
*$Y_{3\alpha'}$ (Di-Le^A)	$[M+Na]^+$	987.0	214.7	2.3(33)
*α-cyclodextrin	$[M+Na]^+$	995.6	200.7	0.5(4)
$^{0,2}X_{1\beta \text{ or } 3\alpha''}$-$N_2$ (Di-Le^A)	$[M+Na]^+$	1001.0	209.3	1.8(5)
$^{0,2}X_{2\alpha'' \text{ or } 1\beta}$-$N_2$ (Le^ALe^x)	$[M+Na]^+$	1001.0	217.7	2.1(9)
*P1 penta	$[M+Na]^+$	1002.4	206.2	0.6(30)
*M-N_2 (GNLNLN)	$[M+Na]^+$	1015.9	220.6	2.3(24)
*Y_5-N_2 (H-type2-LN-LN)	$[M+Na]^+$	1016.0	220.2	2.2(4)
$^{1,5}A_4$ (Di-Le^A)	$[M+Na]^+$	1018.0	208.6	4.0(5)
*LNDFH1	$[M+Na]^+$	1023.0	225.6	1.1(18)
*LNDFH2	$[M+Na]^+$	1023.0	220.6	1.0(18)
*GNLNLN	$[M+Na]^+$	1043.9	230.5	0.8(25)
*B_4 (Di-Le^A)	$[M+Na]^+$	1046.0	228.0	2.4(13)
C_4 (Le^ALe^x)	$[M+Na]^+$	1064.0	225.2	2.8(17)
*C_4 (Di-Le^A)	$[M+Na]^+$	1064.0	225.4	2.4(30)
$^{2,4}X_{3\alpha'}$ (Le^ALe^x)	$[M+Na]^+$	1073.0	227.3	1.4(5)
M-N_2 (Le^ALe^x)	$[M+Na]^+$	1105.0	232.4	1.5(23)
*M-N_2 (Di-Le^A)	$[M+Na]^+$	1105.0	230.9	1.0(37)
Le^ALe^x	$[M+Na]^+$	1133.0	237.9	3.3(25)
*Di-Le^A	$[M+Na]^+$	1133.0	238.9	3.1(49)
*β-cyclodextrin	$[M+Na]^+$	1157.0	231.4	0.6(4)
*Y_6-N_2 (H-type2-LN-LN)	$[M+Na]^+$	1178.0	232.0	1.4(7)
*Tri-LacNAc	$[M+Na]^+$	1206.0	232.6	0.6(5)
*Y_6 (H-type2-LN-LN)	$[M+Na]^+$	1206.0	238.7	4.2(8)

*C_7 (H-type2-LN-LN)	$[M+Na]^+$	1283.0	243.2	4.0(8)
*M-N_2 (H-type2-LN-LN)	$[M+Na]^+$	1324.2	245.5	0.4(7)
*H-type2-LN-LN	$[M+Na]^+$	1352.2	252.1	0.6(7)

Footnotes on table nomenclature:

1. Carbohydrate nomenclature:

2'F-B type 2	Galα1-3[Fucα1-2]Galβ1-4[Fucα1-3]GlcNAcβ-Sp
3'SLN-Lec	Neu5Acα2-3Galβ1-4GlcNAcβ1-3Galβ1-3GlcNAcβ-Sp
α-cyclodextrin	Cyclomaltohexaose
β-cyclodextrin	Cyclomaltoheptaose
B2-tri	Galα1-3Galβ1-4GlcNAcβ-Sp
B tetra type 1	Galα1-3[Fucα1-2]Galβ1-3GlcNAcβ-Sp
Di-Le^A	Galβ1-3[Fucα1-4]GlcNAcβ1-3Galβ1-3[Fucα1-4]GlcNAcβ-Sp
Di-Le^c	Galβ1-3GlcNAcβ1-3Galβ1-3GlcNAcβ-Sp
Galα3-type1	Galα1-3Galβ1-3GlcNAcβ-Sp
GNLNLN	GlcNAcβ1-3(Galβ1-4GlcNAcβ1-3)$_2$β-Sp
H-type2-LN-LN	Fucα1-2(Galβ1-4GlcNAcβ1-3)$_3$β -Sp
Lac	Galβ1-4Glcβ-Sp
Lactose	Galβ1-4Glc
LacNAc	Galβ1-4GlcNAcβ-Sp
Le^ALe^x	Galβ1-3[Fucα1-4]GalNAcβ1-3Galβ1-4[Fucα1-3]GlcNAcβ-Sp
Le^c	Galβ1-3GlcNAcβ-Sp
LN	Galβ1-4GlcNAc
LNDFH1	Fucα1-2Galβ1-3[Fucα1-4]GlcNAcβ1-3Galβ1-4Glc
LNDFH2	Galβ1-3[Fucα1-4]GlcNAcβ1-3Galβ1-4[Fucα1-3]Glc
LNFP1	Fucα1-2Galβ1-3GlcNAcβ1-3Galβ1-4Glc
LNFP2	Galβ1-3[Fucα1-4]GlcNAcβ1-3Galβ1-4Glc
LNFP3	Galβ1-4[Fucα1-3]GlcNAcβ1-3Galβ1-4Glc
LNFP5	Galβ1-3GlcNAcβ1-3Galβ1-4[Fucα1-3]Glc
LNnT	Galβ1-4GlcNAcβ1-3Galβ1-4Glcβ-Sp
LNT	Galβ1-3GlcNAcβ1-3Galβ1-4GlcNAcβ-Sp
Maltose	Glcα1-4Glc
P1 antigen	Galα1-4Galβ1-4GlcNAcβ1-3Galβ1-4Glcβ-Sp
P1 penta	Galb1-3GalNAcβ1-3Galα1-4Galβ1-4GlcNAcβ-Sp
P1 tri	Galα1-4Galβ1-4GlcNAcβ-Sp
Pk	Galα1-4Galβ1-4Glcβ-Sp
Tri-LacNAc	(Galβ1-4GlcNAcβ1-3)$_3$β-Sp

Fuc - Fucose
Gal - Galactose
Glc - Glucose
GlcNAc - N-acetylglucosamine
GalNAc – N-acetylgalactosamine

Neu5Ac - N-Acetylneuraminic Acid
Sp – azide spacer not utilized in these studies but which readily loses N_2 in the MS accounting for some carbohydrate fragment peaks

Fragmentation is in Domon and Costello nomenclature (Figure 1.2).[27]

Table A.2 Oligonucleotide class species and collision cross sections referred to in Chapter II.[2]

Name (parent name if fragmented)	species	*m/z* (Da)	Ω (Å^2)	σ (# of measurements)
d2-G-H_2O (GACT)	$[M+H]^+$	492.1	129.2	0.3(6)
w2-G-H_2O (TCAG)	$[M+H]^+$	492.1	137.7	0.5(6)
w2-C-H_2O (TGAC)	$[M+H]^+$	492.6	135.5	0.4(6)
d2-C-H_2O or x2-T-H_2O (CAGT)	$[M+H]^+$	492.9	125.7	0.5(6)
a2 (TCGA)	$[M+H]^+$	514.1	134.3	0.5(6)
a2 (TCAG)	$[M+H]^+$	514.1	138.2	0.3(6)
a2 (TCG)	$[M+H]^+$	514.1	150.9	0.4(6)
a2-T (ACTG)	$[M+H]^+$	524.1	137.9	0.5(6)
z2 or a2 (GCAT)	$[M+H]^+$	539.1	141.6	0.4(6)
w2 (GCT)	$[M+H]^+$	610.1	154.9	0.6(6)
w2 (GTC)	$[M+H]^+$	612.1	145.5	0.4(6)
c2 (GCT)	$[M+H]^+$	618.1	163.1	0.5(6)
w2 (TGAC)	$[M+H]^+$	621.1	153.2	0.6(6)
w2 (TGCA)	$[M+H]^+$	621.1	156.7	0.3(6)
w2 (CGTA)	$[M+H]^+$	636.1	163.5	0.1(6)
w2 (GCTA)	$[M+H]^+$	636.1	165.1	0.4(6)
w2 (CGAT)	$[M+H]^+$	636.1	152	0.4(6)
w2 (GCAT)	$[M+H]^+$	636.1	153.7	0.2(6)
w2 (ACTG)	$[M+H]^+$	652.1	142.1	0.7(6)
w2 (CTG)	$[M+H]^+$	652.1	161.9	0.2(6)
w2 (TCAG)	$[M+H]^+$	661.1	158.4	0.2(6)
TGC-G (TGC)	$[M+H]^+$	710.2	171	1.3(6)
GTC-G (GTC)	$[M+H]^+$	710.2	172.5	0.2(6)
GCT-G (GCT)	$[M+H]^+$	710.2	176	0.9(6)
a3-G (ATGC)	$[M+H]^+$	716.2	171.7	0.3(6)
a3-C (TACG)	$[M+H]^+$	716.2	170.5	0.4(6)
a3-G (TAGC)	$[M+H]^+$	716.2	173.7	0.3(6)
a3-C (ATCG)	$[M+H]^+$	716.2	172.2	0.1(6)
CGT-C (CGT)	$[M+H]^+$	750.2	170.9	0.3(6)
TCG-C (TCG)	$[M+H]^+$	750.2	182.9	1.0(6)
CTG-C (CTG)	$[M+H]^+$	750.2	176.3	1.3(6)
x3-G or w3-G-H_2O (CATG)	$[M+H]^+$	796.1	179.8	0.4(6)
x3-G or w3-G-H_2O (CTAG)	$[M+H]^+$	796.1	181.6	0.8(6)
c3-G or x3-C (GATC)	$[M+H]^+$	796.1	181.8	0.3(6)
c3-G (GTAC)	$[M+H]^+$	796.1	179.2	0.3(6)
w3-C (GACT)	$[M+H]^+$	814.1	156.1	0.4(6)
w3-G or d3-C (CATG)	$[M+H]^+$	814.1	179.5	0.7(6)
w3-G or d3-C (CTAG)	$[M+H]^+$	814.1	186.4	1.3(6)
d3-G or w3-C (GATC)	$[M+H]^+$	814.1	182	0.3(6)
d3-G or w3-C (GTAC)	$[M+H]^+$	814.1	183.1	0.3(6)
w3-G (CTGA)	$[M+H]^+$	814.1	170.4	0.8(6)
w3-C (GCAT)	$[M+H]^+$	814.1	180.3	0.4(6)
w3-C (GTCA)	$[M+H]^+$	814.1	172.1	0.8(6)

w3-G (CAGT)	$[M+H]^+$	814.3	172	0.7(6)
CGT	$[M+H]^+$	861.2	187.6	0.6(6)
TCG	$[M+H]^+$	861.2	186.1	0.4(6)
TGC	$[M+H]^+$	861.2	190.2	0.3(6)
GTC	$[M+H]^+$	861.2	187.2	0.1(6)
GCT	$[M+H]^+$	861.2	198.3	0.1(6)
CTG	$[M+H]^+$	861.2	190.5	0.2(6)
w3 (GCTA)	$[M+H]^+$	925.2	187.8	0.1(6)
w3 (GACT)	$[M+H]^+$	925.2	191.4	0.3(6)
w3 (GATC)	$[M+H]^+$	925.2	193.8	0.2(6)
w3 (GTAC)	$[M+H]^+$	925.2	197.3	0.1(6)
w3 (GCAT)	$[M+H]^+$	925.2	200.6	0.5(6)
w3 (GTCA)	$[M+H]^+$	925.2	202.3	0.2(6)
w3 (CAGT)	$[M+H]^+$	965.2	197.9	0.5(6)
w3 (CGTA)	$[M+H]^+$	965.2	193	0.6(6)
W3 (ACTG)	$[M+H]^+$	965.2	199.1	0.3(6)
w3 (CTAG)	$[M+H]^+$	965.2	191.2	0.5(6)
w3 (CGAT)	$[M+H]^+$	965.2	200.5	0.3(6)
w3 (CTGA)	$[M+H]^+$	965.2	202.6	0.3(6)
GACT-G (GACT)	$[M+H]^+$	1023.2	211.9	0.4(6)
GCTA-G (GCTA)	$[M+H]^+$	1023.2	209.2	0.8(6)
GATC-G (GATC)	$[M+H]^+$	1023.2	212.5	0.4(6)
GTAC-G (GTAC)	$[M+H]^+$	1023.2	211.4	0.5(6)
GCAT-G (GCAT)	$[M+H]^+$	1023.2	215	0.6(6)
GTCA-G (GTCA)	$[M+H]^+$	1023.2	216.3	0.7(6)
ATGC-C (ATGC)	$[M+H]^+$	1063.2	213.2	0.6(6)
CAGT-C (CAGT)	$[M+H]^+$	1063.2	214.4	0.8(6)
CGTA-C (CGTA)	$[M+H]^+$	1063.2	215.7	0.8(6)
CGAT-C (CGAT)	$[M+H]^+$	1063.2	216.3	0.7(6)
CGTA	$[M+H]^+$	1174.2	234	0.5(6)
ACGT	$[M+H]^+$	1174.3	219.3	0.3(6)
AGTC	$[M+H]^+$	1174.3	214.3	0.4(6)
ATGC	$[M+H]^+$	1174.3	232.3	0.3(6)
CAGT	$[M+H]^+$	1174.3	220.7	0.5(6)
GCTA	$[M+H]^+$	1174.3	223.1	0.7(6)
TACG	$[M+H]^+$	1174.3	231.9	0.5(6)
GACT	$[M+H]^+$	1174.3	228.6	0.2(6)
GCTA	$[M+H]^+$	1174.3	223.3	0.6(6)
TCGA	$[M+H]^+$	1174.3	217.2	0.5(6)
ACTG	$[M+H]^+$	1174.3	227.4	0.4(6)
CATG	$[M+H]^+$	1174.3	216.7	0.4(6)
CTAG	$[M+H]^+$	1174.3	231.6	0.3(6)
GATC	$[M+H]^+$	1174.3	210.7	0.4(6)
GTAC	$[M+H]^+$	1174.3	224.1	0.3(6)
TAGC	$[M+H]^+$	1174.3	220.3	0.4(6)
TGAC	$[M+H]^+$	1174.3	224.3	0.4(6)
AGCT	$[M+H]^+$	1174.3	232.4	0.5(6)
ATCG	$[M+H]^+$	1174.3	226.2	0.6(6)

CGAT	$[M+H]^+$	1174.3	215.4	0.4(6)
CTGA	$[M+H]^+$	1174.3	231.4	0.4(6)
GCAT	$[M+H]^+$	1174.3	229.1	0.5(6)
TCAG	$[M+H]^+$	1174.3	233	0.1(6)
TGCA	$[M+H]^+$	1174.3	230	0.3(6)

Footnotes on table nomenclature:

2. Oligonucleotide nomenclature:

G - Guanine
A - Adenine
C - Cytosine
T – Thymine

Oligonucleotide fragmentation is specified in McLucky nomenclature.[175] In this table, tentative fragment ion assignments are given by the predominant fragmentation channels observed previously.

Table A.3 Lipid class species and collision cross sections referred to in Chapter II.[3]

Name (parent name if fragmented)	species	*m/z* (Da)	Ω (Å^2)	σ (# of measurements)
PE 34:2	$[M+H]^+$	716.5	206.9	2.0(29)
PE 34:1	$[M+H]^+$	718.5	205.8	4.3(29)
SM (36:1)	$[M+H]^+$	731.6	221.1	2.0(33)
PE 34:2	$[M+Na]^+$	738.5	213.5	2.1(29)
PE 34:1	$[M+Na]^+$	740.5	214.7	1.5(29)
SM (36:1)	$[M+Na]^+$	753.6	221.3	2.6(33)
PC 34:2	$[M+H]^+$	758.6	217.4	3.2(33)
SM (38:1)	$[M+H]^+$	759.7	229.8	3.4(33)
PC 34:1	$[M+H]^+$	760.6	219.1	2.7(33)
PE 36:4	$[M+Na]^+$	762.5	214.4	1.6(29)
PE 36:2	$[M+Na]^+$	766.5	220.9	2.7(29)
PE 36:1	$[M+Na]^+$	768.6	221.7	4.8(29)
PC 34:2	$[M+Na]^+$	780.6	218.9	2.8(33)
SM (38:1)	$[M+Na]^+$	781.6	231.3	2.5(33)
PC 34:1	$[M+Na]^+$	782.6	221.7	3.2(33)
PC 36:2	$[M+H]^+$	786.6	222.6	2.2(33)
SM (40:1)	$[M+H]^+$	787.7	232.2	5.0(33)
PE 38:5	$[M+Na]^+$	788.5	220.6	5.2(29)
PC 36:1	$[M+H]^+$	788.6	227.4	4.3(33)
PE 38:4	$[M+Na]^+$	790.5	228.1	3.6(29)
CB (40:1)	$[M+Na]^+$	806.6	232.9	2.4(33)
PC 36:2	$[M+Na]^+$	808.6	226.7	4.6(33)
CB (39:1)h	$[M+Na]^+$	808.6	236.6	2.9(33)
PS 36:2	$[M+Na]^+$	810.5	217.1	5.5(29)
PC 36:1	$[M+Na]^+$	810.6	228.1	2.0(33)
PS 36:1	$[M+Na]^+$	812.5	222.6	2.4(29)
SM (42:2)	$[M+H]^+$	813.7	241.8	2.5(33)
SM (42:1)	$[M+H]^+$	815.7	242.1	6.3(33)
CB (40:2)h	$[M+Na]^+$	820.6	236.2	5.6(33)
CB (40:1)h	$[M+Na]^+$	822.6	234.6	5.3(33)
CB (42:6)	$[M+Na]^+$	824.6	237.9	1.9(33)
CB (42:2)	$[M+Na]^+$	832.7	238.8	1.7(33)
PS 38:4	$[M+Na]^+$	834.5	225.5	2.1(29)
CB (42:1)	$[M+Na]^+$	834.7	239.3	2.6(33)
SM (42:2)	$[M+Na]^+$	835.7	239.4	2.8(33)
CB (41:1)h	$[M+Na]^+$	836.7	240.2	3.4(33)
SM (42:1)	$[M+Na]^+$	837.7	239.3	4.7(33)
PS 38:1	$[M+Na]^+$	840.6	222.6	5.5(29)
CB (42:3)h	$[M+Na]^+$	846.6	238.8	2.2(33)
CB (42:2)h	$[M+Na]^+$	848.7	240.3	2.7(33)
CB (44:7)	$[M+Na]^+$	850.6	242.8	1.9(33)
CB (44:6)	$[M+Na]^+$	852.6	243.3	3.7(33)
PS 40:6	$[M+Na]^+$	858.5	231.9	2.8(29)

CB (44:2)	$[M+Na]^+$	860.7	245.9	5.2(33)
CB (44:1)	$[M+Na]^+$	862.7	244.3	5.5(33)
CB (44:8)h	$[M+Na]^+$	864.6	245.2	2.9(33)
CB (44:7)h	$[M+Na]^+$	866.6	252.2	5.1(33)
SM (44:1)	$[M+Na]^+$	866.7	247.9	4.3(33)
CB (44:2)h	$[M+Na]^+$	876.7	246.7	3.7(33)
PS 42:9	$[M+Na]^+$	880.5	238	1.7(29)
PS 42:8	$[M+Na]^+$	882.5	230.8	3.0(29)
PC 42:1	$[M+Na]^+$	894.7	238.2	2.3(33)
PC 42:0	$[M+Na]^+$	896.7	246.3	2.1(33)

Footnotes on table nomenclature:

3. Lipid nomenclature :

Glycerophospholipids:

Ex. PC X:Y

PC, PE, PS = abbreviated names phosphatidylcholine, phosphatidylethanolamine, phosphatidylserine.

X = total number of carbons in fatty acid chains
Y = total number of double bonds in fatty acid chains

Sphingolipids:

Ex. SM (x:y)

SM, CB = abbreviated names sphingomyelin, cerebroside

x = total number of carbons in the amide linked fatty acid of the ceramide plus eighteen carbons from the sphingosine backbone
y = total number of double bonds, one trans double bond in the sphingosine backbone plus the number of double bonds in the amide linked fatty acid of the ceramide

( ) = used to distinguish sphingolipid from glycerophospholipid nomenclature in the table

Hydroxylation on Cerebrosides:

Ex. CB (x:y)h

h = denotes hydroxylation on the number two carbon (from carbonyl) of the amide linked fatty acid.

APPENDIX B

TABULAR DATA FOR SIMULTANEOUS GLYCOMICS IDENTIFICATIONS

Table B.1 Peptide signals identified from specified glycoproteins studied in this work. All are using MALDI unless specified otherwise.

Protein	*m/z* (Da)	Species	Peptide
RNAse B	858.4	$[M+H]^+$	YPNCAYK
RNAse B	880.3	$[M+Na]^+$	YPNCAYK
RNAse B	1447.9	$[M+H]^+$	ETGSSKYNCAYK
RNAse B	1470.1	$[M+Na]^+$	ETGSSKYNCAYK
RNAse B	2168.1	$[M+H]^+$	HIIVACEGNPYVPVHFDASV
RNAse B	2190.0	$[M+Na]^+$	HIIVACEGNPYVPVHFDASV
RNAse B	2330.6	$[M+Na]^+$	QHMDSSTSAASSSNYCNQMMK
RNAseB (ESI)	611.4	$[M+Na]^+$	ETAAAK
RNAseB (ESI)	685.4	$[M+Na]^+$	TTQANK
RNAseB (ESI)	858.4	$[M+H]^+$	YPNCAYK
RNAseB (ESI)	880.4	$[M+Na]^+$	YPNCAYK
RNAseB (ESI)	576.9	$[M+2H]^{+2}$	KETAAAKFER
RNAseB (ESI)	724.6	$[M+2H]^{+2}$	ETGSSKYPNCAYK
RNAseB (ESI)	1084.2	$[M+2H]^{+2}$	HIIVACEGNPYVPVHFDASV
RNAseB (ESI)	1087.2	$[M+2H]^{+2}$	NGQTNCYQSYSMSITDCR
RNAseB (ESI)	1095.2	$[M+H+Na]^{+2}$	HIIVACEGNPYVPVHFDASV
RNAseB (ESI)	1098.2	$[M+H+Na]^{+2}$	NGQTNCYQSYSMSITDCR
RNAseB (ESI)	1154.6	$[M+2H]^{+2}$	QHMDSSTSAASSSNYCNQMMK
ovalbumin	888.6	$[M+H]^+$	IKVYLPR
ovalbumin	1190.6	$[M+H]^+$	ADHPFLFCIK
ovalbumin	1209.5	$[M+H]^+$	DEDTQAMPFR
ovalbumin	1212.6	$[M+Na]^+$	ADHPFLFCIK
ovalbumin	1345.7	$[M+H]^+$	HIATNAVLFFGR
ovalbumin	1368.0	$[M+Na]^+$	HIATNAVLFFGR
ovalbumin	1465.8	$[M+H]^+$	YPILPEYLQCVK
ovalbumin	1488.1	$[M+Na]^+$	YPILPEYLQCVK
ovalbumin	1555.7	$[M+H]^+$	AFKDEDTQAMPFR
ovalbumin	1578.1	$[M+Na]^+$	AFKDEDTQAMPFR
ovalbumin	1581.7	$[M+H]^+$	LTEWTSSNVMEER
ovalbumin	1687.8	$[M+H]^+$	GGLEPINFQTAADQAR
ovalbumin	1710.2	$[M+Na]^+$	GGLEPINFQTAADQAR
ovalbumin	1731.9	$[M+H]^+$	HIATNAVLFFGRCVSP
ovalbumin	1754.3	$[M+Na]^+$	HIATNAVLFFGRCVSP

ovalbumin	1773.9	$[M+H]^+$	ISQAVHAAHAEINEAGR
ovalbumin	1796.3	$[M+Na]^+$	ISQAVHAAHAEINEAGR
ovalbumin	1859.0	$[M+H]^+$	ELINSWVESQTNGIIR
ovalbumin	1881.8	$[M+Na]^+$	ELINSWVESQTNGIIR
ovalbumin	1951.0	$[M+H]^+$	LTEWTSSNVMEERKIK
ovalbumin	2008.9	$[M+H]^+$	EVVGSAEAGVDAASVSEEFR
ovalbumin	2027.1	$[M+H]^+$	YPILPEYLQCVKELYR
ovalbumin	2227.6	$[M+H]^+$	LYAEERYPILPEYLQCVK
ovalbumin	2249.8	$[M+H]^+$	ELYRGGLEPINFQTAADQAR
ovalbumin	2281.2	$[M+H]^+$	DILNQITKPNDVYSFSLASR
ovalbumin	2305.6	$[M+Na]^+$	DILNQITKPNDVYSFSLASR
ovalbumin	2460.3	$[M+H]^+$	NVLQPSSVDSQTAMVLVNAIVFK
ovalbumin	2483.4	$[M+Na]^+$	NVLQPSSVDSQTAMVLVNAIVFK
fetuin	522.3	$[M+H]^+$	HLPR
fetuin	544.3	$[M+H]^+$	LCPGR
fetuin	545.3	$[M+Na]^+$	HLPR
fetuin	557.3	$[M+H]^+$	VWPR
fetuin	579.3	$[M+Na]^+$	VWPR
fetuin	653.3	$[M+Na]^+$	GSVIQK
fetuin	726.4	$[M+H]^+$	IRYFK
fetuin	748.4	$[M+Na]^+$	IRYFK
fetuin	767.3	$[M+Na]^+$	QYGFCK
fetuin	774.4	$[M+H]^+$	AHYDLR
fetuin	787.4	$[M+H]^+$	EVVDPTK
fetuin	789.5	$[M+H]^+$	CNLLAEK
fetuin	809.4	$[M+Na]^+$	EVVDPTK
fetuin	812.4	$[M+Na]^+$	CNLLAEK
fetuin	816.4	$[M+H]^+$	ALGGEDVR
fetuin	839.5	$[M+H]^+$	IRYFKI
fetuin	840.4	$[M+Na]^+$	ALGGEDVR
fetuin	1072.9	$[M+H]^+$	IPLDPVAGYK
fetuin	1094.5	$[M+Na]^+$	IPLDPVAGYK
fetuin	1155.0	$[M+H]^+$	HTLNQIDSVK
fetuin	1177.0	$[M+Na]^+$	HTLNQIDSVK
fetuin	1253.0	$[M+H]^+$	LCPGRIRYFK
fetuin	1270.1	$[M+H]^+$	QDGQFSVLFTK
fetuin	1275.0	$[M+Na]^+$	LCPGRIRYFK
fetuin	1291.9	$[M+Na]^+$	QDGQFSVLFTK
fetuin	1431.3	$[M+Na]^+$	CDSSPDSAEDVRK
fetuin	1474.8	$[M+H]^+$	TPIVGQPSIPGGPVR
fetuin	1497.3	$[M+Na]^+$	TPIVGQPSIPGGPVR
fetuin	1525.1	$[M+Na]^+$	GYKHTLNQIDSVK
fetuin	1626.8	$[M+H]^+$	LCPDCPLLAPLNDSR

fetuin	1649.7	$[M+Na]^+$	LCPDCPLLAPLNDSR
fetuin	1692.9	$[M+H]^+$	HTLNQIDSVKVWPR
fetuin	1754.9	$[M+H]^+$	KLCPDCPLLAPLNDSR
fetuin	1778.4	$[M+Na]^+$	KLCPDCPLLAPLNDSR
fetuin	1920.9	$[M+H]^+$	QQTQHAVEGDCDIHVLK
fetuin	1943.5	$[M+Na]^+$	QQTQHAVEGDCDIHVLK
fetuin	2120.9	$[M+H]^+$	HTFSGVASVESSSGEAFHVG K
fetuin	2142.8	$[M+Na]^+$	HTFSGVASVESSSGEAFHVG K
fetuin	2462.3	$[M+H]^+$	AQFVPLPVSVSVEFAVAATD CIAK
fetuin	2485.3	$[M+Na]^+$	AQFVPLPVSVSVEFAVAATD CIAK
fetuin	2531.1	$[M+H]^+$	QDGQFSVLFTKCDSSPDSAE DVR
fetuin	3016.7	$[M+H]^+$	VVHAVEVALATFNAESNGSY LQLVEISR
fetuin	3402.6	$[M+H]^+$	IPLDPVAGYKEPACDDPDTE QAALAAVDYINK
HGP	696.3	$[M+H]^+$	EYQTR
HGP	777.4	$[M+H]^+$	ENGTISR
HGP	806.4	$[M+H]^+$	KQEEGES
HGP	826.7	$[M+H]^+$	QHEKER
HGP	961.4	$[M+H]^+$	DKCEPLEK
HGP	983.6	$[M+Na]^+$	DKCEPLEK
HGP	994.8	$[M+H]^+$	TEDTIFLR
HGP	1016.5	$[M+Na]^+$	TEDTIFLR
HGP	1091.5	$[M+H]^+$	ERKQEEGES
HGP	1113.0	$[M+H]^+$	SDVVYTDWK
HGP	1134.5	$[M+Na]^+$	SDVVYTDWK
HGP	1161.0	$[M+H]^+$	WFYIASAFR
HGP	1182.9	$[M+Na]^+$	WFYIASAFR
HGP	1241.0	$[M+H]^+$	SDVVYTDWKK or CEPLEKQHEK
HGP	1263.0	$[M+Na]^+$	SDVVYTDWKK or CEPLEKQHEK
HGP	1483.0	$[M+H]^+$	DKCEPLEKQHEK or SDVVYTDWKKDK
HGP	1579.0	$[M+H]^+$	IPKSDVVYTDWKK
HGP	1671.4	$[M+H]^+$	TEDTIFLREYQTR
HGP	1686.2	$[M+H]^+$	EQLGEFYEALDCLR
HGP	1708.8	$[M+H]^+$	NWGLSVYADKPETTK
HGP	1730.7	$[M+Na]^+$	NWGLSVYADKPETTK
HGP	1753.9	$[M+H]^+$	YVGGQEHFAHLLILR
HGP	1773.8	$[M+Na]^+$	YVGGQEHFAHLLILR
HGP	1789.6	$[M+H]^+$	DTKTYMLAFDVNDEK
HGP	1813.6	$[M+Na]^+$	DTKTYMLAFDVNDEK
HGP	1858.5	$[M+H]^+$	QDQCIYNTTYLNVQR
HGP	1882.3	$[M+Na]^+$	QDQCIYNTTYLNVQR
HGP	1937.7	$[M+H]^+$	WFYIASAFRNEEYNK
HGP	2098.5	$[M+H]^+$	YVGGQEHFAHLLILRDTK

HGP	2616.3	$[M+H]^+$	QDQCIYNTTYLNVQRENGTI SR
HGP	2895.7	$[M+H]^+$	SVQEIQATFFYFTPNKTEDT IFLR
HGP	2919.7	$[M+Na]^+$	SVQEIQATFFYFTPNKTEDT IFLR
HGP	3135.2	$[M+H]^+$	TYMLAFDVNDEKNWGLSVYA DKPETTK
HGP	3158.6	$[M+Na]^+$	TYMLAFDVNDEKNWGLSVYA DKPETTK

Table B.2 Carbohydrate signals identified from specified glycoproteins studied in this work. All are using MALDI unless specified otherwise.[1]

Protein	*m/z* (Da)	Species	Carbohydrate
RNAse B	1257.7	$[M+Na]^+$	$Man_5GlcNAc_2$
RNAse B	1271.8	$[M+K]^+$	$Man_5GlcNAc_2$
RNAse B	1419.9	$[M+Na]^+$	$Man_6GlcNAc_2$
RNAse B	1433.7	$[M+K]^+$	$Man_6GlcNAc_2$
RNAse B	1581.9	$[M+Na]^+$	$Man_7GlcNAc_2$
RNAse B	1744.0	$[M+Na]^+$	$Man_8GlcNAc_2$
RNAse B	1905.9	$[M+Na]^+$	$Man_9GlcNAc_2$
RNAseB (ESI)	603.0	$[M+H]^+$	$C^{2,5}X_{Man}$
RNAseB (ESI)	696.9	$[M+H]^+$	$C^{1,5}X_{Man}$
RNAseB (ESI)	782.9	$[M+H]^+$	$^{1,5}A_{Man}$
RNAseB (ESI)	798.8	$[M+Na]^+$	$^{1,5}X_{Man}$
RNAseB (ESI)	918.8	$[M+Na]^+$	$C^{1,5}X_{Man}$
RNAseB (ESI)	934.8	$[M+Na]^+$	$C^{0,2}X_{Man}$
RNAseB (ESI)	1004.9	$[M+Na]^+$	$^{1,4}A_{Man}$
RNAseB (ESI)	1114.7	$[M+H]^+$	$^{0,2}X_{Man}$
RNAseB (ESI)	1140.9	$[M+Na]^+$	$^{2,5}A_{GlcNAc}$
RNAseB (ESI)	1234.7	$[M+H]^+$	$Man_5GlcNAc_2$
RNAseB (ESI)	1240.8	$[M+Na]^+$	$Man_5GlcNAc_2$-H_20
RNAseB (ESI)	1256.7	$[M+Na]^+$	$Man_5GlcNAc_2$
RNAseB (ESI)	1382.8	$[M+Na]^+$	$Man_6GlcNAc_2$-$2H_2O$
RNAseB (ESI)	1522.3	$[M+H]^+$	$Man_7GlcNAc_2$-$2H_2O$
ovalbumin	1257.8	$[M+Na]^+$	$Hex_2Man_3GlcNAc_2$
ovalbumin	1298.9	$[M+Na]^+$	$HexHexNAcMan_3GlcNAc_2$
ovalbumin	1339.8	$[M+Na]^+$	$HexNAc_2Man_3GlcNAc_2$
ovalbumin	1419.8	$[M+Na]^+$	$Hex_3Man_3GlcNAc_2$
ovalbumin	1501.9	$[M+Na]^+$	$HexHexNAc_2Man_3GlcNAc_2$
ovalbumin	1542.9	$[M+Na]^+$	$HexNAc_3Man_3GlcNAc_2$
ovalbumin	1581.8	$[M+Na]^+$	$Hex_4Man_3GlcNAc_2$
ovalbumin	1622.6	$[M+Na]^+$	$Hex_3HexNAcMan_3GlcNAc_2$
ovalbumin	1664.0	$[M+Na]^+$	$Hex_2HexNAc_2Man_3GlcNAc_2$
ovalbumin	1704.9	$[M+Na]^+$	$HexHexNAc_3Man_3GlcNAc_2$
ovalbumin	1745.9	$[M+Na]^+$	$HexNAc_4Man_3GlcNAc_2$
ovalbumin	1867.0	$[M+Na]^+$	$Hex_2HexNAc_3Man_3GlcNAc_2$
ovalbumin	1908.0	$[M+Na]^+$	$HexHexNAc_4Man_3GlcNAc_2$
ovalbumin	1949.2	$[M+Na]^+$	$HexNAc_5Man_3GlcNAc_2$
ovalbumin	2029.0	$[M+Na]^+$	$Hex_3HexNAc_3Man_3GlcNAc_2$
ovalbumin	2070.3	$[M+Na]^+$	$Hex_2HexNAc_4Man_3GlcNAc_2$
ovalbumin	2111.5	$[M+Na]^+$	$HexHexNAc_5Man_3GlcNAc_2$
ovalbumin	2152.7	$[M+Na]^+$	$HexNAc_6Man_3GlcNAc_2$
ovalbumin	2273.4	$[M+Na]^+$	$Hex_2HexNAc_5Man_3GlcNAc_2$

ovalbumin	2314.7	$[M+Na]^+$	$HexHexNAc_6Man_3GlcNAc_2$
ovalbumin	2476.8	$[M+Na]^+$	$Hex_2HexNAc_6Man_3GlcNAc_2$
ovalbumin	2638.0	$[M+Na]^+$	$Hex_3HexNAc_6Man_3GlcNAc_2$
fetuin	1298.8	$[M+Na]^+$	$HexHexNAcMan_3GlcNAc_2$
fetuin	1341.7	$[M+Na]^+$	$HexNAc_2Man_3GlcNAc_2$
fetuin	1501.8	$[M+Na]^+$	$HexHexNAc_2Man_3GlcNAc_2$
fetuin	1664.0	$[M+Na]^+$	$Hex_2HexNAc_2Man_3GlcNAc_2$
fetuin	1867.3	$[M+Na]^+$	$Hex_2HexNAc_3Man_3GlcNAc_2$
fetuin	1911.3	$[M+Na]^+$	$HexHexNAc_4Man_3GlcNAc_2$
fetuin	1955.1	$[M+Na]^+$	$Hex_2HexNAc_2NeuAcMan_3GlcNAc_2$
fetuin	1977.2	$[M+2Na-H]^+$	$Hex_2HexNAc_2NeuAcMan_3GlcNAc_2$
fetuin	2029.1	$[M+Na]^+$	$Hex_3HexNAc_3Man_3GlcNAc_2$
fetuin	2244.5	$[M+Na]^+$	$Hex_2HexNAc_2NeuAc_2Man_3GlcNAc_2$
fetuin	2266.3	$[M+2Na-H]^+$	$Hex_2HexNAc_2NeuAc_2Man_3GlcNAc_2$
fetuin	2276.6	$[M+Na]^+$	$Hex_2HexNAc_5Man_3GlcNAc_2$
fetuin	2320.6	$[M+Na]^+$	$Hex_3HexNAc_3NeuAcMan_3GlcNAc_2$
fetuin	2342.6	$[M+2Na-H]^+$	$Hex_3HexNAc_3NeuAcMan_3GlcNAc_2$
fetuin	2611.9	$[M+Na]^+$	$Hex_3HexNAc_3NeuAc_2Man_3GlcNAc_2$
fetuin	2633.8	$[M+2Na-H]^+$	$Hex_3HexNAc_3NeuAc_2Man_3GlcNAc_2$
fetuin	2655.8	$[M+3Na-2H]^+$	$Hex_3HexNAc_3NeuAc_2Man_3GlcNAc_2$
fetuin	2903.0	$[M+Na]^+$	$Hex_3HexNAc_3NeuAc_3Man_3GlcNAc_2$
fetuin	2925.0	$[M+2Na-H]^+$	$Hex_3HexNAc_3NeuAc_3Man_3GlcNAc_2$
fetuin	2947.0	$[M+3Na-2H]^+$	$Hex_3HexNAc_3NeuAc_3Man_3GlcNAc_2$
fetuin	2968.9	$[M+4Na-3H]^+$	$Hex_3HexNAc_3NeuAc_3Man_3GlcNAc_2$
fetuin	3193.7	$[M+Na]^+$	$Hex_3HexNAc_3NeuAc_4Man_3GlcNAc_2$
fetuin	3216.1	$[M+2Na-H]^+$	$Hex_3HexNAc_3NeuAc_4Man_3GlcNAc_2$
fetuin	3238.1	$[M+3Na-2H]^+$	$Hex_3HexNAc_3NeuAc_4Man_3GlcNAc_2$
fetuin	3260.1	$[M+4Na-3H]^+$	$Hex_3HexNAc_3NeuAc_4Man_3GlcNAc_2$
fetuin	3282.1	$[M+5Na-4H]^+$	$Hex_3HexNAc_3NeuAc_4Man_3GlcNAc_2$
HGP	1298.8	$[M+Na]^+$	$HexHexNAcMan_3GlcNAc_2$
HGP	1321.0	$[M+Na]^+$	$HexNAc_2Man_3GlcNAc_2$
HGP	1342.6	$[M+Na]^+$	$HexNAc_2Man_3GlcNAc_2$
HGP	1502.0	$[M+Na]^+$	$HexHexNAc_2Man_3GlcNAc_2$
HGP	1664.0	$[M+Na]^+$	$Hex_2HexNAc_2Man_3GlcNAc_2$
HGP	1911.2	$[M+Na]^+$	$HexHexNAc_4Man_3GlcNAc_2$
HGP	1955.2	$[M+Na]^+$	$Hex_2HexNAc_2NeuAcMan_3GlcNAc_2$
HGP	2029.3	$[M+Na]^+$	$Hex_3HexNAc_3Man_3GlcNAc_2$
HGP	2175.4	$[M+Na]^+$	$Hex_3HexNAc_3DeoxyhexMan_3GlcNAc_2$
HGP	2246.1	$[M+Na]^+$	$Hex_2HexNAc_2NeuAc_2Man_3GlcNAc_2$
HGP	2268.5	$[M+2Na-H]^+$	$Hex_2HexNAc_2NeuAc_2Man_3GlcNAc_2$
HGP	2290.5	$[M+3Na-2H]^+$	$Hex_2HexNAc_2NeuAc_2Man_3GlcNAc_2$
HGP	2320.6	$[M+Na]^+$	$Hex_3HexNAc_3NeuAcMan_3GlcNAc_2$
HGP	2342.6	$[M+2Na-H]^+$	$Hex_3HexNAc_3NeuAcMan_3GlcNAc_2$

HGP	2394.7	$[M+Na]^+$	$Hex_2HexNAc_2DeoxyhexNeuAc_2Man_3GlcNAc_2$
HGP	2466.5	$[M+Na]^+$	$Hex_3HexNAc_3DeoxyhexNeuAcMan_3GlcNAc_2$
HGP	2488.6	$[M+2Na-H]^+$	$Hex_3HexNAc_3DeoxyhexNeuAcMan_3GlcNAc_2$
HGP	2611.8	$[M+Na]^+$	$Hex_3HexNAc_3NeuAc_2Man_3GlcNAc_2$
HGP	2633.8	$[M+2Na-H]^+$	$Hex_3HexNAc_3NeuAc_2Man_3GlcNAc_2$
HGP	2655.8	$[M+3Na-2H]^+$	$Hex_3HexNAc_3NeuAc_2Man_3GlcNAc_2$
HGP	2686.0	$[M+Na]^+$	$Hex_4HexNAc_4NeuAcMan_3GlcNAc_2$
HGP	2707.9	$[M+2Na-H]^+$	$Hex_4HexNAc_4NeuAcMan_3GlcNAc_2$
HGP	2903.4	$[M+Na]^+$	$Hex_3HexNAc_3NeuAc_3Man_3GlcNAc_2$
HGP	2925.0	$[M+2Na-H]^+$	$Hex_3HexNAc_3NeuAc_3Man_3GlcNAc_2$
HGP	2947.0	$[M+3Na-2H]^+$	$Hex_3HexNAc_3NeuAc_3Man_3GlcNAc_2$
HGP	2969.0	$[M+4Na-3H]^+$	$Hex_3HexNAc_3NeuAc_3Man_3GlcNAc_2$
HGP	3268.1	$[M+Na]^+$	$Hex_4HexNAc_4NeuAc_3Man_3GlcNAc_2$
HGP	3291.1	$[M+2Na-H]^+$	$Hex_4HexNAc_4NeuAc_3Man_3GlcNAc_2$
HGP	3312.1	$[M+3Na-2H]^+$	$Hex_4HexNAc_4NeuAc_3Man_3GlcNAc_2$
HGP	3334.3	$[M+4Na-3H]^+$	$Hex_4HexNAc_4NeuAc_3Man_3GlcNAc_2$

Table B.3 Most likely contributors to lipid signals in human milk sample.[2]

Experimental *m/z* (Da)	Expected *m/z* (Da)	Species	Lipid
703.6	**703.6**	$[M+Na]^+$	**TG 39:1**
	703.6	$[M+H]^+$	**SM(d18:1/16:0)**
725.6	**725.6**	$[M+Na]^+$	**SM(d18:1/16:0)**
	725.6	$[M+Na]^+$	**TG 41:3**
782.6	**782.6**	$[M+Na]^+$	**PC 34:1**
	782.6	$[M+Na]^+$	**PE 37:1**
	781.6	$[M+Na]^+$	**TG 45:3**
	781.6	$[M+Na]^+$	**SM(d18:1/20:0)**
	782.5	$[M+K]^+$	**PC o,p34:2**
	782.5	$[M+K]^+$	**PE o,p37:2**
	782.5	$[M+K]^+$	**PC 33:2**
	782.5	$[M+K]^+$	**PE 36:2**
	782.6	$[M+H]^+$	**PC 36:4**
784.7	**784.6**	$[M+Na]^+$	**PC 34:0**
	784.6	$[M+Na]^+$	**PE 37:0**
	783.6	$[M+Na]^+$	**TG 45:2**
	783.6	$[M+Na]^+$	**SM(d18:0/20:0)**
	784.6	$[M+K]^+$	**PC o,p34:1**
	784.6	$[M+K]^+$	**PE o,p37:1**
	784.5	$[M+K]^+$	**PC 33:1**
	784.5	$[M+K]^+$	**PE 36:1**
	784.6	$[M+H]^+$	**PC 36:3**
786.7	**786.5**	$[M+Na]^+$	**PC 35:6**
	786.5	$[M+Na]^+$	**PE 38:6**
	785.7	$[M+Na]^+$	**TG 45:1**
	786.6	$[M+K]^+$	**PC o,p34:0**
	786.6	$[M+K]^+$	**PE o,p37:0**
	786.5	$[M+K]^+$	**PC 33:0**
	786.5	$[M+K]^+$	**PE 36:0**
	786.6	$[M+H]^+$	**PC 36:2**
788.7	**788.5**	$[M+Na]^+$	**PC 35:5**
	788.5	$[M+Na]^+$	**PE 38:5**
	787.7	$[M+Na]^+$	**TG 45:0**
	788.5	$[M+K]^+$	**PC 34:6**
	788.5	$[M+K]^+$	**PE 37:6**
	787.7	$[M+H]^+$	**SM (d18:1/22:0)**
	788.6	$[M+H]^+$	**PC 36:1**
806.6	**806.6**	$[M+Na]^+$	**PC o,p37:3**
	806.6	$[M+Na]^+$	**PE o,p40:3**
	806.6	$[M+Na]^+$	**PE 39:3**

	806.6	$[M+Na]^+$	**PC 36:3**
	805.6	$[M+Na]^+$	**TG 47:5**
	806.5	$[M+K]^+$	**PC o,p36:4**
	806.5	$[M+K]^+$	**PE o,p39:4**
	806.5	$[M+K]^+$	**PC 35:4**
	806.5	$[M+K]^+$	**PE 38:4**
	806.6	$[M+H]^+$	**PC 38:6**
808.7	**808.6**	$[M+Na]^+$	**PC o,p37:2**
	808.6	$[M+Na]^+$	**PE o,p40:2**
	808.6	$[M+Na]^+$	**PE 39:2**
	808.6	$[M+Na]^+$	**PC 36:2**
	807.6	$[M+Na]^+$	**TG 47:4**
	808.6	$[M+K]^+$	**PC o,p36:3**
	808.6	$[M+K]^+$	**PE o,p39:3**
	808.5	$[M+K]^+$	**PC 35:3**
	808.5	$[M+K]^+$	**PE 38:3**
	808.6	$[M+H]^+$	**PC 38:5**
810.7	**810.6**	$[M+Na]^+$	**PC o,p37:1**
	810.6	$[M+Na]^+$	**PE o,p40:1**
	810.6	$[M+Na]^+$	**PE 39:1**
	810.6	$[M+Na]^+$	**PC 36:1**
	810.5	$[M+Na]^+$	**PE 40:8**
	809.7	$[M+Na]^+$	**TG 47:3**
	809.7	$[M+Na]^+$	**SM(d18:1/22:0)**
	810.6	$[M+K]^+$	**PC o,p36:2**
	810.6	$[M+K]^+$	**PE o,p39:2**
	810.5	$[M+K]^+$	**PC 35:2**
	810.5	$[M+K]^+$	**PE 38:2**
	810.6	$[M+H]^+$	**PC 38:4**
813.8	**813.7**	$[M+Na]^+$	**TG 47:1**
	813.7	$[M+H]^+$	**SM(d18:1/24:1)**
815.8	**815.7**	$[M+Na]^+$	**TG 47:0**
	815.7	$[M+H]^+$	**SM(d18:1/24:0)**
825.8	**825.7**	$[M+Na]^+$	**TG 48:2**
	825.6	$[M+K]^+$	**SM(d18:1/22:0)**
827.8	**827.7**	$[M+Na]^+$	**TG 48:1**
	827.6	$[M+K]^+$	**SM(d18:0/22:0)**
835.7	**835.7**	$[M+Na]^+$	**TG 49:4**
	835.7	$[M+Na]^+$	**SM(d18:1/24:1)**
837.8	**837.7**	$[M+Na]^+$	**TG 49:3**
	837.7	$[M+Na]^+$	**SM(d18:1/24:0)**
851.8	**851.7**	$[M+Na]^+$	**TG 50:3**
	851.7	$[M+Na]^+$	**SM(d18:1/25:0)**

	851.6	$[M+K]^+$	**SM(d18:1/24:1)**
853.8	**853.7**	$[M+Na]^+$	**TG 50:2**
	853.7	$[M+K]^+$	**SM(d18:0/24:1)**
	853.7	$[M+K]^+$	**SM(d18:1/24:0)**
855.8	**855.7**	$[M+Na]^+$	**TG 50:1**
	855.7	$[M+K]^+$	**SM(d18:0/24:0)**
879.8	**879.7**	$[M+Na]^+$	**TG 52:3**
	879.7	$[M+K]^+$	**SM(d18:1/26:1)**
881.8	**881.8**	$[M+Na]^+$	**TG 52:2**
	881.7	$[M+K]^+$	**SM(d18:1/26:0)**
	881.7	$[M+K]^+$	**SM(d18:0/26:1)**
883.8	**883.8**	$[M+Na]^+$	**TG 52:1**
	883.7	$[M+K]^+$	**SM(d18:0/26:0)**

Table B.4 Identified carbohydrates in human milk sample.[1]

m/z (Da)	Species	Glycan	Common Name
511.2	$[M+Na]^+$	FucGalGlc	Fucosyl-lactose
657.2	$[M+Na]^+$	$Fuc_2GalGlc$	Difucosyl-lactose
673.3	$[M+K]^+$	$Fuc_2GalGlc$	Difucosyl-lactose
727.1	$[M+Na]^+$	$Gal_2GlcGlcNAc$	Lacto-N-tetraose
743.0	$[M+K]^+$	$Gal_2GlcGlcNAc$	Lacto-N-tetraose
802.7	$[M+Na]^+$	FucGalGlcNeuAc	Sialyl-lactose
876.3	$[M+Na]^+$	$FucGal_2GlcGlcNAc$	Lacto-N-fucopentaose
1022.3	$[M+Na]^+$	$Fuc_2Gal_2GlcGlcNAc$	Lacto-N-difucohexaose
1038.4	$[M+K]^+$	$Fuc_2Gal_2GlcGlcNAc$	Lacto-N-difucohexaose
1095.4	$[M+Na]^+$	$Gal_3GlcGlcNAc_2$	Lacto-N-hexaose
1100.1	$[M+K]^+$	$Gal_3GlcGlcNAc_2$	Lacto-N-hexaose

Footnotes on table nomenclature:

1. Carbohydrate nomenclature:

Deoxyhex – Deoxyhexose, *i.e.* fucose
Fuc – Fucose
Hex – Hexose, *i.e.* glucose
Gal – Galactose
Glc – Glucose
HexNAc – *N*-acetylhexosamine, *i.e. N*-acetylglucosamine
GlcNAc – *N*-acetylglucosamine
GalNAc – *N*-acetylgalactosamine
NeuAc – *N*-Acetylneuraminic acid, *i.e.* sialic acid

All fragmentation is in Domon and Costello nomenclature.[27]

2. Lipid nomenclature:

SM - Sphingomyelin
TG - Triacylglycerol
PE - Phosphatidylethanolamine
PC - Phosphatidylcholine

Glycerophospholipids:
Ex. PC X:Y
X = total number of carbons in fatty acyl chains
Y = total number of double bonds in fatty acyl chains

Sphingolipids:
Ex. SM (X:Y/x:y)
X = total number of carbons in the sphingosine backbone
x = total number of carbons in the amide linked fatty acid
Y = total number of double bonds in the spingosine backbone
y = total number of double bonds in the amide linked fatty acid

( ) = used to distinguish sphingolipid from glycerophospholipid nomenclature in the table

APPENDIX C

REFERENCES OF ADAPTATION FOR CHAPTERS

Chapter I: Sections adapted from Larissa S. Fenn and John A. McLean, "Biomolecular Structural Separations by Ion Mobility-Mass Spectrometry: New Prospects for Systems Biology", *Analytical and Bioanalytical Chemistry* **2008**, *391*, 905-909, and John A. McLean, Larissa S. Fenn, and Jeffrey R. Enders, "Ion mobility-mass spectrometry Imaging", *Mass Spectrometric Imaging: History, Fundamentals and Protocols,* **Methods in Molecular Biology Series**, Jonathan V. Sweedler and Stanislav Rubakhin, eds. September 2010.

Chapter II: Adapted from Larissa S. Fenn, Michal Kliman, Ablatt Mahsut, Sophie R. Zhao, and John A. McLean, "Characterizing Ion Mobility-Mass Spectrometry Conformation Space for the Analysis of Complex Biological Samples", *Analytical and Bioanalytical Chemistry* **2009**, *394*, 235-244.

Chapter III: Adapted from Larissa S. Fenn and John A. McLean, "Structural resolution of positional and structural carbohydrate isomers based on gas-phase ion mobility-mass spectrometry", submitted to *Physical Chemistry & Chemical Physics*

Chapter IV: Adapted from Larissa S. Fenn and John A. McLean, "Simultaneous glycoproteomic strategies utilizing ion mobility-mass spectrometry", *Molecular BioSystems* **2009**, 5, 1298-1302.

Chapter V: Adapted from Larissa S. Fenn and John A. McLean, "Enhanced carbohydrate structural selectivity by boronic acid derivitization and ion mobility-mass spectrometry analysis", *Chemical Communications*, **2008**, *43*, 5505-5507.

REFERENCES

1. Bahl, O. P., *Glycoconjugates: Composition, Structure, and Function*. Marcel Dekker: New York, NY, 1992; p 1-12.

2. Gorelik, E.; Galili, U.; Raz, A., "On the Role of Cell Surface Carbohydrates and their Binding Proteins (lectins) in Tumor Metastasis." *Cancer and Metastasis Reviews* **2001,** *20*, 245-277.

3. Montreuil, J.; Vliegenthart, J. F. G.; Schachter, H., *Glycoproteins I*. Elsevier Science New York, NY, 1995; p 644.

4. Rudd, P. M.; Elliott, T.; Cresswell, P.; Wilson, I. A.; Dwek, R. A., "Glycosylation and the Immune System." *Science* **2001,** *291*, 2370-2376.

5. Harvey, D. J., "Identification of protein-bound carbohydrates by mass spectrometry." *Proteomics* **2001,** *1*, 311-328.

6. Morelle, W.; Canis, K.; Chirat, F.; Faid, V.; Michalski, J.-C., "The use of mass spectrometry for the proteomic analysis of glycosylation." *Proteomics* **2006,** *6*, 3993-4015.

7. Hernández-Borges, J.; Neusüß, C.; Cifuentes, A.; Pelzing, M., "On-line capillary electrophoresis-mass spectrometry for the analysis of biomolecules." *Electrophoresis* **2004,** *25*, 2257-2281.

8. Patel, T.; Bruce, J.; Merry, A.; Bigge, C.; Wormald, M.; Parekh, R.; Jaques, A., "Use of hydrazine to release in intact and unreduced form both N- and O-linked oligosaccharides from glycoproteins." *Biochemistry* **1993,** *32*, 679-693.

9. Patel, T. P.; Parekh, R. B., Release of oligosaccharides from glycoproteins by hydrazinolysis. In *Methods Enzymol.*, Lennarz, W. J.; Hart, G. W., Eds. Academic Press: 1994; Vol. 230, pp 57-66.

10. Takasaki, S.; Mizuochi, T.; Kobata, A.; Victor, G., Hydrazinolysis of asparagine-linked sugar chains to produce free oligosaccharides. In *Methods Enzymol.*, Ginsburg, V., Ed. Academic Press: 1982; Vol. 83, pp 263-268.

11. An, H. J.; Peavy, T. R.; Hedrick, J. L.; Lebrilla, C. B., "Determination of N-Glycosylation Sites and Site Heterogeneity in Glycoproteins." *Anal. Chem.* **2003,** *75*, 5628-5637.

12. Juhasz, P.; Martin, S. A., "The utility of nonspecific proteases in the characterization of glycoproteins by high-resolution time-of-flight mass spectrometry." *Int. J. Mass Spectrom. Ion Processes* **1997,** *169-170*, 217-230.

13. Liu, X.; McNally, D. J.; Nothaft, H.; Szymanski, C. M.; Brisson, J.-R.; Li, J., "Mass Spectrometry-Based Glycomics Strategy for Exploring N-Linked Glycosylation in Eukaryotes and Bacteria." *Anal. Chem.* **2006,** *78*, 6081-6087.

14. Yamagaki, T.; Nakanishi, H., "Ion intensity analysis of post-source decay fragmentation in curved-field reflectron matrix-assisted laser desorption/ionization time-of-flight mass spectrometry of carbohydrates: For structural characterization of glycosylation in proteome analysis." *Proteomics* **2001,** *1*, 329-339.

15. Ashline, D. J.; Lapadula, A. J.; Liu, Y.-H.; Lin, M.; Grace, M.; Pramanik, B.; Reinhold, V. N., "Carbohydrate Structural Isomers Analyzed by Sequential Mass Spectrometry." *Anal. Chem.* **2007,** *79*, 3830-3842.

16. Hardy, M. R.; Townsend, R. R., "Separation of positional isomers of oligosaccharides and glycopeptides by high-performance anion-exchange chromatography with pulsed amperometric detection." *Proc. Natl. Acad. Sci. U. S. A.* **1988,** *85*, 3289-3293.

17. Meyer, B.; Möller, H., "Conformation of Glycopeptides and Glycoproteins." *Top. Curr. Chem.* **2007,** *267*, 187-251.

18. Maslen, S.; Sadowski, P.; Adam, A.; Lilley, K.; Stephens, E., "Differentiation of Isomeric N-Glycan Structures by Normal-Phase Liquid Chromatographyâˆ'MALDI-TOF/TOF Tandem Mass Spectrometry." *Anal. Chem.* **2006,** *78*, 8491-8498.

19. Bruggink, C.; Wuhrer, M.; Koeleman, C. A. M.; Barreto, V.; Liu, Y.; Pohl, C.; Ingendoh, A.; Hokke, C. H.; Deelder, A. M., "Oligosaccharide analysis by capillary-scale high-pH anion-exchange chromatography with on-line ion-trap mass spectrometry." *Journal of Chromatography B* **2005,** *829*, 136-143.

20. Torto, N.; Hofte, A.; Hoeven, R. v. d.; Tjaden, U.; Gorton, L.; Marko-Varga, G.; Bruggink, C.; Greef, J. v. d., "Microdialysis introduction high-performance anion-exchange chromatography/ionspray mass spectrometry for monitoring of on-line desalted carbohydrate hydrolysates." *J. Mass Spectrom.* **1998,** *33*, 334-341.

21. Costello, C. E.; Contado-Miller, J. M.; Cipollo, J. F., "A Glycomics Platform for the Analysis of Permethylated Oligosaccharide Alditols." *J. Am. Soc. Mass Spectrom.* **2007,** *18*, 1799-1812.

22. Anumula, K. R.; Dhume, S. T., "High resolution and high sensitivity methods for oligosaccharide mapping and characterization by normal phase high performance liquid chromatography following derivatization with highly fluorescent anthranilic acid." *Glycobiology* **1998,** *8*, 685-694.

23. Wuhrer, M.; Koeleman, C. A. M.; Hokke, C. H.; Deelder, A. M., "Nano-scale liquid chromatography-mass spectrometry of 2-aminobenzamide-labeled oligosaccharides at low femtomole sensitivity." *Int. J. Mass Spectrom.* **2004,** *232*, 51-57.

24. Scrivens, J. H.; Jackson, A. T.; Jennings, K. R.; Jennings, R. C. K.; Everall, N. J., "High energy collision-induced dissociation (CID) product ion spectra of isomeric polyhydroxy sugars." *Int. J. Mass Spectrom.* **2003,** *230*, 201-208.

25. Rouse, J. C.; Strang, A.-M.; Yu, W.; Vath, J. E., "Isomeric Differentiation of Asparagine-Linked Oligosaccharides by Matrix-Assisted Laser Desorption-Ionization Postsource Decay Time-of-Flight Mass Spectrometry." *Anal. Biochem.* **1998,** *256*, 33-46.

26. Spina, E.; Cozzolino, R.; Ryan, E.; Garozzo, D., "Sequencing of oligosaccharides by collision-induced dissociation matrix-assisted laser desorption/ionization mass spectrometry." *J. Mass Spectrom.* **2000,** *35*, 1042-1048.

27. Domon, B.; Costello, C. E., "A systematic nomenclature for carbohydrate fragmentations in FAB-MS/MS spectra of glycoconjugates." *Glycoconjugate J.* **1988,** *5*, 397-409.

28. Stahl, B.; Steup, M.; Karas, M.; Hillenkamp, F., "Analysis of neutral oligosaccharides by matrix-assisted laser desorption ionization mass spectrometry." *Anal. Chem.* **1991,** *63*, 1463-1466.

29. Lemoine, J.; Fournet, B.; Despeyroux, D.; Jennings, K. R.; Rosenberg, R.; de Hoffmann, E., "Collision-induced dissociation of alkali metal cationized and permethylated oligosaccharides: Influence of the collision energy and of the collision gas for the assignment of linkage position." *J. Am. Soc. Mass Spectrom.* **1993,** *4*, 197-203.

30. Harvey, D. J.; Hunter, A. P.; Bateman, R. H.; Brown, J.; Critchley, G., "Relationship between in-source and post-source fragment ions in the matrix-assisted laser desorption (ionization) mass spectra of carbohydrates recorded with reflectron time-of-flight mass spectrometers." *Int. J. Mass Spectrom.* **1999,** *188*, 131-146.

31. Zubarev, R. A.; Kelleher, N. L.; McLafferty, F. W., "Electron Capture Dissociation of Multiply Charged Protein Cations. A Nonergodic Process." *J. Am. Chem. Soc.* **1998,** *120*, 3265-3266.

32. Syka, J. E. P.; Coon, J. J.; Schroeder, M. J.; Shabanowitz, J.; Hunt, D. F., "Peptide and protein sequence analysis by electron transfer dissociation mass spectrometry." *Proc. Natl. Acad. Sci. U. S. A.* **2004,** *101*, 9528-9533.

33. McLean, J. A.; Ruotolo, B. T.; Gillig, K. J.; Russell, D. H., "Ion mobility-mass spectrometry: a new paradigm for proteomics." *Int. J. Mass Spectrom.* **2005,** *240*, 301-315.

34. Clemmer, D. E.; Jarrold, M. F., "Ion mobility measurements and their applications to clusters and biomolecules." *J. Mass Spectrom.* **1997,** *32*, 577-592.

35. Baumbach, J., "Process analysis using ion mobility spectrometry." *Anal. Bioanal. Chem.* **2006,** *384*, 1059-1070.

36. Mason, E. A.; McDaniel, E. W., *Transport Properties of Ions in Gases*. John Wiley and Sons: Indianapolis, IN, 1988.

37. Eiceman, G. A.; Karpas, Z., *Ion Mobility Spectrometry, Second Edition*. 2005; p 360

38. McAfee, K. B., Jr.; Edelson, D., "Identification and Mobility of Ions in a Townsend Discharge by Time-resolved Mass Spectrometry." *Proc. Phys. Soc.* **1963,** *81*, 382-384.

39. Barnes, W. S.; Martin, D. W.; McDaniel, E. W., "Mass spectrographic identification of the ion observed in hydrogen mobility experiments." *Phys. Rev. Lett.* **1961,** *6*, 110-111.

40. Gieniec, J.; Mack, L. L.; Nakamae, K.; Gupta, C.; Kumar, V.; Malcolm, D., "Electrospray mass spectroscopy of macromolecules: Application of an ion-drift spectrometer." *Biomed. Spectrom.* **1984,** *11*, 259-268.

41. von Helden, G.; Wyttenbach, T.; Bowers, M. T., "Inclusion of a MALDI ion source in the ion chromatography technique: conformational information on polymer and biomolecular ions " *Int. J. Mass Spectrom. Ion Processes* **1995,** *146-147*, 349-364.

42. Shelimov, K. B.; Clemmer, D. E.; Hudgins, R. R.; Jarrold, M. F., "Protein structure in vacuo: Gas-phase confirmations of BPTI and cytochrome c." *J. Am. Chem. Soc.* **1997,** *119*, 2240-2248.

43. von Helden, G.; Wyttenbach, T.; Bowers, M. T., "Conformation of Macromolecules in the Gas-Phase - Use of Matrix-Assisted Laser-Desorption Methods in Ion Chromatography." *Science* **1995,** *267*, 1483-1485.

44. Wyttenbach, T.; vonHelden, G.; Bowers, M. T., "Gas-phase conformation of biological molecules: Bradykinin." *J. Am. Chem. Soc.* **1996,** *118*, 8355-8364.

45. Myung, S.; Lee, Y. J.; Moon, M. H.; Taraszka, J.; Sowell, R.; Koeniger, S.; Hilderbrand, A. E.; Valentine, S. J.; Cherbas, L.; Cherbas, P.; Kaufmann, T. C.; Miller, D. F.; Mechref, Y.; Novotny, M. V.; Ewing, M. A.; Sporleder, C. R.; Clemmer, D. E., "Development of high-sensitivity ion trap ion mobility spectrometry time-of-flight techniques: A high-throughput nano-LC-IMS-TOF separation of peptides arising from a Drosophila protein extract." *Anal. Chem.* **2003,** *75*, 5137-5145.

46. Isailovic, D.; Kurulugama, R. T.; Plasencia, M. D.; Stokes, S. T.; Kyselova, Z.; Goldman, R.; Mechref, Y.; Novotny, M. V.; Clemmer, D. E., "Profiling of Human Serum Glycans Associated with Liver Cancer and Cirrhosis by IMSâˆ'MS." *J. Prot. Res.* **2008,** *7*, 1109-1117.

47. Liu, X.; Plasencia, M.; Ragg, S.; Valentine, S. J.; Clemmer, D. E., "Development of high throughput dispersive LC-ion mobility-TOFMS techniques for analysing the human plasma proteome." *Brief Funct Genomic Proteomic* **2004,** *3*, 177-186.

48. Liu, X. Y.; Valentine, S. J.; Plasencia, M. D.; Trimpin, S.; Naylor, S.; Clemmer, D. E., "Mapping the human plasma proteome by SCX-LC-IMS-MS." *J. Am. Soc. Mass Spectrom.* **2007,** *18*, 1249-1264.

49. Valentine, S. J.; Plasencia, M. D.; Liu, X. Y.; Krishnan, M.; Naylor, S.; Udseth, H. R.; Smith, R. D.; Clemmer, D. E., "Toward plasma proteome profiling with ion mobility-mass spectrometry." *J. Prot. Res.* **2006,** *5*, 2977-2984.

50. Liu, X. Y.; Miller, B. R.; Rebec, G. V.; Clemmer, D. E., "Protein expression in the striatum and cortex regions of the brain for a mouse model of Huntington's disease." *J. Prot. Res.* **2007,** *6*, 3134-3142.

51. Taraszka, J. A.; Kurulugama, R.; Sowell, R. A.; Valentine, S. J.; Koeniger, S. L.; Arnold, R. J.; Miller, D. F.; Kaufman, T. C.; Clemmer, D. E., "Mapping the proteome of Drosophila melanogaster: Analysis of embryos and adult heads by LC-IMS-MS methods." *J. Prot. Res.* **2005,** *4*, 1223-1237.

52. Benesch, J. L. P.; Ruotolo, B. T.; Simmons, D. A.; Robinson, C. V., "Protein complexes in the gas phase: Technology for structural genomics and proteomics." *Chem. Rev.* **2007,** *107*, 3544-3567.

53. Ruotolo, B. T.; Hyung, S. J.; Robinson, P. M.; Giles, K.; Bateman, R. H.; Robinson, C. V., "Ion mobility-mass spectrometry reveals long-lived, unfolded intermediates in the dissociation of protein complexes." *Angew. Chem., Int. Ed. Engl.* **2007,** *46*, 8001-8004.

54. Ruotolo, B. T.; Giles, K.; Campuzano, I.; Sandercock, A. M.; Bateman, R. H.; Robinson, C. V., "Evidence for macromolecular protein rings in the absence of bulk water." *Science* **2005,** *310*, 1658-1661.

55. Jackson, S. N.; Ugarov, M.; Egan, T.; Post, J. D.; Langlais, D.; Schultz, J. A.; Woods, A. S., "MALDI-ion mobility-TOFMS imaging of lipids in rat brain tissue." *J. Mass Spectrom.* **2007,** *42*, 1093-1098.

56. McLean, J. A.; Ridenour, W. B.; Caprioli, R. M., "Profiling and imaging of tissues by imaging ion mobility-mass spectrometry." *J. Mass Spectrom.* **2007,** *42*, 1099-1105.

57. Mason, E. A., Ion Mobility: Its Role in Plasma Chromatography. In *Plasma Chromatography*, Carr, T. W., Ed. Plenum Press: New York, NY, 1984; pp 43-93.

58. Revercomb, H. E.; Mason, E. A., "Theory of plasma chromatography/gaseous electrophoresis. Review." *Anal. Chem.* **1975,** *47*, 970-983.

59. Ruotolo, B. T.; Benesch, J. L. P.; Sandercock, A. M.; Hyung, S.-J.; Robinson, C. V., "Ion mobility-mass spectrometry analysis of large protein complexes." *Nat. Protocols* **2008,** *3*, 1139-1152.

60. Williams, J. P.; Scrivens, J. H., "Coupling desorption electrospray ionisation and neutral desorption/extractive electrospray ionisation with a travelling-wave based ion mobility mass spectrometer for the analysis of drugs." *Rapid Commun. Mass Spectrom.* **2008,** *22*, 187-196.

61. Fenn, L. S.; McLean, J. A., "Biomolecular structural separations by ion mobility-mass spectrometry." *Anal. Bioanal. Chem.* **2008,** *391*, 905-909.

62. Hoaglund-Hyzer, C. S.; Counterman, A. E.; Clemmer, D. E., "Anhydrous Protein Ions." *Chem. Rev.* **1999,** *99*, 3037-3080.

63. Jarrold, M. F., "Peptides and proteins in the vapor phase." *Annu. Rev. Phys. Chem.* **2000,** *51*, 179-207.

64. Wyttenbach, T.; Bowers, M. T., Gas-phase conformations: The ion mobility/ion chromatography method. In *Top. Curr. Chem.*, 2003; Vol. 225, pp 207-232.

65. Lee, S.; Wyttenbach, T.; Bowers, M. T., "Gas phase structures of sodiated oligosaccharides by ion mobility/ion chromatography methods." *Int. J. Mass Spectrom. Ion Processes* **1997,** *167-168*, 605-614.

66. Dwivedi, P.; Wu, P.; Klopsch, S. J.; Puzon, G. J.; Xun, L.; Hill, H. H., Jr., "Metabolic profiling by ion mobility mass spectrometry (IMMS)." *Metabolomics* **2008,** *4*, 63-80.

67. Ruotolo, B. T.; Verbeck; Thomson, L. M.; Woods, A. S.; Gillig, K. J.; Russell, D. H., "Distinguishing between Phosphorylated and Nonphosphorylated Peptides with Ion Mobility-Mass Spectrometry." *J. Prot. Res.* **2002,** *1*, 303-306.

68. Tao, L.; McLean, J. R.; McLean, J. A.; Russell, D. H., "A Collision Cross-Section Database of Singly-Charged Peptide Ions." *J. Am. Soc. Mass Spectrom.* **2007,** *18*, 1232-1238.

69. Furche, F.; Ahlrichs, R.; Weis, P.; Jacob, C.; Gilb, S.; Bierweiler, T.; Kappes, M. M., "The structures of small gold cluster anions as determined by a combination of ion mobility measurements and density functional calculations." *J. Chem. Phys.* **2002,** *117*, 6982-6990.

70. Shvartsburg, A. A.; Smith, R. D., "Fundamentals of Traveling Wave Ion Mobility Spectrometry." *Anal. Chem.* **2008,** *80*, 9689-9699.

71. Ridenour, W. B.; Kliman, M.; McLean, J. A.; Caprioli, R. M., "Structural Characterization of Phospholipids and Peptides Directly from Tissue Sections by MALDI Traveling-Wave Ion Mobility-Mass Spectrometry." *Anal. Chem. 82*, 1881-1889.

72. Mason, E. A.; McDaniel, E. W., Measurement of drift velocities and longitudinal diffusion coefficients. In *Transport Properties of Ions in Gases*, John Wiley & Sons: New York, NY, 1988; pp 31-102.

73. Sundarapandian, S.; May, J. C.; McLean, J. A., "Dual Source Ion Mobility-Mass Spectrometer for Direct Comparison of Electrospray Ionization and MALDI Collision Cross Section Measurements." *Anal. Chem.* **2010,** *DOI: 10.1021/ac902980r*.

74. Giles, K.; Pringle, S. D.; Worthington, K. R.; Little, D.; Wildgoose, J. L.; Bateman, R. H., "Applications of a travelling wave-based radio-frequency-only stacked ring ion guide." *Rapid Commun. Mass Spectrom.* **2004,** *18*, 2401-2414.

75. Pringle, S. D.; Giles, K.; Wildgoose, J. L.; Williams, J. P.; Slade, S. E.; Thalassinos, K.; Bateman, R. H.; Bowers, M. T.; Scrivens, J. H., "An investigation of the mobility separation of some peptide and protein ions using a new hybrid

quadrupole/travelling wave IMS/oa-ToF instrument." *Int. J. Mass Spectrom.* **2007,** *261*, 1-12.

76. Vakhrushev, S. Y.; Langridge, J.; Campuzano, I.; Hughes, C.; Peter-Katalinic, J., "Ion Mobility Mass Spectrometry Analysis of Human Glycourinome." *Anal. Chem.* **2008,** *80*, 2506-2513.

77. Riba-Garcia, I.; Giles, K.; Bateman, R. H.; Gaskell, S. J., "Evidence for Structural Variants of a- and b-Type Peptide Fragment Ions Using Combined Ion Mobility/Mass Spectrometry." *J. Am. Soc. Mass Spectrom.* **2008,** *19*, 609-613.

78. Clowers, B. H.; Dwivedi, P.; Steiner, W. E.; Hill, H. H.; Bendiak, B., "Separation of Sodiated Isobaric Disaccharides and Trisaccharides Using Electrospray Ionization-Atmospheric Pressure Ion Mobility-Time of Flight Mass Spectrometry." *J. Am. Soc. Mass Spectrom.* **2005,** *16*, 660-669.

79. Dwivedi, P.; Bendiak, B.; Clowers, B. H.; Hill Jr, H. H., "Rapid Resolution of Carbohydrate Isomers by Electrospray Ionization Ambient Pressure Ion Mobility Spectrometry-Time-of-Flight Mass Spectrometry (ESI-APIMS-TOFMS)." *J. Am. Soc. Mass Spectrom.* **2007,** *18*, 1163-1175.

80. Leavell, M. D.; Gaucher, S. P.; Leary, J. A.; Taraszka, J. A.; Clemmer, D. E., "Conformational studies of Zn-ligand-hexose diastereomers using ion mobility measurements and density functional theory calculations." *J. Am. Soc. Mass Spectrom.* **2002,** *13*, 284-293.

81. Lee, D.-S.; Wu, C.; Hill, H. H., "Detection of carbohydrates by electrospray ionization-ion mobility spectrometry following microbore high-performance liquid chromatography." *J. Chromatogr. A* **1998,** *822*, 1-9.

82. Liu, Y.; Clemmer, D. E., "Characterizing Oligosaccharides Using Injected-Ion Mobility/Mass Spectrometry." *Anal. Chem.* **1997,** *69*, 2504-2509.

83. Hoaglund, C. S.; Valentine, S. J.; Clemmer, D. E., "An Ion Trap Interface for ESI Ion Mobility Experiments." *Anal. Chem.* **1997,** *69*, 4156-4161.

84. Clowers, B. H.; Hill, H. H., Jr., "Mass Analysis of Mobility-Selected Ion Populations Using Dual Gate, Ion Mobility, Quadrupole Ion Trap Mass Spectrometry." *Anal. Chem.* **2005,** *77*, 5877-5885.

85. Williams, J. P.; Grabenauer, M.; Holland, R. J.; Carpenter, C. J.; Wormald, M. R.; Giles, K.; Harvey, D. J.; Bateman, R. H.; Scrivens, J. H.; Bowers, M. T., "Characterization of simple isomeric oligosaccharides and the rapid separation of glycan mixtures by ion mobility mass spectrometry." *Int. J. Mass Spectrom.* **2010,** *In Press, Corrected Proof*.

86. Zhu, M.; Bendiak, B.; Clowers, B.; Hill, H., "Ion mobility-mass spectrometry analysis of isomeric carbohydrate precursor ions." *Anal. Bioanal. Chem.* **2009,** *394*, 1853-1867.

87. Yamagaki, T.; Sato, A., "Peak width-mass correlation in CID MS/MS of isomeric oligosaccharides using traveling-wave ion mobility mass spectrometry." *J. Mass Spectrom.* **2009,** *44*, 1509-1517.

88. Yamagaki, T.; Sato, A., "Isomeric Oligosaccharides Analyses Using Negative-ion Electrospray Ionization Ion Mobility Spectrometry Combined with Collision-induced Dissociation MS/MS." *Anal. Sci.* **2009,** *25*, 985-988.

89. Gabryelski, W.; Froese, K. L., "Rapid and sensitive differentiation of anomers, linkage, and position isomers of disaccharides using High-Field Asymmetric Waveform Ion Mobility Spectrometry (FAIMS)." *J. Am. Soc. Mass Spectrom.* **2003,** *14*, 265-277.

90. Olivova, P.; Chen, W.; Chakraborty, A. B.; Gebler, J. C., "Determination of N-glycosylation sites and site heterogeneity in a monoclonal antibody by electrospray quadrupole ion-mobility time-of-flight mass spectrometry." *Rapid Commun. Mass Spectrom.* **2008,** *22*, 29-40.

91. Plasencia, M. D.; Isailovic, D.; Merenbloom, S. I.; Mechref, Y.; Clemmer, D. E., "Resolving and Assigning N-Linked Glycan Structural Isomers from Ovalbumin by IMS-MS." *J. Am. Soc. Mass Spectrom.* **2008,** *19*, 1706-1715.

92. Kelleher, N. L., "Top-Down Proteomics." *Anal. Chem.* **2004,** *76*, 196 A-203 A.

93. Hood, L.; Heath, J. R.; Phelps, M. E.; Lin, B., "Systems Biology and New Technologies Enable Predictive and Preventative Medicine." *Science* **2004,** *306*, 640-643.

94. Huang, S.; Wikswo, J., "Dimensions of systems biology." *Rev. Physiol. Biochem. Pharmacol.* **2007,** *157*, 81-104.

95. Peterson, R. T., "Chemical biology and the limits of reductionism." *Nat. Chem. Biol.* **2008,** *4*, 635-638.

96. Simon, G. M.; Cravatt, B. F., "Challenges for the 'chemical-systems' biologist." *Nat. Chem. Biol.* **2008,** *4*, 639-642.

97. Van Regenmortel, M. H. V., "Reductionism and complexity in molecular biology " *EMBO Reports* **2004,** *5*, 1016-1020.

98. Mesleh, M. F.; Hunter, J. M.; Shvartsburg, A. A.; Schatz, G. C.; Jarrold, M. F., "Structural information from ion mobility measurements: Effects of the long-range potential." *J. Phys. Chem.* **1996,** *100*, 16082-16086.

99. Shvartsburg, A. A.; Jarrold, M. F., "An exact hard-spheres scattering model for the mobilities of polyatomic ions." *Chem. Phys. Lett.* **1996,** *261*, 86-91.

100. Vonhelden, G.; Wyttenbach, T.; Bowers, M. T., "Conformation of Macromolecules in the Gas-Phase - Use of Matrix-Assisted Laser-Desorption Methods in Ion Chromatography." *Science* **1995,** *267*, 1483-1485.

101. Clemmer, D. E.; Hudgins, R. R.; Jarrold, M. F., "Naked Protein Conformations: Cytochrome c in the Gas Phase." *J. Am. Chem. Soc.* **1995,** *117*, 10141-10142.

102. Mao, Y.; Ratner, M. A.; Jarrold, M. F., "One Water Molecule Stiffens a Protein." *J. Am. Chem. Soc.* **2000,** *122*, 2950-2951.

103. Koomen, J. M.; Ruotolo, B. T.; Gillig, K. J.; McLean, J. A.; Russell, D. H.; Kang, M. J.; Dunbar, K. R.; Fuhrer, K.; Gonin, M.; Schultz, J. A., "Oligonucleotide analysis with MALDI-ion-mobility-TOFMS." *Anal. Bioanal. Chem.* **2002,** *373*, 612-617.

104. Karas, M.; Hillenkamp, F., "Laser desorption ionization of proteins with molecular masses exceeding 10,000 daltons." *Anal. Chem.* **1988,** *60*, 2299-2301.

105. Sud, M.; Fahy, E.; Cotter, D.; Brown, A.; Dennis, E. A.; Glass, C. K.; Merrill, A. H., Jr.; Murphy, R. C.; Raetz, C. R. H.; Russell, D. W.; Subramaniam, S., "LMSD: LIPID MAPS structure database." *Nucleic Acids Res.* **2007,** *35*, D527-532.

106. Jackson, S. N.; Wang, H.-Y. J.; Woods, A. S., "In Situ Structural Characterization of Glycerophospholipids and Sulfatides in Brain Tissue Using MALDI-MS/MS " *J. Am. Soc. Mass Spectrom.* **2007,** *18*, 17-26.

107. Case, D. A.; Cheatham, T. E.; Darden, T.; Gohlke, H.; Luo, R.; Merz, K. M.; Onufriev, A.; Simmerling, C.; Wang, B.; Woods, R. J., "The Amber biomolecular simulation programs." *J. Comput. Chem.* **2005,** *26*, 1668-1688.

108. Frisch, M. J.; Trucks, G. W.; Schlegel, H. B.; Scuseria, G. E.; Robb, M. A.; Cheeseman, J. R.; Montgomery, J. A.; Vreven, T.; Kudin, K. N.; Burant, J. C.; Millam, J. M.; Iyengar, S. S.; Tomasi, J.; Barone, V.; Mennucci, B.; Cossi, M.; Scalmani, G.; Rega, N.; Petersson, G. A.; Nakatsuji, H.; Hada, M.; Ehara, M.; Toyota, K.; Fukuda, R.; Hasegawa, J.; Ishida, M.; Nakajima, T.; Honda, Y.; Kitao, O.; Nakai, H.; Klene, M.; Li, X.; Knox, J. E.; Hratchian, H. P.; Cross, J. B.; Bakken, V.; Adamo, C.; Jaramillo, J.; Gomperts, R.; Stratmann, R. E.; Yazyev,

O.; Austin, A. J.; Cammi, R.; Pomelli, C.; Ochterski, J. W.; Ayala, P. Y.; Morokuma, K.; Voth, G. A.; Salvador, P.; Dannenberg, J. J.; Zakrzewski, V. G.; Dapprich, S.; Daniels, A. D.; Strain, M. C.; Farkas, O.; Malick, D. K.; Rabuck, A. D.; Raghavachari, K.; Foresman, J. B.; Ortiz, J. V.; Cui, Q.; Baboul, A. G.; Clifford, S.; Cioslowski, J.; Stefanov, B. B.; Liu, G.; Liashenko, A.; Piskorz, P.; Komaromi, I.; Martin, R. L.; Fox, D. J.; Keith, T.; Al-Laham, M. A.; Peng, C. Y.; Nanayakkara, A.; Challacombe, M.; Gill, P. M. W.; Johnson, B.; Chen, W.; Wong, M. W.; Gonzalez, C.; Pople, J. A. *Gaussian 03, Revision D.01*, Gaussian, Inc.: Wallingford, CT, 2004.

109. Bayly, C. I.; Cieplak, P.; Cornell, W. D.; Kollman, P. A., "A Well-Behaved Electrostatic Potential Based Method Using Charge Restraints for Deriving Atomic Charges - the Resp Model." *J. Phys. Chem.* **1993,** *97*, 10269-10280.

110. Cornell, W. D.; Cieplak, P.; Bayly, C. I.; Gould, I. R.; Merz, K. M.; Ferguson, D. M.; Spellmeyer, D. C.; Fox, T.; Caldwell, J. W.; Kollman, P. A., "A Second Generation Force Field for the Simulation of Proteins, Nucleic Acids, and Organic Molecules." *J. Am. Chem. Soc.* **1995,** *117*, 5179-5197.

111. Barton, G. J. *OC - A cluster analysis program*, University of Dundee: Dundee, Scotland, UK, 1993, 2002.

112. Smith, J. *Suppose – superposition software*, Vanderbilt University: Nashville, TN, 2006.

113. Ruotolo, B. T.; Gillig, K. J.; Stone, E. G.; Russell, D. H.; Fuhrer, K.; Gonin, M.; Schultz, J. A., "Analysis of protein mixtures by matrix-assisted laser desorption ionization-ion mobility-orthogonal-time-of-flight mass spectrometry " *J. Am. Soc. Mass Spectrom.* **2002,** *219*, 253-267.

114. Woods, A. S.; Koomen, J. M.; Ruotolo, B. T.; Gillig, K. J.; Russel, D. H.; Fuhrer, K.; Gonin, M.; Egan, T. F.; Schultz, J. A., "A study of peptide–peptide interactionsusing MALDI ion mobility o-TOF and ESI mass spectrometry." *J. Am. Soc. Mass Spectrom.* **2002,** *13*, 166-169.

115. Merenbloom, S. I.; Koeniger, S. L.; Valentine, S. J.; Plasencia, M. D.; Clemmer, D. E., "IMS-IMS and IMS-IMS-IMS/MS for Separating Peptide and Protein Fragment Ions." *Anal. Chem.* **2006,** *78*, 2802-2809.

116. Myung, S.; Wiseman, J. M.; Valentine, S. J.; Takats, Z.; Cooks, R. G.; Clemmer, D. E., "Coupling Desorption Electrospray Ionization with Ion Mobility/Mass Spectrometry for Analysis of Protein Structure: Evidence for Desorption of Folded and Denatured States." *J. Phys. Chem. B* **2006,** *110*, 5045-5051.

117. Dwivedi, P.; Wu, C.; Matz, L. M.; Clowers, B. H.; Seims, W. F.; Hill, H. H., Jr., "Gas-phase chiral separations by ion mobility spectrometry." *Anal. Chem.* **2006,** *78*, 8200-8206.

118. Gidden, J.; Bowers, M. T., "Gas-phase conformations of deprotonated trinucleotides (dGTT(-), dTGT(-), and dTTG(-)): The question of zwitterion formation." *J. Am. Soc. Mass Spectrom.* **2003,** *14*, 161-170.

119. Baker, E. S.; Bowers, M. T., "B-DNA Helix Stability in a Solvent-Free Environment." *J. Am. Soc. Mass Spectrom.* **2007,** *18*, 1188-1195.

120. Gidden, J.; Ferzoco, A.; Baker, E. S.; Bowers, M. T., "Duplex formation and the onset of helicity in poly d(CG)(n) oligonucleotides in a solvent-free environment." *J. Am. Chem. Soc.* **2004,** *126*, 15132-15140.

121. Baker, E. S.; Manard, M. J.; Gidden, J.; Bowers, M. T., "Structural Analysis of Metal Interactions with the Dinucleotide Duplex, dCG.dCG, Using Ion Mobility Mass Spectrometry." *J. Phys. Chem. B* **2005,** *109*, 4808-4810.

122. Baker, E. S.; Bernstein, S. L.; Bowers, M. T., "Structural characterization of G-quadruplexes in deoxyguanosine clusters using ion mobility mass spectrometry." *J. Am. Soc. Mass Spectrom.* **2005,** *16*, 989-997.

123. Baker, E. S.; Bernstein, S. L.; Gabelica, V.; De Pauw, E.; Bowers, M. T., "G-quadruplexes in telomeric repeats are conserved in a solvent-free environment." *Int. J. Mass Spectrom.* **2006,** *253*, 225-237.

124. Gabelica, V.; Baker, E. S.; Teulade-Fichou, M. P.; De Pauw, E.; Bowers, M. T., "Stabilization and structure of telomeric and c-myc region intramolecular G-quadruplexes: The role of central cations and small planar ligands." *J. Am. Chem. Soc.* **2007,** *129*, 895-904.

125. Baker, E. S.; Lee, J. T.; Sessler, J. L.; Bowers, M. T., "Cyclo[n]pyrroles: Size and Site-Specific Binding to G-Quadruplexes." *J. Am. Chem. Soc.* **2006,** *128*, 2641-2648.

126. Thalassinos, K.; Slade, S. E.; Jennings, K. R.; Scrivens, J. H.; Giles, K.; Wildgoose, J.; Hoyes, J.; Bateman, R. H.; Bowers, M. T., "Ion mobility mass spectrometry of proteins in a modified commercial mass spectrometer " *Int. J. Mass Spectrom.* **2004,** *236*, 55-63.

127. Baumketner, A.; Bernstein, S. L.; Wyttenbach, T.; Bitan, G.; Teplow, D. B.; Bowers, M. T.; Shea, J.-E., "Amyloid beta-protein monomer structure: A computational and experimental study." *Protein Sci.* **2006,** *15*, 420-428.

128. Bernstein, S. L.; Liu, D.; Wyttenbach, T.; Bowers, M. T.; Lee, J. C.; Gray, H. B.; Winkler, J. R., "α-Synuclein: Stable compact and extended monomeric structures and pH dependence of dimer formation." *J. Am. Soc. Mass Spectrom.* **2004,** *15*, 1435-1443.

129. Barran, P. E.; Polfer, N. C.; Campopiano, D. J.; Clarke, D. J.; Langridge-Smith, P. R. R.; Langley, R. J.; Govan, J. R. W.; Maxwell, A.; Dorin, J. R.; Millar, R. P.; Bowers, M. T., "Is it biologically relevant to measure the structures of small peptides in the gas-phase?" *Int. J. Mass Spectrom.* **2005,** *240*, 273-284.

130. Ruotolo, B. T.; Gillig, K. J.; Woods, A. S.; Egan, T. F.; Ugarov, M. V.; Schultz, J. A.; Russell, D. H., "Analysis of Phosphorylated Peptides by Ion Mobility-Mass Spectrometry." *Anal. Chem.* **2004,** *76*, 6727-6733.

131. Jackson, S. N.; Wang, H.-Y. J.; Woods, A. S.; Ugarov, M.; Egan, T.; Schultz, J. A., "Direct tissue analysis of phospholipids in rat brain using MALDI-TOFMS and MALDI-ion mobility-TOFMS." *J. Am. Soc. Mass Spectrom.* **2005,** *16*, 133-138.

132. Woods, A. S.; Ugarov, M.; Egan, T.; Koomen, J.; Gillig, K. J.; Fuhrer, K.; Gonin, M.; Schultz, J. A., "Lipid/peptide/nucleotide separation with MALDI-ion mobility-TOF MS." *Anal. Chem.* **2004,** *76*, 2187-2195.

133. Ruotolo, B. T.; McLean, J. A.; Gillig, K. J.; Russell, D. H., "Peak capacity of ion mobility mass spectrometry: the utility of varying drift gas polarizability for the separation of tryptic peptides." *J. Mass Spectrom.* **2004,** *39*, 361-367.

134. Cancilla, M. T.; Penn, S. G.; Carroll, J. A.; Lebrilla, C. B., "Coordination of Alkali Metals to Oligosaccharides Dictates Fragmentation Behavior in Matrix Assisted Laser Desorption Ionization/Fourier Transform Mass Spectrometry." *J. Am. Chem. Soc.* **1996,** *118*, 6736-6745.

135. Cancilla, M. T.; Penn, S. G.; Lebrilla, C. B., "Alkaline Degradation of Oligosaccharides Coupled with Matrix-Assisted Laser Desorption/Ionization Fourier Transform Mass Spectrometry: A Method for Sequencing Oligosaccharides." *Anal. Chem.* **1998,** *70*, 663-672.

136. Cancilla, M. T.; Wong, A. W.; Voss, L. R.; Lebrilla, C. B., "Fragmentation Reactions in the Mass Spectrometry Analysis of Neutral Oligosaccharides." *Anal. Chem.* **1999,** *71*, 3206-3218.

137. Harvey, D. J., "Ionization and collision-induced fragmentation of N-linked and related carbohydrates using divalent cations." *J. Am. Soc. Mass Spectrom.* **2001,** *12*, 926-937.

138. Leavell, M. D.; Leary, J. A., "Stabilization and linkage analysis of metal-ligated sialic acid containing oligosaccharides." *J. Am. Soc. Mass Spectrom.* **2001,** *12*, 528-536.

139. Dinya, Z.; Benke, P.; Györgydeák, Z.; Somsák, L.; Jekö, J.; Pintér, I.; Kuszman, J.; Praly, J.-P., "Mass spectrometric studies of anomeric glycopyranosyl azides." *J. Mass Spectrom.* **2001,** *36*, 211-219.

140. Fenn, L. S.; Kliman, M.; Mahsut, A.; Zhao, S. R.; McLean, J. A., "Characterizing ion mobility-mass spectrometry conformation space for the analysis of complex biological samples." *Anal. Bioanal. Chem.* **2009,** *394*, 235-244.

141. Cooper, C. A.; Gasteiger, E.; Packer, N., "GlycoMod - A software Tool for Determining Glycosylation Compositions from Mass Spectrometric Data " *Proteomics* **2001,** *1*.

142. Cooper, C. A.; Gasteiger, E.; Packer, N., Predicting Glycan Composition from Experimental Mass Using GlycoMod In *Handbook of Proteomic Methods* Conn, P. M., Ed. Humana Press: Totowa, NJ, 2003; pp 225-232.

143. Gasteiger, E.; Gattiker, A.; Hoogland, C.; Ivanyi, I.; Appel, R. D.; Bairoch, A., "ExPASy: the proteomics server for in-depth protein knowledge and analysis." *Nucleic Acids Res.* **2003,** *31*, 3784-3788.

144. Gasteiger, E.; Hoogland, C.; Gattiker, A.; Duvaud, S.; Wilkins, M. R.; Appel, R. D.; Bairoch, A., Protein Identification and Analysis Tools on the ExPASy Server. In *The Proteomics Protocols Handbook*, Walker, J. M., Ed. Humana Press: New York, NY, 2005; pp 571-607.

145. Wilkins, M. R.; Lindskog, I.; Gasteiger, E.; Bairoch, A.; Sanchez, J.-C.; Hochstrasser, D. F.; Appel, R. D., "Detailed peptide characterisation using PEPTIDEMASS - a World-Wide Web accessible tool." *Electrophoresis* **1997,** *18*, 403-408.

146. Plummer, T. H.; Elder, J. H.; Alexander, S.; Phelan, A. W.; Tarentino, A. L., "Demonstration of peptide:N-glycosidase F activity in endo-beta-N-acetylglucosaminidase F preparations." *J. Biol. Chem.* **1984,** *259*, 10700-10704.

147. Balaguer, E.; Neususs, C., "Glycoprotein Characterization Combining Intact Protein and Glycan Analysis by Capillary Electrophoresis-Electrospray Ionization-Mass Spectrometry." *Anal. Chem.* **2006,** *78*, 5384-5393.

148. Lattova, E.; Perreault, H.; Krokhin, O., "Matrix-assisted laser desorption/ionization tandem mass spectrometry and post-source decay

fragmentation study of phenylhydrazones of N-linked oligosaccharides from ovalbumin." *J. Am. Soc. Mass Spectrom.* **2004,** *15*, 725-735.

149. Lattová, E.; Snovida, S.; Perreault, H.; Krokhin, O., "Influence of the Labeling Group on Ionization and Fragmentation of Carbohydrates in Mass Spectrometry." *J. Am. Soc. Mass Spectrom.* **2005,** *16*, 683-696.

150. Mechref, Y.; Novotny, M. V., "Mass Spectrometric Mapping and Sequencing of N-Linked Oligosaccharides Derived from Submicrogram Amounts of Glycoproteins." *Anal. Chem.* **1998,** *70*, 455-463.

151. Snovida, S. I.; Chen, V. C.; Krokhin, O.; Perreault, H., "Isolation and Identification of Sialylated Glycopeptides from Bovine a1-Acid Glycoprotein by Off-Line Capillary Electrophoresis MALDI-TOF Mass Spectrometry." *Anal. Chem.* **2006,** *78*, 6556-6563.

152. Snovida, S. I.; Chen, V. C.; Perreault, H., "Use of a 2,5-Dihydroxybenzoic Acid/Aniline MALDI Matrix for Improved Detection and On-Target Derivatization of Glycans: A Preliminary Report." *Anal. Chem.* **2006,** *78*, 8561-8568.

153. Harvey, D. J.; Wing, D. R.; Küster, B.; Wilson, I. B. H., "Composition of N-linked carbohydrates from ovalbumin and co-purified glycoproteins." *J. Am. Soc. Mass Spectrom.* **2000,** *11*, 564-571.

154. Imre, T.; Schlosser, G.; Pocsfalvi, G.; Siciliano, R.; Molnár-Szöllosi, É.; Kremmer, T.; Malorni, A.; Vékey, K., "Glycosylation site analysis of human alpha-1-acid glycoprotein (AGP) by capillary liquid chromatography - electrospray mass spectrometry." *J. Mass Spectrom.* **2005,** *40*, 1472-1483.

155. Kang, P.; Mechref, Y.; Klouckova, I.; Novotny, M. V., "Solid-phase permethylation of glycans for mass spectrometric analysis." *Rapid Commun. Mass Spectrom.* **2005,** *19*, 3421-3428.

156. Kremmer, T.; É, S.; Boldizsár, M.; Vincze, B.; Ludányi, K.; Imre, T.; Schlosser, G.; Vékey, K., "Liquid chromatographic and mass spectrometric analysis of human serum acid alpha-1-glycoprotein." *Biomed. Chromatogr.* **2004,** *18*, 323-329.

157. Küster, B.; Wheeler, S. F.; Hunter, A. P.; Dwek, R. A.; Harvey, D. J., "Sequencing of N-Linked Oligosaccharides Directly from Protein Gels: In-Gel Deglycosylation Followed by Matrix-Assisted Laser Desorption/Ionization Mass Spectrometry and Normal-Phase High-Performance Liquid Chromatography." *Anal. Biochem.* **1997,** *250*, 82-101.

158. Treuheit, M. J.; Costello, C. E.; Halsall, H. B., "Analysis of the five glycosylation sites of human alpha 1-acid glycoprotein." *Biochem. J.* **1992,** *283*, 105-112.

159. Jensen, R. G., "The lipids in human milk." *Prog. Lipid Res.* **1996,** *35*, 53-92.

160. Ninonuevo, M. R.; Park, Y.; Yin, H.; Zhang, J.; Ward, R. E.; Clowers, B. H.; German, J. B.; Freeman, S. L.; Killeen, K.; Grimm, R.; Lebrilla, C. B., "A Strategy for Annotating the Human Milk Glycome." *J. Agric. Food Chem.* **2006,** *54*, 7471-7480.

161. Ninonuevo, M. R.; Perkins, P. D.; Francis, J.; Lamotte, L. M.; LoCascio, R. G.; Freeman, S. L.; Mills, D. A.; German, J. B.; Grimm, R.; Lebrilla, C. B., "Daily Variations in Oligosaccharides of Human Milk Determined by Microfluidic Chips and Mass Spectrometry." *J. Agric. Food Chem.* **2007,** *56*, 618-626.

162. Kunz, C.; Rudloff, S.; Baier, W.; Klein, N.; Strobel, S., "OLIGOSACCHARIDES IN HUMAN MILK: Structural, Functional, and Metabolic Aspects." *Annu. Rev. Nutr.* **2000,** *20*, 699-722.

163. Stahl, B.; Thurl, S.; Zeng, J. R.; Karas, M.; Hillenkamp, F.; Steup, M.; Sawatzki, G., "Oligosaccharides from Human Milk as Revealed by Matrix-Assisted Laser Desorption/Ionization Mass Spectrometry." *Anal. Biochem.* **1994,** *223*, 218-226.

164. Casado, B.; Affolter, M.; Kussmann, M., "OMICS-rooted studies of milk proteins, oligosaccharides and lipids." *J. Proteomics* **2009,** *73*, 196-208.

165. Wilson, N. L.; Robinson, L. J.; Donnet, A.; Bovetto, L.; Packer, N. H.; Karlsson, N. G., "Glycoproteomics of Milk: Differences in Sugar Epitopes on Human and Bovine Milk Fat Globule Membranes." *J. Prot. Res.* **2008,** *7*, 3687-3696.

166. Creaser, C. S.; Griffiths, J. R.; Stockton, B. M., "Gas-phase ion mobility studies of amines and polyether/amine complexes using tandem quadrupole ion trap/ion mobility spectrometry." *Eur. J. Mass Spectrom.* **2000,** *6*, 213-218.

167. Hilderbrand, A. E.; Myung, S.; Clemmer, D. E., "Exploring Crown Ethers as Shift Reagents for Ion Mobility Spectrometry." *Anal. Chem.* **2006,** *78*, 6792-6800.

168. James, T., "Saccharide-Selective Boronic Acid Based Photoinduced Electron Transfer (PET) Fluorescent Sensors." *Top. Curr. Chem.* **2007,** *277*, 107-152.

169. James, T. D.; Phillips, M. D.; Shinkai, S., *Boronic Acids in Saccharide Sensing*. Royal Society of Chemistry: Cambridge, UK, 2006.

170. Wang, W.; Gao, X.; Wang, B., "Boronic Acid-Based Sensors." *Curr. Org. Chem.* **2002,** *6*, 1285-1317.

171. Lorand, J. P.; Edwards, J. O., "Polyol Complexes and Structure of the Benzeneboronate Ion." *J. Org. Chem.* **1959,** *24*, 769-774.

172. Pikulski, M.; Hargrove, A.; Shabbir, S. H.; Anslyn, E. V.; Brodbelt, J. S., "Sequencing and Characterization of Oligosaccharides Using Infrared Multiphoton Dissociation and Boronic Acid Derivatization in a Quadrupole Ion Trap." *J. Am. Soc. Mass Spectrom.* **2007,** *18*, 2094-2106.

173. Williams, D.; Young, M. K., "Analysis of neutral isomeric low molecular weight carbohydrates using ferrocenyl boronate derivatization and tandem electrospray mass spectrometry." *Rapid Commun. Mass Spectrom.* **2000,** *14*, 2083-2091.

174. Young, M. K.; Dinh, N.; Williams, D., "Analysis of N-acetylated hexosamine monosaccharides by ferrocenyl boronation and tandem electrospray ionization mass spectrometry." *Rapid Commun. Mass Spectrom.* **2000,** *14*, 1462-1467.

175. McLuckey, S. A.; Habibi-Goudarzi, S., "Decompositions of multiply charged oligonucleotide anions." *J. Am. Chem. Soc.* **1993,** *115*, 12085-12095.

Larissa S. Fenn

7408 East Winchester Dr.
Antioch, TN 37013

Email: larissa.fenn@gmail.com
Cell : (478)319-8637

Education[i]

Vanderbilt University, Nashville, TN
Attended: August 2005 to present
Advisor: Prof. John A. McLean
Degree obtained: Ph.D. in Analytical Chemistry
Dissertation title: Detection and characterization of glycans and glycoconjugates using ion mobility-mass spectrometry
GPA: 3.687

Mercer University, Macon, GA
Attended: August 2001-May 2005
Degree obtained: Bachelor of Science in Chemistry with Departmental Honors, minor in mathematics
GPA: 3.69 *cum laude*

University of Wales, Swansea, Great Britain
Attended: August 2002-May 2003
Participated in Study Abroad Program

Research Experience

Vanderbilt University Graduate School – McLean lab, March 2006-May 2010
Specialize in ion mobility-mass spectrometry instrumentation – research grade and commercial (Waters Synapt); Matrix-assisted laser desorption/ionization and electrospray ionization; concentrated on biological samples with particular attention to carbohydrates and glycoproteins

Work Experience

Rayonier, Inc., Jesup, GA
May-August 2002-2004
Customer Service Internship
Immediate supervisor – Kimberly Jones (912) 588-8000
Duties – Prepared shipment and insurance documents for air, land, and sea deliveries; Communicated with international offices; Converted all archived shipment bills for a period of approximately ten years to electronic format

Selected Honors and Awards

2009 Barbara Stull Graduate Student Award from the Society of Applied Spectroscopy received at Federation of Analytical Chemistry and Spectroscopy Societies (FACSS) annual conference

[i] CV completed April 12th, 2010

2009 Vanderbilt University Graduate School Dissertation Enhancement Grant for travel to study in the lab of Dr. J. Sabine Becker at the Research Centre Juelich, Germany

2009, 2008, 2007 Vanderbilt Institute for Chemical Biology Annual Retreat Poster Award

2008, 2007 35th and 34th Annual FACSS Conference Poster Award

2008, 2007 Society for Applied Spectroscopy Piedmont Section Award for Travel to FACSS meeting in Reno, NV, and Memphis, TN

2008 Nomination by Nashville Chapter of the Philanthropic Educational Organization (P.E.O.) for National Scholar Award

2007 Outstanding Teaching Assistant Award from the Student Affiliates of the American Chemical Society (Department of Chemistry, Vanderbilt University)

2006 Tennessee Academy of Science Annual Meeting Student Oral Presentation Award

2006 Wallace Odell DuVall Excellence in Leadership Award (Scholarship for graduate study, Mercer University)

2005 Iota Sigma Pi (National Honor Society for Women in Chemistry) undergraduate award, Mercer University

2004 ACS Division of Analytical Chemistry Undergraduate Award, Mercer University

2004 Summer Undergraduate Research Experience (SURE), Emory University

Publications – Peer Reviewed

13. **Larissa S. Fenn** and John A. McLean, "Simultaneous glycoproteomic strategies utilizing ion mobility-mass spectrometry", *Molecular BioSystems* **2009**, 5, 1298-1302. (Featured on front cover of Nov. 2009 issue)

12. **Larissa S. Fenn**, Michal Kliman, Ablatt Mahsut, Sophie R. Zhao, and John A. McLean, "Characterizing Ion Mobility-Mass Spectrometry Conformation Space for the Analysis of Complex Biological Samples", *Analytical and Bioanalytical Chemistry* **2009**, *394*, 235-244.

11. **Larissa S. Fenn** and John A. McLean, "Enhanced carbohydrate structural selectivity by boronic acid derivitization and ion mobility-mass spectrometry analysis", *Chemical Communications*, **2008**, *43*, 5505-5507.

10. **Larissa S. Fenn** and John A. McLean, "Biomolecular Structural Separations by Ion Mobility-Mass Spectrometry: New Prospects for Systems Biology", *Analytical and Bioanalytical Chemistry* **2008**, *391*, 905-909.

9. John A. McLean, **Larissa S. Fenn,** and Jeffrey R. Enders, "Ion mobility-mass spectrometry Imaging", *Mass Spectrometric Imaging: History, Fundamentals and Protocols,* **Methods in Molecular Biology Series**, Jonathan V. Sweedler and Stanislav Rubakhin, eds. September 2010.

8. Kellen M. Harness, **Larissa S. Fenn**, David E. Cliffel, and John A. McLean, "Analysis of capping structural motifs on gold nanoparticles by ion mobility-mass spectrometry" Accepted, *Analytical Chemistry*

7. John A. McLean and **Larissa S. Fenn**, "Structural separations by ion mobility-MS for the characterization of glycoproteins", in preparation for *Mass Spectrometry of Glycoproteins,* **Methods in Molecular Biology Series**, Steven Patrie and Jennifer Kohler, eds.

6. LaKedra S. Pam, **Larissa L. Spell**, and James T. Kindt, "Simulation and theory of flexible equilibrium polymers under poor solvent conditions", *The Journal of Chemical Physics* **2007,** *126*, 134906.

5. **Larissa S. Fenn** and John A. McLean, "Differentiation of carbohydrate structural isomers using MALDI-Ion Mobility-Mass Spectrometry", in preparation for submission to *Physical Chemistry & Chemical Physics*

4. **Larissa S. Fenn**, Cody Goodwin, Brian O. Bachmann, and John A. McLean, "Exploring conformation space for cyclic peptide natural products using ion mobility-mass spectrometry", In preparation for submission to *Journal of the American Chemical Society*

3. Whitney B. Ridenour, Michal Kliman, **Larissa S. Fenn,** John A. McLean, Richard M. Caprioli. "Structural characterization of pharmaceutical compounds by ion mobility-mass spectrometry". In preparation for submission to *Analytical Chemistry*

2. **Larissa S. Fenn** and John A. McLean, "Simultaneous glycoproteomics and glycolipidomics utilizing ion mobility-mass spectrometry", In preparation for submission to *Analytical Chemistry*

1. **Larissa S. Fenn,** Jerry Thomas (Molecular Probes), and John A. McLean, "Enhanced carbohydrate structural selectivity by derivitization using click chemistry", in preparation for submission

Publications – Proceedings Papers

3. **L.S. Fenn**, M. Kliman, A. Mahsut, S. Zhao, T.J. Kerr, R.L. Gant, J.A. McLean, "Integrated 'omics' on the basis of structural separations by ion mobility-mass spectrometry", Proceedings of the American Society for Mass Spectrometry 57th Annual Conference, **2009**

2. **L.S. Fenn**, J.A. McLean, "Ion mobility shift strategies for structural characterization of carbohydrates", Proceedings of the American Society for Mass Spectrometry 56th Annual Conference, **2008**

1. **L.S. Fenn**, J.A. McLean, "Simultaneous glycomic and proteomic strategies using structural mass spectrometry", Proceedings of the American Society for Mass Spectrometry 55th Annual Conference, **2007**

Presentations

27. **L.S. Fenn**, C. Goodwin, B.O. Bachmann, J.A. McLean, *Structural characterization of natural products from complex biological mixtures using ion mobility-mass spectrometry*, 36th Annual Federation of Analytical Chemistry and Spectroscopy Societies conference, Louisville, KY (October 2009) (invited talk)

26. **L.S. Fenn**, M. Kliman, R.L. Gant, T.J. Kerr, J.A. McLean*, Characterization of complex biological samples on the basis of structural separations by ion mobility-mass spectrometry*, 18th International Mass Spectrometry Conference, Bremen, Germany (Sept. 2009)

25. **L.S. Fenn**, M. Kliman, J.A. McLean, *Integrated 'omics' on the basis of structural separations by ion mobility-mass spectrometry*, 5th Annual Meeting of the Vanderbilt Institute for Chemical Biology, Nashville, TN (August 2009)

24. **L.S. Fenn**, M. Kliman, A. Mahsut, S. Zhao, T.J. Kerr, R.L. Gant, J.A. McLean, *Integrated 'omics' on the basis of structural separations by ion mobility-mass spectrometry*, American Society for Mass Spectrometry Annual Conference, Philadelphia, PA (June 2009)

23. **L.S. Fenn**, M. Kliman, A. Mahsut, S. Zhao, T.J. Kerr, R.L. Gant, J.A. McLean, *Integrated 'Omics' Using Structural Mass Spectrometry Strategies,* Southeast Regional Meeting of the American Chemical Society, Nashville, TN (November 2008)

22. C.R. Goodwin, A.P. Gies, D.M. Hercules, **L.S. Fenn**, J.A. McLean, *MALDI-IM-TOF-MS and CID Fragmentation Studies of Polyurethanes,* Southeast Regional Meeting of the American Chemical Society, Nashville, TN (November 2008)

21. A.P. Gies, **L.S. Fenn**, M. Kliman, J.A. McLean, D.M. Hercules, *MALDI-TOF MS Identification of Poly(p-phenylene terephthalamide) Branching and Metathesis Products*, Southeast Regional Meeting of the American Chemical Society, Nashville, TN (November 2008)

20. **L.S. Fenn** and J.A. McLean, *Simultaneous glycoproteomic strategies utilizing ion mobility-mass spectrometry: New insights from structural separations*, 35th Annual Federation of Analytical Chemistry and Spectroscopy Societies conference, Reno, NV (October 2008)

19. **L.S. Fenn** and J.A. McLean, *Ion mobility shift strategies for structural characterization of carbohydrates,* 4th Annual Meeting of the Vanderbilt Institute for Chemical Biology, Nashville, TN (August 2008)

18. J. R. Enders, **L. S. Fenn**, M. F. Aldersley, J. P. Ferris, P. C. Joshi, J. A. McLean, D. Zagorevski, *Ion Mobility Mass Spectrometry of the Products of*

Oligomerization of Activated Nucleotides with Montmorillonite, American Society for Mass Spectrometry Annual Conference, Denver, CO (June 2008)

17. **L.S. Fenn** and J.A. McLean, *Ion mobility shift strategies for structural characterization of carbohydrates,* American Society for Mass Spectrometry Annual Conference, Denver, CO (June 2008)

16. **L.S. Fenn** and J.A. McLean, *Structural Separations of Positional and Structural Carbohydrate Isomers using Ion Mobility-Mass Spectrometry,* American Society for Mass Spectrometry Sanibel Conference, Ion Mobility and Related Emerging Areas, Daytona, FL, (January 2008)

15. **L. S. Fenn** and J. A. McLean, *Structural Characterization Strategies for Simultaneous Glycomics and Proteomics using Ion Mobility-Mass Spectrometry,* 34th Annual Federation of Analytical Chemistry and Spectroscopy Societies conference, Memphis, TN (October 2007).

14. N.V. Arinze, J.R. McLean, **L.S. Fenn**, J.A. McLean, *A Critical Comparison of Positively and Negatively-Charged Ion Structures using Ion Mobility-Mass Spectrometry*, 34th Annual Federation of Analytical Chemistry and Spectroscopy Societies conference, Memphis, TN (October 2007).

13. **L. S. Fenn** and J. A. McLean, *Simultaneous glycomic and proteomic strategies using structural mass spectrometry*, 3rd Annual Meeting of the Vanderbilt Institute for Chemical Biology, Nashville, TN (August 9th, 2007).

12. J. A. McLean, **L. S. Fenn,** T. Kerr, *Structural mass spectrometry separation strategies for proteomics, glycomics, and lipidomics: Ion mobility-MS and imaging ion mobility-MS*, Protein Society 21st Annual Symposium, Boston, MA (July 2007).

11. **L.S. Fenn** and J.A. McLean, *Simultaneous glycomic and proteomic strategies using structural mass spectrometry*, 55th Annual Meeting of the American Society for Mass Spectrometry, Indianapolis, IN (June 2007).

10. M. V. Ugarov, T. F. Egan, J. A. Schultz, **L. S. Fenn**, M. Kliman, J. A. McLean, S. N. Jackson, H.-Y. J. Wang, and A. S. Woods, *Study of Lipids in Tissues by Ion Mobility Time-Of-Flight Mass Spectrometry*, 55th Annual Meeting of the American Society for Mass Spectrometry, Indianapolis, IN (June 2007).

9. J. A. McLean and **L. L. Spell**, *Structural Ion Mobility-Mass Spectrometry Strategies for Glycomics and Glycoproteomics*, Pittsburgh Conference on Analytical Chemistry and Applied Spectroscopy (PITTCON) Conference, Chicago, IL (March 2007).

8. **L.S. Fenn** and J.A. McLean, *Strategies in Glycomics and Proteomics using Structural Mass Spectrometry,* Vanderbilt University Center in Molecular Toxicology 40th Anniversary Symposium "Advances in Mass Spectrometry" Nashville, TN (April 14th, 2007).

7. **L.S. Fenn** and J.A. McLean, *Simultaneous glycomic and proteomic strategies using structural mass spectrometry*, Vanderbilt University Graduate Student Research Day, Nashville, TN (April 6th, 2007).

6. **L.S. Fenn**, T. Kerr, and J.A. McLean, *Advanced Structural Mass Spectrometry Approaches for Proteomics and Biophysics,* St. Jude Children's Research Hospital/Vanderbilt Institute for Chemical Biology Retreat, Florence, AL (March 23, 2007).

5. **L.S. Fenn** and J.A. McLean, *High-throughput detection and characterization of glycopeptides and glycoproteins using advanced structural mass spectrometry,* Tennessee Academy of Science Annual Meeting, Austin Peay University, Clarksville, TN (November 17th, 2006).

4. **L.L. Spell** and J.A. McLean, *Advanced Structural Mass Spectrometry Approaches to Proteomics and Biophysics,* 2nd Annual Vanderbilt Institute for Chemical Biology Retreat, Nashville, TN (August 8th, 2006).

3. **L. L. Spell**, M. Golden, and A.J. Pounds, *ab initio Study of Hydroxyl Radical Initiated Reactions of Elemental Mercury,* Mercer University Academic Research and Scholarly Activity, Macon, GA (May 2005).

2. F. Mobini, D. Moshkelani, **L. L. Spell**, B. Rainwater, N. C. Dopke, *Maintaining Traditions yet Making it New: A SAACS Chapter Celebrates National Chemistry Week,* Southeastern Conference of the American Chemical Society, Raleigh-Durham, NC (November 13, 2004).

1. **L. L. Spell**, M. Golden, and A.J. Pounds, *Exploring Conformational Space,* Mercer University Symposium for Undergraduate Research, Macon, GA (May 2002).

Academic Volunteer Activities

1. Vanderbilt University Department of Chemistry Steering Committee (2005-2007)

2. Vanderbilt Institute of Chemical Biology Annual Retreat Planning Committee (2009)

Professional Memberships/Leadership

1. American Society for Mass Spectrometry

2. American Chemical Society

3. Society for Applied Spectroscopy

4. Coblenz Society

Teaching Experience

Teaching assistant, Analytical Chemistry Lab

September-December 2009, January-May 2007
Vanderbilt University, Department of Chemistry

Teaching assistant, General Chemistry Lab
August 2005-May 2006
Vanderbilt University, Department of Chemistry

Teaching assistant, Organic Chemistry Lab
January-May 2005
Mercer University, Department of Chemistry

Student instructor, August 2004-May 2005
Mercer University, Department of Interdisciplinary Studies

Volunteer Activities

Adventure Science Center Special Event Volunteer, Nashville, TN (2009)

TWISTER (Tennessee Women in Science, Technology, and Engineering) volunteer, Nashville, TN (2009)

Vistacare hospice patient care volunteer, Macon, GA (2001-2005)

British Red Cross Oncology Volunteer, Singleton Hospital, Swansea, Wales, UK (2002-2003)